

**STRUCTURAL STUDIES ON CHIRAL Cu(II) COMPLEXES:
ENANTIO-SPECIFIC INCLUSION OF CHIRAL GUEST MOLECULES,
PERFECTLY POLAR ORDERING AND HELICAL ASSEMBLIES**

**A THESIS
SUBMITTED FOR THE DEGREE OF
DOCTOR OF PHILOSOPHY**

**BY
M. VAMSEE KRISHNA**



**SCHOOL OF CHEMISTRY
UNIVERSITY OF HYDERABAD
HYDERABAD 500 046
INDIA**

JUNE 2005



Dedicated to my beloved mother Late Smt. Muppidi Bharathi

CONTENTS

STATEMENT	i
CERTIFICATE	ii
ACKNOWLEDGEMENT	iii

CHAPTER 1

Introduction

1.1. Abstract	1
1.2. Introduction	2
1.3. Aim of the Present Investigation	13
1.4. References	15

CHAPTER 2

Synthesis of the enantiomers of a chiral dinuclear copper(II) complex: Selective inclusion of chlorinated solvents and enantio-specific inclusion of chiral 1,2-dichloroethane rotamers in the crystal lattice

2.1. Abstract	21
2.2. Introduction	22
2.3. Experimental	23
2.4. Results and Discussion	29
2.5. Conclusion	49
2.6. References	49

CHAPTER 3

Inclusion compounds of polar solvents with chiral Cu(II) complexes: Perfectly polar alignment of guest and host molecules and enantio-specific inclusion of chiral 1,2-dihaloethane rotamers

3.1. Abstract	53
---------------	----

3.2. Introduction	54
3.3. Experimental	55
3.4. Results and Discussion	62
3.5. Conclusion	82
3.6. References	82

CHAPTER 4

Mononuclear copper(II) complexes with chloro-substituted chiral reduced Schiff bases: Activated $\text{CH}\cdots\text{O}$ interaction induced self -assembly to homo chiral helices

4.1. Abstract	85
4.2. Introduction	86
4.3. Experimental	87
4.4. Results and Discussion	93
4.5. Conclusion	106
4.6. References	106

CHAPTER 5

Inclusion properties of Cu(II) complexes of bromo substituted chiral reduced Schiff bases: Stabilization of guest molecules *via* $\text{O}-\text{H}\cdots\text{O}$ interactions

5.1. Abstract	109
5.2. Introduction	110
5.3. Experimental	111
5.4. Results and Discussion	117
5.5. Conclusion	128
5.6. References	129


List of Publications	131
-----------------------------	-----

STATEMENT

I here by declare that the matter embodied in the thesis is the result of investigation carried out by me in the School of Chemistry, University of Hyderabad, Hyderabad, India, under the supervisions of Prof. P. S. Zacharias and Prof. Samudranil Pal.

In keeping with the general practice of reporting scientific observations, due acknowledgements have been made wherever the work described is based on the findings of other investigators. Any omission, which might have occurred by oversight or error is regretted.

18-06-05



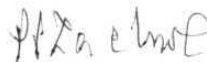
M. Vamsee Krishna

CERTIFICATE

Certified that the work contained in the thesis entitled “**Structural Studies on Chiral Cu(II) Complexes: Enantio-specific Inclusion of Chiral Guest Molecules, Perfectly Polar Ordering and Helical Assemblies**” has been carried out by Mr. M. Vamsee Krishna under our supervisions and the same has not been submitted elsewhere for a degree.

Hyderabad

June 2005



Prof. P. S. Zacharias

(Supervisor)



Dean

School of Chemistry

Dean

School of Chemistry

University of Hyderabad.

Hyderabad 500 046, India.



Prof. Samudranil Pal

(Co-supervisor)

ACKNOWLEDGEMENT

I express my deep sense of gratitude and profound thanks to my thesis supervisors **Prof. P. S. Zacharias** and **Prof. Samudranil Pal** for their invaluable guidance, inspiration, and constant encouragement through out the course of this work.

I thank Prof. M. Periasamy, Dean, School of Chemistry and former Deans and faculty members of the School for their co-operation on various occasions. I would like to take this opportunity to thank Dr. S. K. Das for his kind help and suggestions. I thank Council of Scientific and Industrial Research, New Delhi for the fellowship.

I wish to thank my friendly and cooperative labmates Dr. K. Srinivas Rao, Dr. Sunil Kumar, Dr. N. Mangayarkarasi, Dr. Satyanarayan Pal, Dr. Tin Htwe, M. Prabhakar, C. P. Pradeep, S. Gupta Sreerama, Sunirban Das, Abhik Mukhopadhyay, Raji Raveendran and Anindita Sarkar for creating cheerful work atmosphere.

I also thank all the staff of the School of Chemistry and COSIST building for their assistance on various occasions. I am grateful to Jaypal, Sreevardhan, Kommana, Thallapally, Raghu, Sampath, Shiva, Praveen, Sastry, Senthil, Sairam, Pavan, Vasulu, Chandu, Srinivasa Reddy, Balu, Jagadeesh, Narsi, Suresh, Shyam, Anoop, Perumal, Philip, Mariappan, Sharath, Ravikanth, Yadaiah, Bhuvan, Devendar, Satish, Raju, Biju, Shivaiah, Madhu, Sridhar and all my other friends from School of Chemistry for their help on various occasions. A special note of thanks to Raghavaiah, Venu, Basavoju, Malla Reddy, Babji and Pradeep for their help and encouragement during my thesis work.

My acknowledgements would not be complete without mentioning the unique contribution made by my father, mother, sister, brother-in-law, and other close relatives. My nieces (Bhavya, Dimpu) and nephew (Sai Sushrith) deserve a word of thanks for their smiles and wishes. Finally, I wish to thank my wife Manasa for her patience and constant encouragement.

M. Vamsee Krishna

Introduction

1.1. Abstract

This chapter describes the chiral porous metal-organic frameworks (MOF's) and their applications towards enantioselective separations, asymmetric catalysis and nonlinear optics. Chiral porous metal-organic frameworks constructed from reduced Schiff base ligands and the scope of present investigation are also discussed.

1.2. Introduction

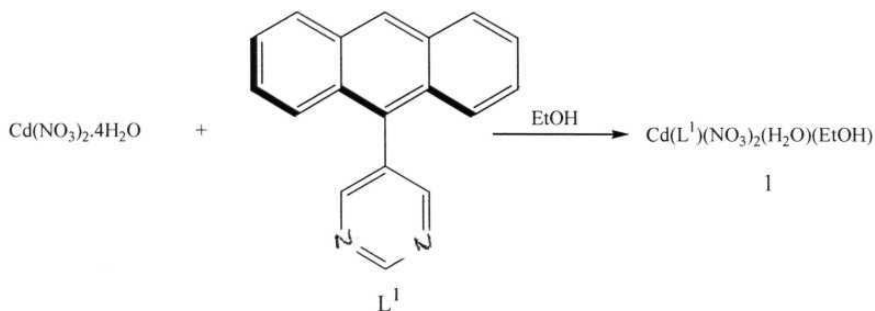
The significance and impact of self-assembly are demonstrated by the porous zeolites that combine the acidic properties of the aluminosilicate with the channels and pores of the supramolecular structure to generate catalytically important materials.¹ The presence of cations inside the channels and cavities of zeolites also make them ideal choices for ion exchange process. They have varied practical applications in the production of many consumer products such as gasoline, detergents etc.² In light of importance of chirality in biological and catalytic process, there have been tremendous research efforts devoted to the development of chiral zeolites. Several attempts to synthesize chiral zeolites found to be unsuccessful. Special design strategies are needed to prepare chiral zeolitic type porous materials that may find application in chirotechnology.³

On the other hand, a major research effort has focused on using the molecular building block approach to generate analogous materials with 3D organic, metal-organic and inorganic frameworks. Strategies for the construction of these solids have utilized metal-ligand coordination, hydrogen-bonding interactions and other non-covalent interactions to link their molecular components.⁴ Number of such frameworks have been found to exhibit desirable zeolitic properties such as stability and micro-porosity of the framework, guest exchange, gas storage and selective catalytic activity.⁵ Recently there has been considerable interest in synthesis of host frameworks with chiral cavities. These solids have potential applications in the separation of enantiomers and in asymmetric catalysis.^{3,6} Especially chiral porous metal-organic frameworks are found to be most reliable catalysts for heterogeneous asymmetric catalysis. Self-assembly of the metal ions linked together by organic bridging ligands lead to the generation of metal-organic frameworks (MOF's). Various structures with interesting composition and topologies have been produced through judicious choice of chiral ligand and metal coordination to construct chiral porous materials with defined pore size. Synthesis and applications of some of the

chiral porous metal-organic frameworks and the aim of the present investigation are described below.

1.2.1. Homochiral porous MOF's constructed from achiral ligands

Spontaneous resolution of an achiral compound on crystallization in the absence of any chiral source is of great interest in recent years.⁷ There are several examples of achiral molecules including simple metal salts which can crystallize in chiral space group. One of the serious inaccuracies for such systems that although single crystals of such compounds lead to homochiral crystals, in bulk sample it may be racemic. Ayoma and coworkers recently reported an interesting example of homochiral crystallization of \uparrow ^{coordination polymer} that are built from achiral components.⁸ They treated $\text{Cd}(\text{NO}_3)_2 \cdot 4\text{H}_2\text{O}$ with achiral 5-(9-anthracenyl pyrimidine) (L^1) and a helical coordination polymer with composition of $\text{Cd}(\text{L}^1)(\text{NO}_3)_2(\text{H}_2\text{O})(\text{EtOH})$ (**1**) was obtained. The Cd^{2+} center adopts octahedral geometry with two pyrimidine ligands (equatorial *cis*), water and ethanol (equatorial *cis*), and two nitrate ions (axial *trans*). X-ray crystallographic analysis reveals that this coordination polymer crystallizes in monoclinic $P2_1$ space group and exhibit helical nature through metal-ligand coordination. Interestingly, adjacent helices adopt the same handedness and linked by the intrastrand H_2O – nitrate hydrogen-bonding interactions. Compound L^1 also forms achiral (*Pbca*) trihydrate adduct $\text{Cd}(\text{L}^1)(\text{NO}_3)_2 \cdot 3\text{H}_2\text{O}$ having nonhelical pyrimidine- Cd^{2+} zigzag chains (Scheme 1). Both chiral and achiral coordination polymers are interconvertable to each other in the solid state upon exchange of volatile ligands. They used the seeding technique to control the chirality of these coordination polymers.



Scheme 1

1.2.2. Homochiral porous MOF's constructed from chiral ligands

One of the easy ways for the synthesis of chiral porous solids is to combine metal salts with well designed chiral ligands. The use of chiral ligand will ensure the chirality in the resulting network structure. Recently, Hosseini and coworkers have designed and synthesized a chiral tecton to coordinate metal centers and generated a perfectly polar 1D network (Figure 1).⁹ The ligand (L^2) consists of a pyridine group on one end and a C_2 -symmetric 2, 6-bis (oxazolyl)-pyridine on the other end, and is thus chiral owing to the use of optically active oxazoline groups. Slow diffusion of EtOH solution of $\text{Co}(\text{II})\text{Cl}_2$ into CHCl_3 solution of L^2 afforded crystals of X-ray quality. Crystal structure analysis revealed that metal-ligand coordination leads to perfectly polar 1D coordination polymer with chiral voids. These voids are occupied by CHCl_3 molecules. It is well known that polar solids have potential applications towards nonlinear optics.

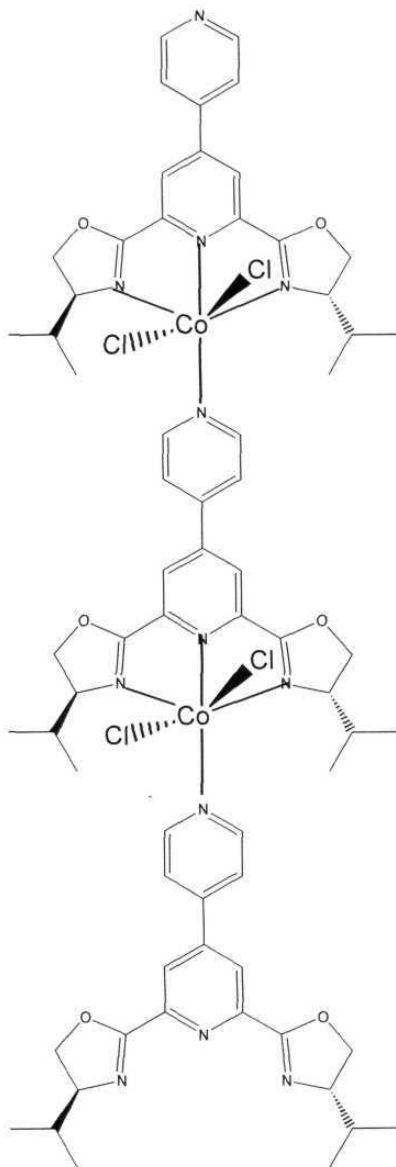


Figure 1. 1D Perfect polar network built from Co(II) and a chiral tecton L².

Recently, Kimoon and coworkers have demonstrated the use of homochiral metal-organic porous material for enantioselective separation and catalysis.¹⁰ The homochiral open-framework solid having the formula of $[\text{Zn}_3(\mu_3\text{-O})(\text{L}^3\cdot\text{H})_6]\cdot 12\text{H}_2\text{O}$ (D-POST) was prepared by the reaction of Zn^{2+} with enantiopure chiral building block derived from D-tartaric acid. The enantiomorphic L-POST is obtained from the enantiomer of L^3 and the Zn^{2+} ion under same condition. In D-POST, three zinc ions are held together with six carboxylate groups of the deprotonated chiral ligand L^3 and bridging oxo group, to form a triangular unit, in which a three-fold axis parallel to the *c*-axis passes through the center of the trinuclear unit. The trinuclear units are further interconnected through coordinate covalent bonds between the zinc ions and pyridyl group of L^3 to generate 2D infinite layers consisting of large edge-sharing chair shaped hexagons with triangular unit at each corner (Figure 2).

Most notably, large 1D chiral channel exists along the *c*-axis with side length of ~ 13.4 Å. The solvent access area of D-POST estimated to be $\sim 47\%$ and these voids are occupied by 47 water molecules per unit cell. The presence of accessible chiral pores in D-POST allows enantioselective inclusion studies. Enantioselective inclusion of chiral metal complexes was studied by using racemic $[\text{Ru}(2,2^1\text{-bipy})_3]\text{Cl}_2$ and ethanol suspension of L-POST. Such enantioselective inclusion of chiral metal complexes in porous materials is unprecedented. The pyridyl groups in D-POST were used to catalyze transesterification reactions. Although the enantiomeric excess in the product of transesterification was rather low ($\sim 8\%$), the enantioselectivity is unprecedented because this asymmetric induction was observed for reaction promoted by a modular porous material (Scheme 2). This creative work triggered interest in using the chiral metal-organic porous materials for asymmetric catalysis. The success of asymmetric catalysis with this kind of porous metal-organic frameworks was realized only very recently.^{6c}

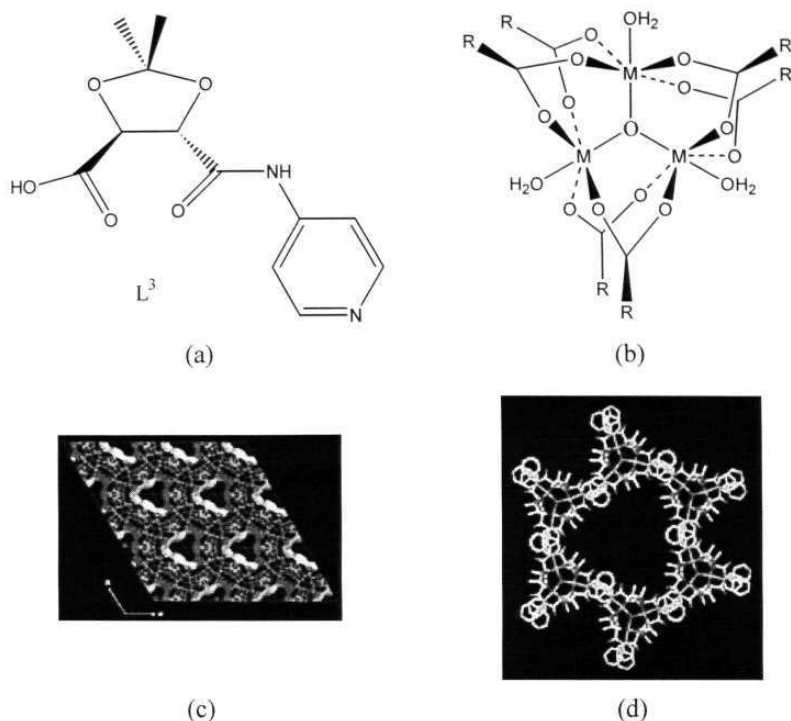
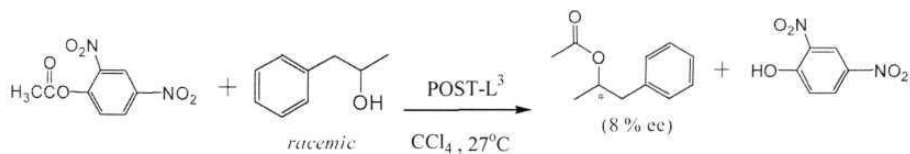


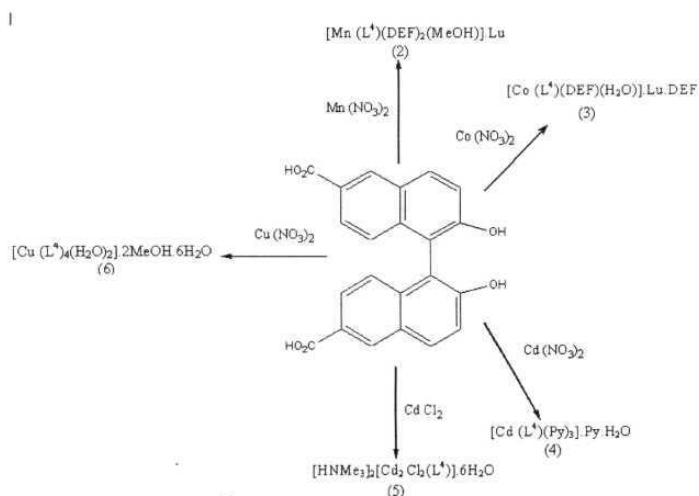
Figure 2. (a) Chiral ligand L^3 , (b) Trinuclear building unit in $POST-L^3$, (c) trigonal channels of $D-POST$, (d) hexagonal framework of $POST-L^3$ that formed from trinuclear building units.



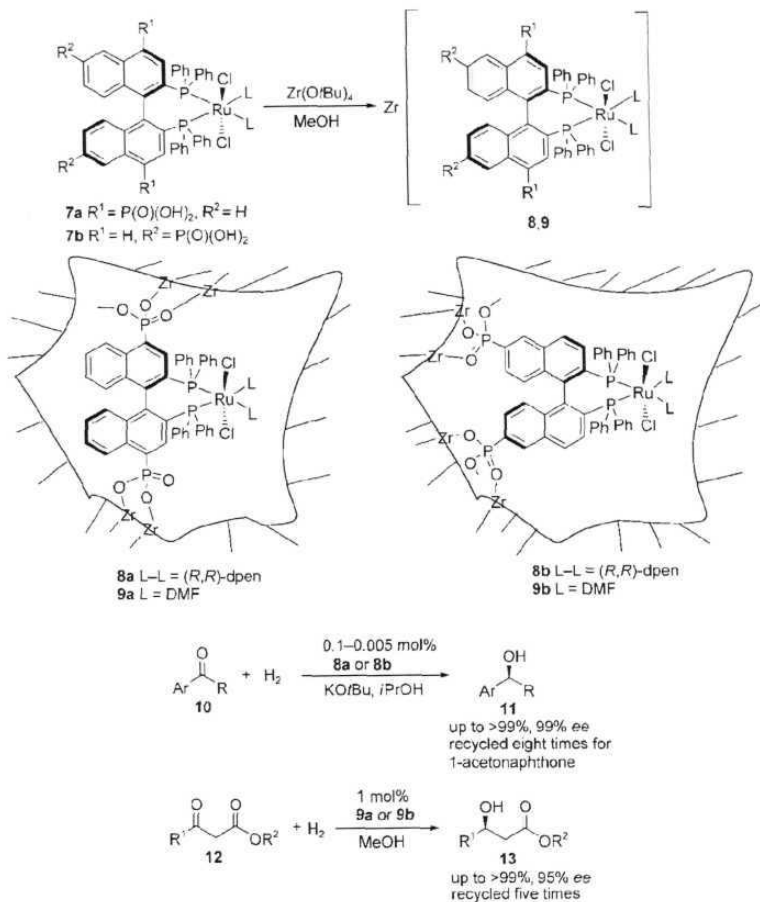
Scheme 2

Lin and coworkers have designed a variety of chiral bridging ligands based on atropisomeric 1,1'-binaphthyl framework. These chiral bridging ligands with twisted di carboxylate group leads to 1D, 2D and 3D MOFs.¹¹ When enantiopure 2,2'-

dihydroxy-1,1'-binaphthylene-6,6'-dicarboxylic acid (H_2L^4) was treated with various metal salts under slightly basic conditions, 1D homochiral MOF's **2-6** with interesting topologies were obtained (Scheme 3). They stated that heterogenation of Noyori's catalysts could be achieved by *insitu* formation of chiral porous hybrid solids such as **8** and **9** through the reaction of zirconium tert-butoxide with chiral bisphosphine/Ru complexes functionalized with phosphonic acid groups, **7** (Scheme 4). Nitrogen adsorption measurements demonstrated that these hybrid solids are highly porous with rather wide pore size distributions. The total BET surface areas of the solids ranges from 328 to 475 m^2g^{-1} with microporous surface area of 60-161 m^2g^{-1} and pore volumes of 0.53-1.02 cm^3g^{-1} . The heterogeneous catalysts **8a** and **8b** show exceptionally high activity and enantioselectivity in the hydrogenation of aromatic ketones, **10**. With 0.1 mol % of catalyst **8a** enantioselectivity up to 99% has been achieved. Interestingly, these porous binaphthol derived Zr phosphonate catalysts provide enantioselectivity superior to that of the parent homogeneous counterpart, the binap/RuCl₂/dppe (dppe = 1,2-diphenylethylenediamine) system developed by Noyori *et al.*¹² The two other catalysts **9a** and **9b** are also used for the asymmetric hydrogenation of β -keto esters (**12**) with good enantioselectivities.



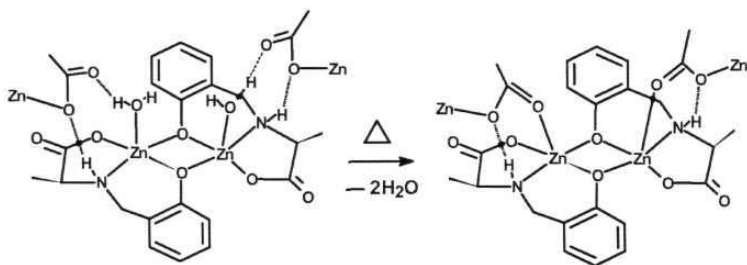
Scheme 3



Scheme 4

1.2.3. Homochiral porous MOF's constructed from chiral reduced Schiff base ligands

Transition metal complexes with chiral Schiff base ligands are known for some time and found applications towards asymmetric catalysis,¹³ nonlinear optics¹⁴ and supramolecular chemistry.¹⁵ Recently tremendous research efforts have been devoted to the synthesis and structural analysis of metal complexes with chiral reduced Schiff bases. Because of their greater flexibility generated by reduced Schiff base $-\text{CH}_2-\text{NH}-$ backbone and the influence of ligand chirality often leads to novel supramolecular networks by self assembly process.¹⁶ It is well known that, the conformational changes in flexible ligands coordinated to metal ions can generate different but closely related network architectures. The conformationally flexible reduced Schiff base ligands are ideal choice for this purpose.¹⁷ These metal complexes have also potential applications towards solid state conversion, DNA cleavage activity¹⁸ and in asymmetric catalysis.¹⁹



Scheme 5

Vittal and coworkers have reported an interesting example of 3D homochiral porous metal-organic framework using the chiral reduced Schiff base *N*-(2-hydroxybenzyl)-*L*-alanine (H_2sala).^{16a,16b,16c} Reaction of H_2sala with $\text{Zn}(\text{OAc})_2$ in presence of NaOH gave a crystalline powder, $[\text{Zn}_2(\text{Sala})_2(\text{H}_2\text{O})_2]$ (**14**). X-ray crystal analysis of this complex revealed that $\text{Zn}(\text{II})$ adopts distorted square pyramidal geometry and the apical position is occupied by a water molecules. These metal

coordinated water molecules are intermolecularly hydrogen bonded to carboxylate groups and a 3D hydrogen bonded network with chiral channels is produced (Figure 3). Topochemical conversion of these hydrogen bonded network generate porous 3D homochiral MOF $[\text{Zn}\{(\text{sala})\}_n]$ (**15**) (Scheme 5; Figure 4). A homochiral 3D Cu(II) MOF that is isostructural to **15** was also obtained in a topochemical conversion. This work represents the “solid state supramolecular synthesis” of MOF. Same authors very recently reported an intriguing example of porous helical coordination polymer with water helical chains inside the channels.^{16h}

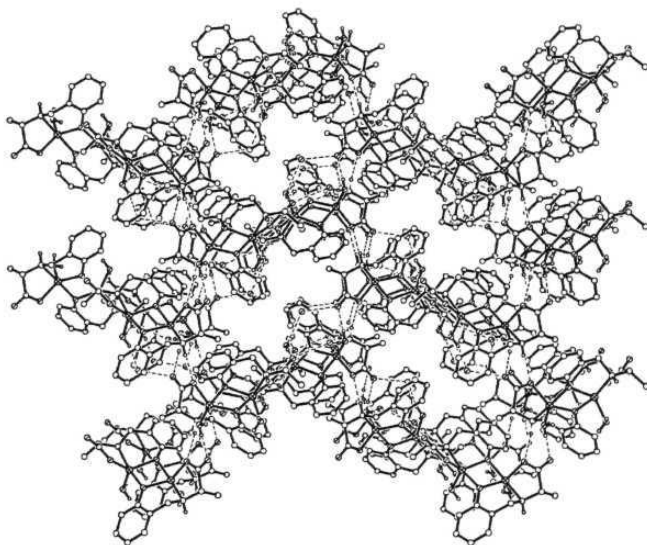


Figure 3. 3D Hydrogen bonded structure of $[\text{Zn}_2(\text{Sala})_2(\text{H}_2\text{O})_2]$ (**14**) with chiral channels.

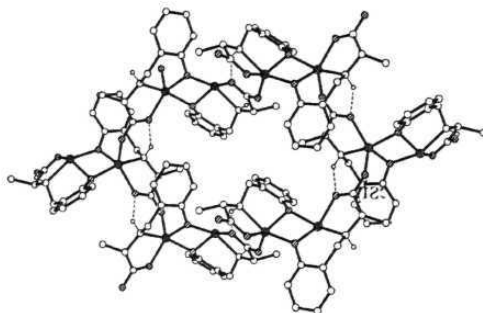


Figure 4. Molecular structure of $[Zn\{(sala)\}_n](15)$

Ray and coworkers recently reported a self-assembled chiral capsule of an octameric Cu(II) complex by using chiral reduced Schiff base N-(2-hydroxybenzyl)-L-histidine (H_2hist) (Figure 5). X-ray analysis shows that unit cell contains two slightly different cup shaped cyclic tetramers. These cyclic tetramers are on the top of each other, thus forming a capsule bound through eight hydrogen bonding interactions between the imidazole NH groups of one tetramer and nonbonded carboxylate-oxygen atoms of the other tetramer. This capsule has four guest pyridine molecules trapped inside the cavity, in which two of the pyridine molecules are held with a combination of hydrogen bonds and Cu(II) coordination.^{16g}

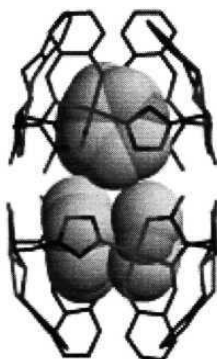


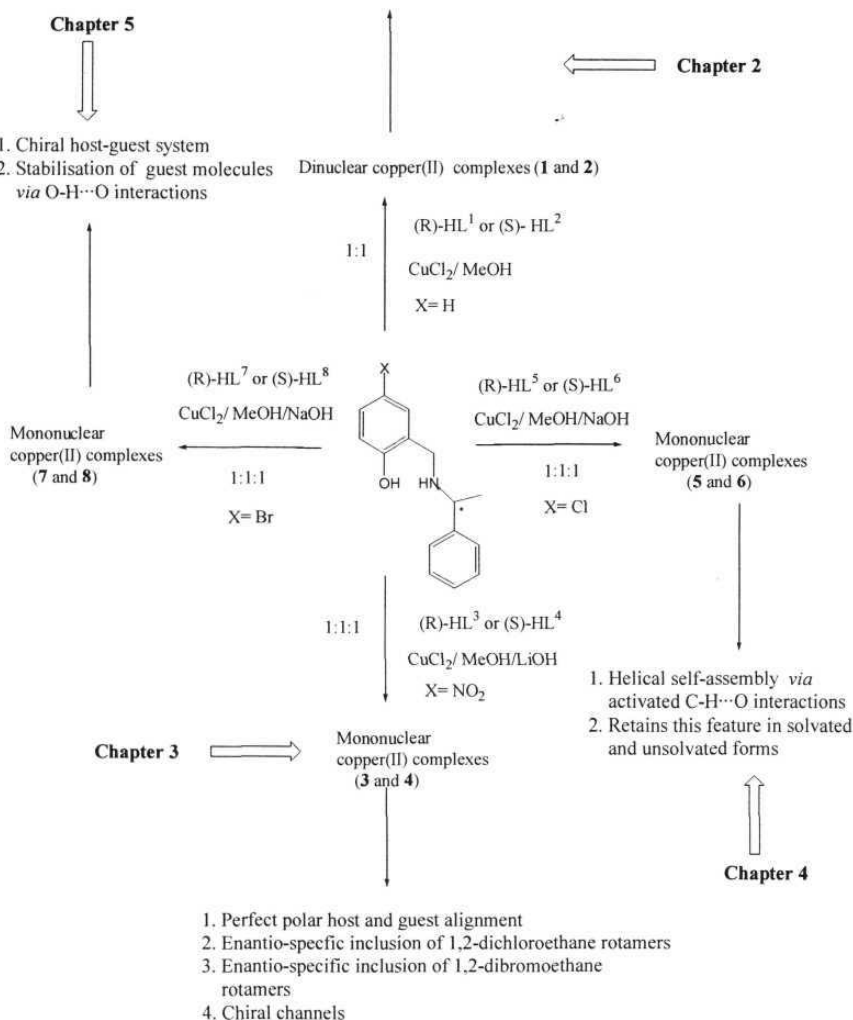
Figure 5. Chiral capsule

1.3. Aim of the present investigation

Due to the significant applications of organic and inorganic (or coordination polymers) porous materials in diverse fields, there have been extensive research attention towards design of new host-guest systems for practical applications. The organic porous solids are designed by considering molecular shape, symmetry, and intermolecular interactions such as hydrogen bonding, weaker halogen...halogen, electrostatic and van der Waals interactions.^{4b} On the other hand, inorganic porous solids are designed primarily by considering metal-ligand coordination, coordination geometry, chemical structure of the organic ligand, metal to ligand ratio, and the coordinating nature of the anions.^{5a,5c} Recently, significant research efforts have been devoted to combine the above two approaches.^{4e,f} Although numerous chiral porous materials are known with hydrogen bonded organic and metal-organic frameworks, there has been shortage of chiral porous solids with organic-inorganic hybrid materials assembled through hydrogen bonds.

While some metal complexes of Schiff bases derived from salicylaldehyde and (R) or (S) α -methylbenzylamine are known,²⁰ no complex of its reduced analogues is reported. We have attempted to synthesize and structurally characterize the copper(II) complexes with bidentate chiral reduced Schiff bases HL¹ to HL⁸. Hydrogen bonding capability and patterns of these ligands play a key role in the formation of various types of molecular assemblies. The results and interesting features are summarized in Scheme 6. The details of these investigations form the subject matter of this thesis.

1. Selective inclusion of chloroalkanes
2. Enantio-specific inclusion of chiral 1,2-dichloroethane rotamers
3. Chiral voids



Scheme 6

1.4. References

- (a) Q. Huo, D. Margolese, U. Ciesla, P. Feng, T. Gier, P. sieger, R. Leon, P. Petroff, F. Schuth and G. Sucky, *Nature*, **1994**, 368, 317; (b) C. Dresge, M. Leonowicz, W. Roth, J. Vartuli and J. Beck, *Nature*, **1992**, 359, 710; (c) M. Davis, C. Saldarriaga, C. Montes, J. Graces and C. Crowder, *Nature*, **1988**, 331, 698; (d) M. Estermann, L. McCusker, C. Baerlocher, A. Merrouche and H. Kessler, *Nature*, **1991**, 352, 320.
- (a) D. W. Breck, *Zeolite molecular Sieves, structure, chemistry, and use*, Wiley, New York, **1974**; (b) R. Szostak, *Molecular Sieves Van Nostand Reinhold*, New York, **1989**; (c) G. Gottardi and E. Galli, *Natural Zeolites*, Springer-Verlag, Berlin, **1985**.
- B. Kesanli and W. Lin, *Coord. Chem. Rev.*, **2003**, 246, 305.
- (a) L. Bramer, *Chem. Soc. Rev.*, **2004**, 32, 476; (b) G. R. Desiraju, *Crystal Engeneering: The Design of Organic Solids*, Elsevier, Amsterdam, **1989**; (c) J.-M. Lehn, *Angew. Chem. Int. Ed. Engl.*, **1990**, 29, 1304; (d) B. Moulton and M. J. Zaworotko, *Chem. Rev.*, **2001**, 101, 1629; (e) A. M. Beatty, *Coord. Chem. Rev.*, **2003**, 246, 131; (f) A. M. Beatty, *CrystEngComm*, **2001**, 51, 1.
- (a) M. J. Zaworotko, *Angew. Chem. Int. Ed.*, **2000**, 39, 3052; (b) M. Eddaoudi, D. B. Moler, H. Li, B. Chen, T. M. Reineke, M. O'Keeffe and O. M. Yaghi, *Acc. Chem. Res.*, **2001**, 34, 319; (c) O. M. Yaghi, H. Li, C. Davis, D. Recharson and L. Groy, *Acc. Chem. Res.*, **1998**, 31, 474; (d) B. F. Abrahams, B. F. Hoskins, D. M. Michail and R. Robson, *Nature*, **1994**, 369, 727; (e) O. M. Yaghi, G. M. Li and H. L. Li, *Nature*, **1995**, 378, 703; (f) S. Noro, S. Kitagawa, M. Kondo and K. Seki, *Angew. Chem. Int. Ed.*, **2000**, 39, 2081; (g) J. L. C. Rowsell, A. R. Millward, K. S. Park and O. M. Yaghi, *J. Am. Chem. Soc.*, **2004**, 126, 5666; (h) M. Fugita, Y.-J. Kwon, S. Washizu and K. Ogura, *J. Am. Chem. Soc.*, **1994**, 116, 1151.
- (a) X. X. Zhang, J. S. Bradshaw and R. M. Izatt, *Chem. Rev.*, **1997**, 97, 3313; (b) E. Brunet, *Chirality*, **2002**, 14, 135; (c) L. Pérez-García and D. B.

- Amabilino, *Chem. Soc. Rev.*, **2002**, 31, 342; (d) L.-X. Dai, *Angew. Chem. Int. Ed.*, **2004**, 43, 5726; (e) M. A. Mateos-Timoneda, M. Crego-Calama and D. N. Reinhoudt, *Chem. Soc. Rev.*, **2004**, 33, 363; (f) R.-G. Xiong, X.-Z. You, B.F. Abrahams, Z.-L. Xue and C.-M. Che, *Angew. Chem. Int. Ed.*, **2001**, 40, 4422.
7. (a) O. R. Evans and W. B. Lin, *Acc. Chem. Res.*, **2002**, 35, 511; (b) E. Q. Gao, S. Q. Bai, Z. M. Wang and C. H. Yan, *J. Am. Chem. Soc.*, **2003**, 125, 4984; (c) L. Han, M. C. Hong, R. H. Wang, J. H. Luo, Z. Z. Lin and D. Q. Yuan, *Chem. Commun.*, **2003**, 2580; (d) M. A. Withersby, A. J. Blake; N. R. Champness, P. Hubberstey and M. Schroder, *Angew. Chem. Int. Ed.*, **1997**, 36, 2327; (e) S. R. Batten, B. F. Hoskins and R. Robson, *Angew. Chem. Int. Ed.*, **1997**, 36, 636.
8. T. Ezuhara, K. Endo and Y. Aoyama, *J. Am. Chem. Soc.*, **1999**, 121, 3279.
9. A. Jouaiti, M. W. Hosseini and N. Kritsakas, *Chem. Commun.*, **2003**, 1388.
10. J. S. Seo, D. Whang, H. Lee, S. I. Jun, J. Oh, Y. J. Jeon and K. Kimoon, *Nature*, **2000**, 404, 982.
11. (a) Y. Cui, L. H. Ngo and W. Lin, *Chem. Commun.*, **2003**, 1388; (b) Y. Cui, L. H. Ngo, P. S. White and W. Lin, *Inorg. Chem.*, **2003**, 42, 652; (c) Y. Cui, L. H. Ngo, P. S. White and W. Lin, *Chem. Commun.*, **2003**, 994; (d) O. R. Evans, D. R. Manke and W. Lin, *Chem. Mater.*, **2002**, 14, 3866; (e) Y. Cui, O. R. Evans, L. H. Ngo, P. S. White and W. Lin, *Angew. Chem. Int. Ed.*, **2002**, 41, 1159; (f) Y. Cui, L. H. Ngo, P. S. White and W. Lin, *Chem. Commun.*, **2002**, 1666; (g) H. L. Ngo and W. Lin, *J. Am. Chem. Soc.*, **2002**, 124, 14298; (h) Y. Cui, S. J. Lee and W. Lin, *J. Am. Chem. Soc.*, **2003**, 125, 6014; (i) O. R. Evans, H. L. Ngo and W. Lin, *J. Am. Chem. Soc.*, **2001**, 123, 10395; (j) A. Hu, H. L. Ngo and W. Lin, *J. Am. Chem. Soc.*, **2003**, 125, 11490; (k) A. Hu, H. L. Ngo and W. Lin, *Angew. Chem. Int. Ed.*, **2004**, 43, 1043; (l) A. Hu, H. L. Ngo and W. Lin, *Angew. Chem. Int. Ed.*, **2004**, 43, 6000.
12. T. Ohkuma and R. Noyori, *Angew. Chem. Int. Ed.*, **2001**, 40, 40.
13. (a) E. N. Jacobson, in Ojima (Ed.), *Catalytic asymmetric Synthesis*, VCH, New York, **1993**; (b) E. N. Jacobson, in E. W. Abel, F. G. A. Stone, G. Wilkinson

- (Eds), *Comprehensive Organometallic Chemistry II*, Vol. 12, Pergamon, New York, **1995**; (c) E. N. Jacobson, W. Zhang, A. R. Muci, J. R. Ecker and L. Deng, *J. Am. Chem. Soc.*, **1991**, 113, 7063; (d) F. Fache, E. Schulz, M. L. Tommasino and M. Lemaire, *Chem. Rev.*, **2000**, 100, 2159; (e) T. Nagata, K. Yoroze, T. Yamada and T. Mukaiyama, *Angew. Chem. Int. Ed.*, **1995**, 34, 2145; (f) T. Nagata, K. Sugi, T. Yamada and T. Mukaiyama, *Synlett.*, **1996**, 1076; (g) R. I. Kureshy, N.H. Khan, S. H. R. Abdi, P. Iyer and A. K. Bhatt, *J. Mol. Catal., A.*, **1997**, 120, 101; (h) R. I. Kureshy, N. H. Khan, S. H. R. Abdi, P. Iyer and A. K. Bhatt, *J. Mol. Catal., A.*, **1997**, 121, 25; (i) R. I. Kureshy, N. H. Khan, S. H. R. Abdi, P. Iyer and A. K. Bhatt, *J. Mol. Catal., A.*, **1998**, 130, 41; (j) A. H. Vetter and A. Berkessel, *Tetrahedron Lett.*, **1998**, 39, 1741; (J) M. Hayshi, T. Inoue, Y. Miyamoto and N. Oguni, *Tetrahedron*, **1994**, 50, 4385; (k) P. Weidong, F. Xiaoming, G. Liuzhu, H. Wenhao, L. Zhi, M. Aiqiao and J. Yaozhong, *Synlett.*, **1996**, 337; (l) J. Yaozhong, G. Liuzhu, F. Xiaoming, H. Wenhao, P. Weidong, L. Zhi and M. Aiqiao, *Tetrahedron*, **1997**, 53, 14327; (m) N. Oguni, K. Tanaka and H. Ishida, *Synlett.*, **1998**, 601; (n) Z. Li, G. Liu, Z. Zheng and H. Chen, *Tetrahedron*, **2000**, 56, 7187; (o) L. Canali and D. C. Sherrington, *Chem. Soc. Rev.*, **1999**, 28, 85.
14. (a) F. Aveseng, P. G. Lacroix, I. Malfant, F. Dahan and K. Nakatani, *J. Mater. Chem.*, **2000**, 10, 1013; (b) G. Lenoble, P. G. Lacroix, J. C. Daran, S. D. Bella and K. Nakatani, *Inorg. Chem.*, **1998**, 37, 2158; (c) S. D. Bella, I. Fragala, I. Ledoux and T. J. Marks, *J. Am. Chem. Soc.*, **1995**, 117, 9481; (d) F. Aveseng, P. G. Lacroix, I. Malfant, G. Lenoble, P. Cassoux, K. Nakatani, I. Maltey-Fanton, J. A. Delare and A. Aukauloo, *Chem. Mater.*, **1999**, 11, 995; (e) F. Aveseng, P. G. Lacroix, I. Malfant, N. Perisse, C. Lepetit and K. Nakatani, *Inorg. Chem.*, **2001**, 40, 3797; (f) C. Evans and D. Luneau, *J. Chem. Soc., Dalton Trans.*, **2002**, 83; (g) S. R. Korupoju, N. Magayakarasi, S. Ameerunisha and P. S. Zacharias, *J. Chem. Soc., Dalton Trans.*, **2000**, 2845.

15. (a) S. G. Telfer, T. Safo, T. Harada, R. Kuroda, J. Lefebvre and D. B. Lenzhoff, *Inorg. Chem.*, **2004**, 43, 6168; (b) A. Fragosio, M. L. Kahn, A. Castineiras, J. P. Sutter, O. Kahn and R. Cao, *Chem. Commun.*, **2000**, 1547; (c) J. Hamblin, L. J. Childs, N. W. Alcock and M. J. Hannon, *J. Chem. Soc., Dalton Trans.*, **2002**, 164; (d) G. C. V. Stain, H. V. Poel, G. V. Koten, A. L. Spek, A. J. Dulsenberg and P. S. Pregosin, *J. Chem. Soc., Chem Commun.*, **1980**, 1016; (e) M. A. Masood, E. J. Enemark and T. D. P. Stack, *Angew. Chem. Int. Ed.*, **1998**, 37, 928; (f) V. Amendola, L. Fabbrizzi, L. Glanelli, C. Maggi, C. Mangano, P. Pallavicini and M. Zema, *Inorg. Chem.*, **2001**, 40, 3579.
16. (a) J. D. Ranford, J. J. Vittal and D. Wu, *Angew. Chem. Int. Ed.*, **1998**, 37, 1114; (b) J. D. Ranford, J. J. Vittal, D. Wu and X. Yang, *Angew. Chem. Int. Ed.*, **1999**, 38, 3498; (c) J. J. Vittal and X. Yang, *Cryst. Growth Des.*, **2002**, 2, 259; (d) C. T. Yang, B. Moubaraki, K. S. Murray, J. D. Ranford and J. J. Vittal, *Inorg. Chem.*, **2001**, 40, 5934; (e) C. T. Yang, B. Moubaraki, K. S. Murray and J. J. Vittal, *Dalton Trans.*, **2003**, 880; (f) C. T. Yang, M. Vetrivelan, X. Yang, B. Moubaraki, K. S. Murray and J. J. Vittal, *Dalton Trans.*, **2004**, 113; (g) M. A. Alam, M. Nethaji and M. Ray, *Angew. Chem. Int. Ed.*, **2003**, 42, 1940; (h) B. Sreenivasulu and J. J. Vittal, *Angew. Chem. Int. Ed.*, **2004**, 43, 5769.
17. B. Sreenivasulu and J. J. Vittal, *Cryst. Growth. Des.*, **2003**, 3, 635.
18. S. R. Korupoju, N. Magayakarasi, P. S. Zacharias, J. Mijuthani and H. Nishihara, *Inorg. Chem.*, **2002**, 41, 4099.
19. J. Gao, J. H. Reibenspies and A. E. Martell, *Angew. Chem. Int. Ed.*, **2003**, 42, 6008.
20. (a) H. Brunner, T. Zwack, M. Zabel, W. Beck and A. Bohm, *Organometallics.*, **2003**, 22, 1741; (b) H. Brunner, H. Oeschey and B. Nuber, *Inorg. Chem.*, **1995**, 34, 3349; (c) H. Brunner, H. Oeschey and B. Nuber, *J. Chem. Soc., Dalton Trans.*, **1996**, 1499; (d) H. Brunner, A. Kollnberger, T.

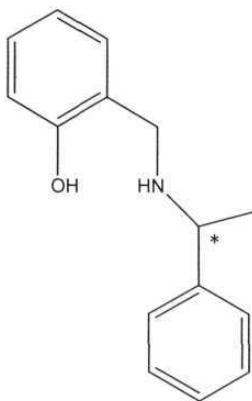
Burgemeister and M. Zabel, *Polyhedron*, **2000**, 19, 1519; (e) H. Brunner, A. Kollnberger and M. Zabel, *Polyhedron*, **2003**, 22, 2639; (f) S. K. Mandal and A. R. Chakravarty, *J. Chem. Soc., Dalton Trans.*, **1992**, 1627; (g) S. K. Mandal and A. R. Chakravarty, *J. Organomet. Chem.*, **1991**, 417, c59; (h) M. L. Loza, J. Parr and A. M. Z. Salwin, *Polyhedron*, **1997**, 16, 2321; (i) H. Brunner, M. Neimetz and M. Zabel, *Z. Natureforsch. B: Chem Sci.*, **2000**, 55, 145; (j) S. K. Mandal and A. R. Chakravarty, *Inorg. Chem.*, **1993**, 32, 3851; (k) H. Brunner, H. Oeschey and B. Nuber, *Angew. Chem. Int. Ed.*, **1994**, 33, 866; (l) H. Sakiyama, H. Okawa, N. Matsumoto and S. Kida, *J. Chem. Soc., Dalton Trans.*, **1990**, 2935; (m) C. Evans and D. Luneau, *J. Chem. Soc., Dalton Trans.*, **2002**, 83; (n) H. Sakiyama, H. Okawa, N. Matsumoto and S. Kida, *Bull. Chem. Soc. Jpn.*, **1991**, 64, 2644; (o) H. Yang, M. A. Khan and K. M. Nicholas, *J. Chem. Soc., Chem. Commun.*, **1992**, 210; (p) H. Yang, M. A. Khan and K. M. Nicholas, *Organometallics*, **1993**, 12, 3485; (q) R. K. Rath, M. Netaji and A. R. Chakravarty, *Polyhedron*, **2000**, 21, 1929.

Synthesis of the enantiomers of a chiral dinuclear copper(II) complex: Selective inclusion of chlorinated solvents and enantio-specific inclusion of chiral 1,2-dichloroethane rotamers in the crystal lattice**2.1. Abstract**

New phenoxy bridged dinuclear copper(II) complexes, $[\text{Cu}_2\text{Cl}_2\text{L}^n_2]$ (**1** ($n = 1$) and **2** ($n = 2$)) have been synthesized using chiral reduced Schiff bases N-(2-hydroxybenzyl)-(R)- α -methylbenzylamine (HL^1) and N-(2-hydroxybenzyl)-(S)- α -methylbenzylamine (HL^2) (H represents dissociable phenolic proton). X-ray crystallographic studies reveal that these complexes can act as good chiral hosts which can enantioselectively accommodate chiral rotamers of 1,2-dichloroethane. The host-guest compounds **1**· CHCl_3 , **2**· CHCl_3 , **1**· $\text{C}_2\text{H}_4\text{Cl}_2$ and **2**· $\text{C}_2\text{H}_4\text{Cl}_2$ crystallize in orthorhombic space group $P2_12_12_1$, whereas **1**· CH_2Cl_2 and **2**· CH_2Cl_2 crystallize in monoclinic space group $P2_1$. In both dinuclear complexes (**1** and **2**) the metal centres are in distorted square-planar geometry and each copper is coordinated by NO_2Cl donor sets provided by one secondary amine nitrogen atom, two bridging phenoxide oxygen atoms and one chloride. Interestingly, the tetrahedral distortions of the square-planar geometry in **1** and **2** are of opposite chirality. In the crystal lattice of **1**·(*P*)- $\text{C}_2\text{H}_4\text{Cl}_2$ and **2**·(*M*)- $\text{C}_2\text{H}_4\text{Cl}_2$, self-assembly *via* intermolecular hydrogen bonding interactions leads to the enantio-selective confinement of chiral rotamers of 1,2-dichloroethane.

2.2. Introduction

Inclusion compounds of guest molecules with various host molecules are useful as media for the molecular recognitions and selective reactions in the solid state.¹ Inclusion compounds are formed by the non-covalent insertion of guest molecules into the host lattice during the crystallization process. Several factors, such as hydrophobic effects, van der Waals and dispersive forces, as well as much stronger ionic and hydrogen bond interactions play a key role in the formation of inclusion compounds.² Importance of chirality in chemical and biological systems is well known. Recently tremendous research efforts have been devoted to careful control of chirality at the molecular and supramolecular levels.³ The separation of enantiomers by using the inclusion phenomenon was known for long time and proven as one of the successful strategies.⁴ This is powerful in many cases and further development of this method is being pursued not only in research laboratories but also in industry. Recently, the enantiocontrol of photocyclization reactions has been studied by using chiral crystalline inclusion compounds.⁵ Other than very few metal-organic host systems,⁶ most of the enantioselective inclusions have been carried out using pure organic chiral host materials.² In this chapter we have discussed the inclusion properties of the enantiomeric pair of complexes $[\text{Cu}_2\text{L}^1_2\text{Cl}_2]$ (**1**) and $[\text{Cu}_2\text{L}^2_2\text{Cl}_2]$ (**2**) with conformationally flexible chiral reduced Schiff bases N-(2-hydroxybenzyl)-(R)- α -methylbenzylamine (HL^1) and N-(2-hydroxybenzyl)-(S)- α -methylbenzylamine (HL^2). These complexes are found to be good flexible hosts, which can accommodate chloro solvents such as dichloromethane, chloroform and 1,2-dichloroethane *via* weak C-H \cdots Cl interactions. Enantio-selective isolation of the right handed (*P*) and the left-handed (*M*) *gauche* form of 1,2-dichloroethane rotamers has been realized in the host lattices formed by **1** and **2**, respectively.



HL¹ = N-(2-hydroxybenzyl)-(R)-α-methylbenzylamine

HL² = N-(2-hydroxybenzyl)-(S)-α-methylbenzylamine

2.3. Experimental

2.3.1. Materials

All commercially available chemicals and the solvents utilized in this work were of analytical grade and were used as obtained. The chemicals and the sources are as follows: Salicylaldehyde, (R)-α-methylbenzylamine and (S)-α-methylbenzylamine, sodium borohydride, Lancaster (England); CDCl₃, methanol, dichloromethane, chloroform, 1,2-dichloroethane, Acros (India); CuCl₂·2H₂O, anhydrous sodium sulphate, S. D. Fine Chem. Ltd. (India).

2.3.2. Physical measurements

Elemental analysis was carried out on a Perkin-Elmer 240C CHN analyzer. Infrared spectra were collected by using KBr pellets on a Jasco-5300 FT-IR spectrophotometer. NMR spectra were recorded on a Bruker ACF-200 spectrometer. A Shimadzu 3101-PC UV/vis/NIR spectrophotometer was used to record the electronic spectra. X-ray crystallographic experiments were performed using a

Bruker-Nonius SMART APEX CCD single crystal diffractometer. A Sherwood scientific magnetic susceptibility balance was used to measure the magnetic moments.

2.3.3. Synthesis of the reduced Schiff bases and the complexes

(a) N-(2-hydroxybenzyl)-(R)- α -methyl benzyl amine, HL¹

A methanol solution (30 ml) of salicylaldehyde (1.22 g, 10 mmol) was added to a methanol solution (30 ml) of (R)- α -methylbenzylamine (1.21 g, 10 mmol) and stirred at room temperature for ½ h. To the resulting yellow solution 0.74 g (20 mmol) of NaBH₄ was added and the mixture was stirred for another ½ h until a colourless solution was obtained. The reaction mixture was evaporated to dryness on a rotary evaporator followed by addition of 100 ml of water. The solid suspended in water was extracted with (2 x 30 ml) CH₂Cl₂. The CH₂Cl₂ extracts were dried over anhydrous Na₂SO₄ and then evaporated to dryness. The compound (HL¹) was obtained in the form of colourless liquid.

Yield	: 1.7 g, (75%)
M. F.	: C ₁₅ H ₁₇ NO
IR (ν cm ⁻¹ , KBr pellet)	: 3292
¹ H NMR (CDCl ₃ , δ , ppm)	: 1.50 (d, 3H, CH ₃), 3.70 and 3.93(2H, CH _A H _B), ~3.81(q, 1H, CH(CH ₃)), 6.77 (d, 1H, <i>ortho</i> to phenolic-OH), 6.86 (d, 1H, <i>ortho</i> to methylene group), 7.19(m, 2H, phenyl protons), 7.27-7.40 (m, 5H, phenyl protons)
Anal. calcd. for C ₁₅ H ₁₇ NO	: C, 79.26; H, 7.54; N, 6.16.
Found	: C, 79.02; H, 7.67; N, 6.25.

(b) N-(2-Hydroxybenzyl)-(S)- α -methyl benzyl amine, HL²

HL² was prepared in similar yield by following the same procedure as described for HL¹ using (S)- α -methylbenzylamine instead of (R)- α -methylbenzylamine.

Yield	: 1.7g, (75%)
-------	---------------

M. F.	: C ₁₅ H ₁₇ NO
IR (ν cm ⁻¹ , KBr pellet)	: 3292
¹ H NMR (CD ₃ CN, δ , ppm)	: 1.50 (d, 3H, CH ₃), 3.70 and 3.93(2H, CH _A H _B), ~ 3.81(q, 1H, CH(CH ₃)), 6.77 (d, 1H, <i>ortho</i> to phenolic- OH), 6.86 (d, 1H, <i>ortho</i> to methylene group), 7.19(m, 2H, phenyl protons), 7.27-7.40 (m, 5H, phenyl protons)
Anal. calcd. for C ₁₅ H ₁₇ NO	: C, 79.26; H, 7.54; N, 6.16.
Found	: C, 79.14; H, 7.71; N, 6.22.

(c) [Cu₂L¹Cl₂] (1): A methanol solution (10 ml) of CuCl₂·2H₂O (0.177 g, 1 mmol) was added to a methanol solution (20 ml) of HL¹ (0.227 g, 1 mmol). The mixture was stirred at room temperature for 1 h. Dark brown solid precipitated was collected by filtration and washed with 10 ml of methanol. Yield: 0.39 g, (60%), Anal. calcd. for Cu₂C₃₀H₃₂N₂O₂Cl₂: C, 55.38; H, 4.96; N, 4.31. Found: 55.45, 5.02, 4.42. Selected infrared bands (cm⁻¹): 3244(m), 2976(w), 2930(w), 2874(w), 1597(s), 1572(m), 1485(s), 1452(s), 1383(w), 1256(s), 1229(w), 1198(w), 1155(w), 1109(m), 1088(w), 1059(w), 1034(w), 972(w), 943(w), 918(w), 876(s), 769(s), 752(s), 700(s), 653(w), 628(w), 590(m), 534(m), 462(m). Electronic spectral data in CHCl₃ (λ , nm (ϵ , M⁻¹cm⁻¹)): 650 sh (345), 430 (3,670), 336 sh (2,520), 268 (12,140). Effective magnetic moment at 298 K: 1.10 μ_B .

(d) [Cu₂L²Cl₂] (2): A methanol solution (10 ml) of CuCl₂·2H₂O (0.177 g, 1 mmol) was added to a methanol solution (20 ml) of HL² (0.227 g, 1 mmol). The mixture was stirred at room temperature for 1 h. Dark brown solid precipitated was collected by filtration and washed with 10 ml of methanol. Yield: 0.39 g, (60%), Anal. calcd. for Cu₂C₃₀H₃₂N₂O₂Cl₂: C, 55.38; H, 4.96; N, 4.31. Found: 55.53, 4.92, 4.36. Selected infrared bands (cm⁻¹): 3244(m), 2976(w), 2932(w), 2874(w), 1597(s), 1572(m), 1485(s), 1452(s), 1383(w), 1256(s), 1229(w), 1198(w), 1155(w), 1109(m), 1088(w), 1059(w), 1034(w), 972(w), 943(w), 918(w), 876(s), 769(s), 752(s), 700(s), 653(w),

628(w), 590(m), 534(m), 462(m). Electronic spectral data in CHCl_3 (λ , nm (ϵ , $\text{M}^{-1}\text{cm}^{-1}$)): 650 sh (353), 430 (4,200), 336 sh (2,990), 268 (13,930). Effective magnetic moment at 298 K: $1.11 \mu_{\text{B}}$.

2.3.4. X-ray crystallography

X-ray data were collected for dark brown crystals of $\mathbf{1} \cdot \text{CH}_2\text{Cl}_2$, $\mathbf{1} \cdot \text{CHCl}_3$, $\mathbf{1} \cdot \text{C}_2\text{H}_4\text{Cl}_2$, $\mathbf{2} \cdot \text{CH}_2\text{Cl}_2$, $\mathbf{2} \cdot \text{CHCl}_3$ and $\mathbf{2} \cdot \text{C}_2\text{H}_4\text{Cl}_2$ on a Bruker-Nonius SMART APEX CCD single crystal diffractometer using graphite monochromated $\text{Mo-K}\alpha$ radiation (0.71073 \AA). The SMART software was used for intensity data acquisition and the SAINT-Plus software⁷ was used for data extraction. In each case, absorption correction was performed with help of SADABS program.⁸ The SHELXTL package⁹ was used for structure solution and least-square refinement on F^2 . All the non hydrogen atoms were refined anisotropically. The secondary amine hydrogen atoms were located in a difference map and refined with geometric restraints. All other hydrogen atoms were included in the structure factor calculation by using a riding model. The ORTEP3¹⁰ and the PLATON¹¹ software were used for molecular graphics. The significant X-ray crystallographic data are given in Tables 1 and 2.

Table 1. Crystallographic data for **1**·CH₂Cl₂, **1**·CHCl₃ and **1**·C₂H₄Cl₂.

Compound	1 ·CH ₂ Cl ₂	1 ·CHCl ₃	1 ·C ₂ H ₄ Cl ₂
Molecular formula	C ₃₁ H ₃₄ Cl ₄ Cu ₂ N ₂ O ₂	C ₃₁ H ₃₃ Cl ₅ Cu ₂ N ₂ O ₂	C ₃₂ H ₃₆ Cl ₄ Cu ₂ N ₂ O ₂
Crystal dimensions / mm	0.15 x 0.28 x 0.48	0.32 x 0.37 x 0.11	0.32 x 0.36 x 0.24
Host-guest ratio	1: 1	1:1	1: 1
<i>T</i> /K	298	298	298
<i>M</i>	735.5	769.9	747.5
Crystal system	Monoclinic	Orthorhombic	Orthorhombic
Space group	<i>P</i> 2 ₁	<i>P</i> 2 ₁ 2 ₁ 2 ₁	<i>P</i> 2 ₁ 2 ₁ 2 ₁
<i>a</i> /Å	8.5479(6)	12.7319(6)	12.822(3)
<i>b</i> /Å	13.0697(9)	13.7805(7)	14.046(3)
<i>c</i> /Å	14.1650(9)	19.4266(100)	18.744(4)
α /°	90	90	90
β /°	90.9410(10)	90	90
γ /°	90	90	90
<i>V</i> /Å ³	1582.28(19)	3408.4(3)	3375.9(12)
<i>Z</i>	2	4	4
Observed reflections	7370	7958	7483
Parameters	378	387	387
Final <i>R</i> indices (<i>I</i> > 2σ(<i>I</i>))	0.0393, 0.1128	0.0516, 0.1327	0.0496, 0.1204
Goodness-of-fit on <i>F</i> ²	1.053	1.018	1.019
Largest hole and peak e/ Å ³	-1.168, 1.123	-0.832, 1.067	-0.646, 0.786

Table 2. Crystallographic data for **2**·CH₂Cl₂, **2**·CHCl₃ and **2**·C₂H₄Cl₂

Compound	2 ·CH ₂ Cl ₂	2 ·CHCl ₃	2 ·C ₂ H ₄ Cl ₂
Molecular formula	C ₃₁ H ₃₄ Cl ₄ Cu ₂ N ₂ O ₂	C ₃₁ H ₃₃ Cl ₅ Cu ₂ N ₂ O ₂	C ₃₂ H ₃₆ Cl ₄ Cu ₂ N ₂ O ₂
Crystal dimensions / mm	0.27 x 0.21 x 0.28	0.40 x 0.28 x 0.16	0.32 x 0.37 x 0.07
Host-guest ratio	1: 1	1:1	1: 1
<i>T</i> /K	298	298	298
<i>M</i>	735.5	769.9	749.5
Crystal system	Monoclinic	Orthorhombic	Orthorhombic
Space group	<i>P</i> 2 ₁	<i>P</i> 2 ₁ 2 ₁ 2 ₁	<i>P</i> 2 ₁ 2 ₁ 2 ₁
<i>a</i> /Å	8.5359(6)	12.7250(7)	12.7982(13)
<i>b</i> /Å	13.0565(10)	13.7785(8)	14.0366(14)
<i>c</i> /Å	14.1597(10)	19.4192(11)	18.7009(19)
<i>α</i> /°	90	90	90
<i>β</i> /°	90.9540(10)	90	90
<i>γ</i> /°	90	90	90
<i>V</i> /Å ³	1577.9(2)	3404.8(3)	3359.5(6)
<i>Z</i>	2	4	4
Observed reflections	7305	7833	7860
Parameters	378	387	387
Final <i>R</i> indices (<i>I</i> > 2σ(<i>I</i>))	0.0403, 0.1162	0.0499, 0.1263	0.0493, 0.1229
Goodness-of-fit on <i>F</i> ²	1.056	0.968	1.057
Largest hole and peak <i>e</i> / Å ³	-1.298, 1.151	-0.799, 1.156	-0.777, 0.951

2.4. Results and discussion

2.4.1. Synthesis and some properties

Unsubstituted chiral reduced Schiff bases HL^1 and HL^2 are prepared by condensation of salicylaldehyde with (R)- or (S)- α -methylbenzylamine followed by reduction with sodiumborohydride in methanol. The elemental analysis and spectral (infrared and proton NMR) data for HL^1 and HL^2 are very similar and consistent with the expected molecular formula and structure. The infrared spectra of HL^1 and HL^2 show bands at $\sim 1589\text{ cm}^{-1}$ and at $\sim 3290\text{ cm}^{-1}$ corresponding to symmetric and asymmetric N—H stretching vibrations respectively. The ^1H NMR spectra of HL^1 - HL^2 display the methyl protons as a doublet at $\sim 1.50\ \delta$. The protons of the methylene group were observed as an AB type quartet centred at $\sim 3.87\ \delta$. The signal for the hydrogen atom attached to the chiral C-atom is expected to be quartet. A signal observed at $\sim 3.81\ \delta$ most likely belongs to this quartet. The remaining part buried under the δ_B signal of the AB type quartet observed due to the methylene group protons. A multiplet centred at $\sim 7.31\ \delta$ corresponding to five protons is assigned to the phenyl group bonded to the chiral C-atom. Two doublets each corresponding to a single proton are observed at 6.77 and 6.86 δ . The former is assigned to the proton *ortho* to the phenolic-OH and the latter is assigned to the proton *ortho* to the methylene group. Multiplets centred at $\sim 7.19\ \delta$ most probably correspond to the remaining two protons of this aromatic ring.

The reactions of HL^1 and HL^2 with $\text{CuCl}_2 \cdot 2\text{H}_2\text{O}$ in methanol (1:1 mole ratio) yielded dark brown microcrystalline complexes of formula $[\text{Cu}_2\text{L}^n\text{Cl}_2]$ (**1** or **2**). The elemental analysis and infrared spectral data for these complexes (**1** and **2**) are very similar and consistent with the expected molecular formula and structure. Representative chemical diagram of these complex molecules are shown in Figure 1. Room temperature (298 K) magnetic moments of **1** and **2** are 1.10 and 1.11 μ_B , respectively. These values suggest very strong antiferromagnetic spin coupling between the diphenoxy-bridged Cu(II) centres.

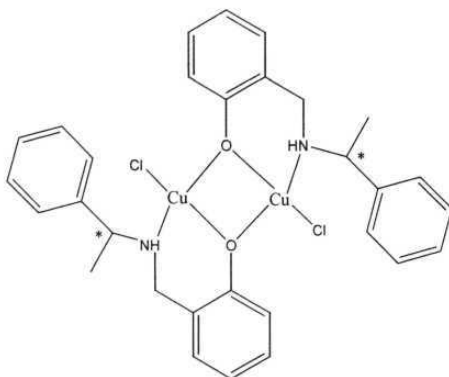


Figure 1. General molecular structure of the binuclear complexes.

The infrared spectra of these complexes show bands at 1597 cm^{-1} and 3244 cm^{-1} corresponding to symmetric and asymmetric stretching of the secondary amine N—H stretching vibrations, respectively. The peaks observed in the range of $2800\text{--}3000\text{ cm}^{-1}$ is most likely due to the aliphatic and aromatic C—H stretches. Electronic spectra of **1** and **2** in CHCl_3 solutions are essentially identical (Figure 2). The low intensity absorption at $\sim 650\text{ nm}$ is assigned to the d-d transition. The other intense bands observed in the range $430\text{--}268\text{ nm}$ are most likely due to ligand-to-metal charge transfer and intraligand transitions.

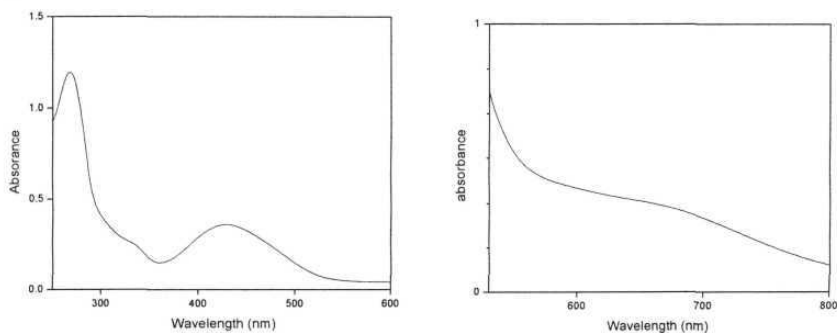


Figure 2. Electronic spectrum of **1** in CHCl_3 .

2.4.2. CSD search

A search for the crystal structures of complexes having formula $[\text{Cu}_2\text{L}_2\text{X}_2]$ (L = monobasic N,O-donor ligand, X = halide) was performed on the Cambridge Structural Database (November 2004 release). Search was restricted to only the phenoxy bridged dinuclear copper(II) complexes. Unexpectedly only eight structures were found with this type of coordination sphere.¹² In all the cases, the ligands are achiral bidentate Schiff base ligands and crystallized in centrosymmetric space groups. The Cu_2O_2 bridging unit is exactly planar for all the complexes because of the crystallographic centre of inversion at its centre. As we expected the torsion angles involving $\text{X}-\text{Cu}\cdots\text{Cu}-\text{X}$ are exactly 180° for all the complexes. This feature indicates the *trans* coordination arrangement of halogen atoms in these complexes. These search results encouraged us to study the X-ray structural features of $[\text{Cu}_2\text{L}^1_2\text{Cl}_2]$ (**1**) and $[\text{Cu}_2\text{L}^2_2\text{Cl}_2]$ (**2**).

2.4.3. Crystallization

Crystallization of the complexes $[\text{Cu}_2\text{L}^1_2\text{Cl}_2]$ (**1**) and $[\text{Cu}_2\text{L}^2_2\text{Cl}_2]$ (**2**) from various common solvents such as methanol, ethanol, acetonitrile, tetrahydrofuran and ethyl acetate found to be unsuccessful. Good quality single crystals for X-ray diffraction were readily obtained from chloroalkane solvents such as dichloromethane, chloroform and 1,2-dichloroethane. In all the cases, solvent molecules are included in 1:1 stoichiometric ratio. Recently, similar kind of highly selective encapsulation of dihalomethanes are reported for *myo*-inositol derivative.¹² Dichloromethane inclusion compounds (**1**· CH_2Cl_2 , **2**· CH_2Cl_2) crystallize in the monoclinic space group $P2_1$. Alternatively, both chloroform (**1**· CHCl_3 , **2**· CHCl_3) and 1,2-dichloroethane (**1**· $\text{C}_2\text{H}_4\text{Cl}_2$, **2**· $\text{C}_2\text{H}_4\text{Cl}_2$) inclusion compounds crystallize in the orthorhombic space group $P2_12_12_1$. All attempts to obtain solvent-free crystals of **1** and **2** were unsuccessful. Thus complexes **1** and **2** are found to provide chiral host frameworks which can accommodate chlorinated solvents.

2.4.4. Description of molecular structures

The field of stereoselective synthesis of coordination compounds using the chiral ligands has developed during the past decade at an increasing rate.¹⁴ To the date, most of the stereoselective synthesis of coordination compounds are limited to the helical chiral self-assembled architectures. Secondary amine N-atom of a reduced Schiff base is a prochiral centre. Metal ion coordination induces chirality to the nitrogen centre. Generally, but not in all the cases, the use of chiral ligand leads to stereo-specific chiral induction. The structures of the inclusion compounds described in this chapter reveal opposite absolute configurations of the chiral C- and N- centres. The S or sinister configuration of the N-centre is found in each of the inclusion compounds where the chiral C-centre is of R or rectus configuration. Similarly the N-centre in the inclusion compounds having S C-centre is found to R. Thus in both the cases the generation of the new chiral centre is heterogeneous. The absolute configurations of all these inclusion complexes are successfully confirmed by flack parameter values¹⁵ and details were given in the Table 3.

Table 3. Absolute configurations of **1**·CH₂Cl₂, **1**·CHCl₃, **1**·C₂H₄Cl₂, **2**·CH₂Cl₂, **2**·CHCl₃ and **2**·C₂H₄Cl₂

Complex	C(8), C(23) configuration	N(1), N(2) Configuration	Flack Parameter value
1 ·CH ₂ Cl ₂	R, R	S, S	0.007(11)
1 ·CHCl ₃	R, R	S, S	-0.014(17)
1 ·C ₂ H ₄ Cl ₂	R, R	S, S	0.026(17)
2 ·CH ₂ Cl ₂	S, S	R, R	0.022(12)
2 ·CHCl ₃	S, S	R, R	-0.029(16)
2 ·C ₂ H ₄ Cl ₂	S, S	R, R	-0.001(17)

The crystal structures of the inclusion compounds confirm the molecular structure shown in Figure 1 for both **1** and **2**. The structures of **1** and **2** are shown in Figure 3. The bond parameters associated with the metal ions are listed in Table 4. In the dimeric structure, the metal centres are tetra coordinated. The approximately square-planar NO₂Cl donor set for each metal centre is provided by one secondary

amine nitrogen atom, two bridging phenolate-oxygen atoms and one chloride. The Cu-Cl distances are within 2.2090(12) - 2.2189(13) Å. The Cu-O distances (1.939(3) - 1.985(3) Å) and the Cu-N distances (1.966(3) - 2.011(4) Å) are comparable to those found in similar complexes.¹² Metal-metal separation is in the range of 3.020-3.027 Å and the Cu-O-Cu bond angles are in the range of 100-103.5°. The molecular structures of **1** and **2** are mirror images of each other (Figure 3). As described in section 2.4.2, the Cu₂O₂ unit is planar due to the crystallographic inversion centre at its centre in structurally known phenoxy-bridged complexes of formula [Cu₂L₂X₂] where L is N,O- donor chelating ligand. As the ligands in **1** and **2** are chiral, both lack the inversion centre and the asymmetric unit contains a full complex molecule in each case. The Cu₂O₂ unit is folded along O1, O2 in both molecules. The fold angles are given in Table 5. The torsion angles involving Cl-Cu...Cu-Cl are 105°, 111°, 112°, 105.1°, 111.5° and 112° for **1**·CH₂Cl₂, **1**·CHCl₃, **1**·C₂H₄Cl₂, **2**·CH₂Cl₂, **2**·CHCl₃ and **2**·C₂H₄Cl₂, respectively. This feature indicates that due to the influence of chirality of the ligand the coordination arrangements for chlorine atoms are in between *cis* and *trans*. The complete structures of each pair of inclusion compounds with opposite chirality show the mirror image relationship. This feature is also extended to the basic coordination sphere in each pair. Mirror image relationships are shown in the Figures 4-6. There is no significant variation in the overall conformations of the dinuclear complex molecules in **1**·CHCl₃ and **1**·C₂H₄Cl₂. It may be noted that both crystallize in the *P*2₁2₁2₁ space group. However, the conformation of **1** in **1**·CH₂Cl₂ that crystallize in the *P*2₁ space group is quite different. The same is true for **2**·CH₂Cl₂ (space group *P*2₁), **2**·CHCl₃ and **2**·C₂H₄Cl₂ (space group *P*2₁2₁2₁). Overlay diagrams of the dinuclear complex molecules in the inclusion compounds of **1** and **2** are shown in Figure 7.

Table 4. Selected bond parameters for **1**·CH₂Cl₂, **1**·CHCl₃, **1**·C₂H₄Cl₂, **2**·CH₂Cl₂, **2**·CHCl₃ and **2**·C₂H₄Cl₂**Bond lengths (Å)**

Compound	1 ·CH ₂ Cl ₂	1 ·CHCl ₃	1 ·C ₂ H ₄ Cl ₂	2 ·CH ₂ Cl ₂	2 ·CHCl ₃	2 ·C ₂ H ₄ Cl ₂
Cu(1)–O(1)	1.944(2)	1.944(3)	1.939(3)	1.941(3)	1.942(3)	1.939(3)
Cu(1)–O(2)	1.965(2)	1.985(3)	1.974(3)	1.964(2)	1.981(3)	1.979(3)
Cu(1)–N(1)	1.993(3)	2.011(4)	2.004(4)	1.991(3)	2.010(4)	2.000(4)
Cu(1)–Cl(1)	2.2108(11)	2.2176(13)	2.2131(13)	2.2090(12)	2.2163(12)	2.2126(13)
Cu(1)–Cu(2)	3.0238(5)	3.0280(8)	3.0253(9)	3.0240(6)	3.0266(7)	3.0198(8)
Cu(2)–O(1)	1.920(2)	1.922(3)	1.926(3)	1.920(3)	1.921(3)	1.924(3)
Cu(2)–O(1)	1.963(2)	1.954(3)	1.961(3)	1.959(3)	1.951(3)	1.962(3)
Cu(2)–N(2)	1.967(3)	1.970(4)	1.978(4)	1.966(3)	1.971(3)	1.971(3)
Cu(2)–Cl(2)	2.2102(10)	2.2189(14)	2.2189(13)	2.2105(11)	2.2174(13)	2.2141(13)

Bond angles (°)

Compound	1 ·CH ₂ Cl ₂	1 ·CHCl ₃	1 ·C ₂ H ₄ Cl ₂	2 ·CH ₂ Cl ₂	2 ·CHCl ₃	2 ·C ₂ H ₄ Cl ₂
O(1)–Cu(1)–O(2)	76.65(10)	76.07(12)	76.44(13)	76.50(10)	75.95(11)	76.65(12)
O(1)–Cu(1)–N(1)	91.53(11)	91.00(16)	91.23(15)	91.56(13)	91.11(14)	91.42(15)
O(2)–Cu(1)–N(1)	167.41(11)	166.79(16)	166.95(15)	167.19(13)	166.72(15)	167.28(15)
O(1)–Cu(1)–Cl(1)	161.45(9)	164.92(12)	165.03(13)	161.51(10)	164.80(11)	164.96(13)
O(2)–Cu(1)–Cl(1)	100.40(8)	100.47(10)	100.47(10)	100.59(9)	100.61(9)	100.48(10)
N(1)–Cu(1)–Cl(1)	92.19(9)	92.72(14)	92.54(12)	92.20(11)	92.66(13)	92.18(12)
O(1)–Cu(1)–Cu(2)	38.23(7)	38.20(9)	38.35(10)	38.21(7)	38.17(8)	38.39(8)
O(2)–Cu(1)–Cu(2)	39.63(7)	39.37(9)	39.60(9)	39.52(8)	39.32(9)	39.78(9)
N(1)–Cu(1)–Cu(2)	129.35(9)	128.41(13)	128.99(11)	129.38(10)	128.51(12)	129.24(12)
Cl(1)–Cu(1)–Cu(2)	132.84(4)	133.69(4)	133.89(5)	132.90(4)	133.68(4)	133.95(4)
O(1)–Cu(2)–O(2)	77.24(10)	77.30(13)	77.05(13)	77.08(10)	77.12(12)	77.41(12)

O(1)-Cu(2)-N(2)	165.17(12)	167.55(17)	166.32(17)	165.14(12)	167.28(17)	166.49(17)
O(2)-Cu(2)-N(2)	93.25(11)	93.15(15)	92.90(14)	93.28(11)	93.26(14)	92.60(14)
O(1)-Cu(2)-Cl(2)	98.70(8)	97.85(11)	98.28(11)	98.75(9)	97.92(10)	98.05(11)
O(2)-Cu(2)-Cl(2)	153.36(9)	155.40(12)	156.11(11)	153.55(10)	155.58(11)	156.46(12)
N(2)-Cu(2)-Cl(2)	94.84(9)	94.12(13)	94.61(12)	94.85(10)	94.23(13)	94.69(12)
O(1)-Cu(2)-Cu(1)	38.78(7)	38.71(9)	38.65(9)	38.70(8)	38.65(8)	38.76(9)
O(2)-Cu(2)-Cu(1)	39.68(7)	40.12(9)	39.92(9)	39.63(7)	40.03(8)	40.20(8)
N(2)-Cu(2)-Cu(1)	132.93(9)	133.07(12)	132.72(11)	132.91(9)	133.11(11)	132.68(11)
Cl(2)-Cu(2)-Cu(1)	126.87(3)	126.46(4)	127.15(5)	126.90(3)	126.53(4)	127.12(4)
Cu(2)-O(1)-Cu(1)	102.98(11)	103.09(13)	103.00(16)	103.09(1)	103.18(12)	102.84(13)
Cu(2)-O(2)-Cu(1)	100.69(10)	100.50(14)	100.48(15)	100.85(11)	100.65(12)	100.01(12)

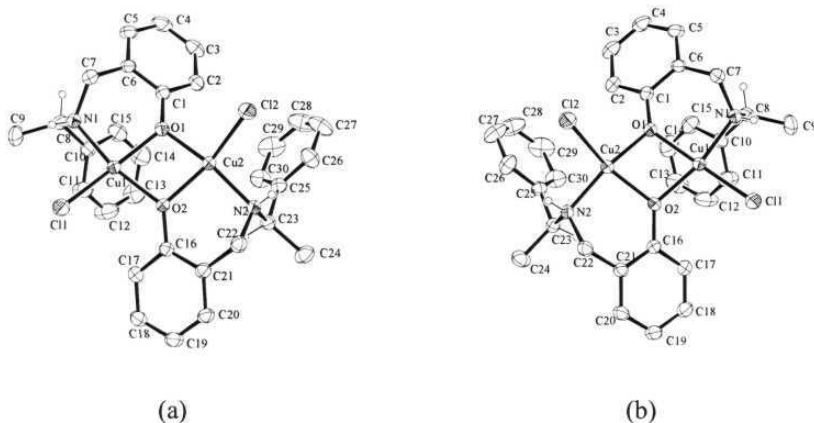


Figure 3. Molecular structures of (a) $[\text{Cu}_2\text{L}^1_2\text{Cl}_2]$ (**1**) and (b) $[\text{Cu}_2\text{L}^2_2\text{Cl}_2]$ (**2**) with the atom-labeling schemes. Hydrogen atoms other than the chiral center hydrogens are omitted for clarity. All non-hydrogen atoms are represented by their 30% probability thermal ellipsoids.

Table 5. Dihedral angle between the Planes defined by Cu1, O1, Cu2 and Cu1, O2, Cu2

Inclusion compound	Dihedral angle between the planes
1 ·CH ₂ Cl ₂	18.61 (0.09)
1 ·CHCl ₃	20.79 (0.14)
1 ·C ₂ H ₄ Cl ₂	20.74 (0.13)
2 ·CH ₂ Cl ₂	18.89 (0.09)
2 ·CHCl ₃	20.98 (0.13)
2 ·C ₂ H ₄ Cl ₂	20.89 (0.14)

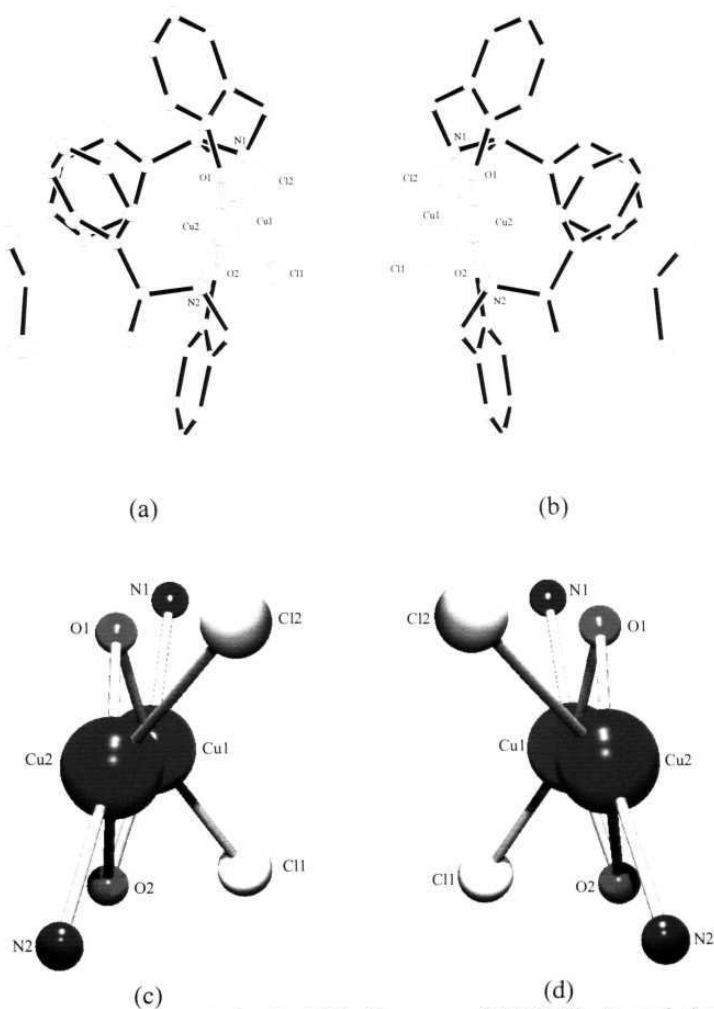


Figure 4. Structures and the $\text{Cu}_2\text{N}_2\text{O}_2\text{Cl}_2$ cores of $2 \cdot \text{CH}_2\text{Cl}_2$ (a and c) and $1 \cdot \text{CH}_2\text{Cl}_2$ (b and d).

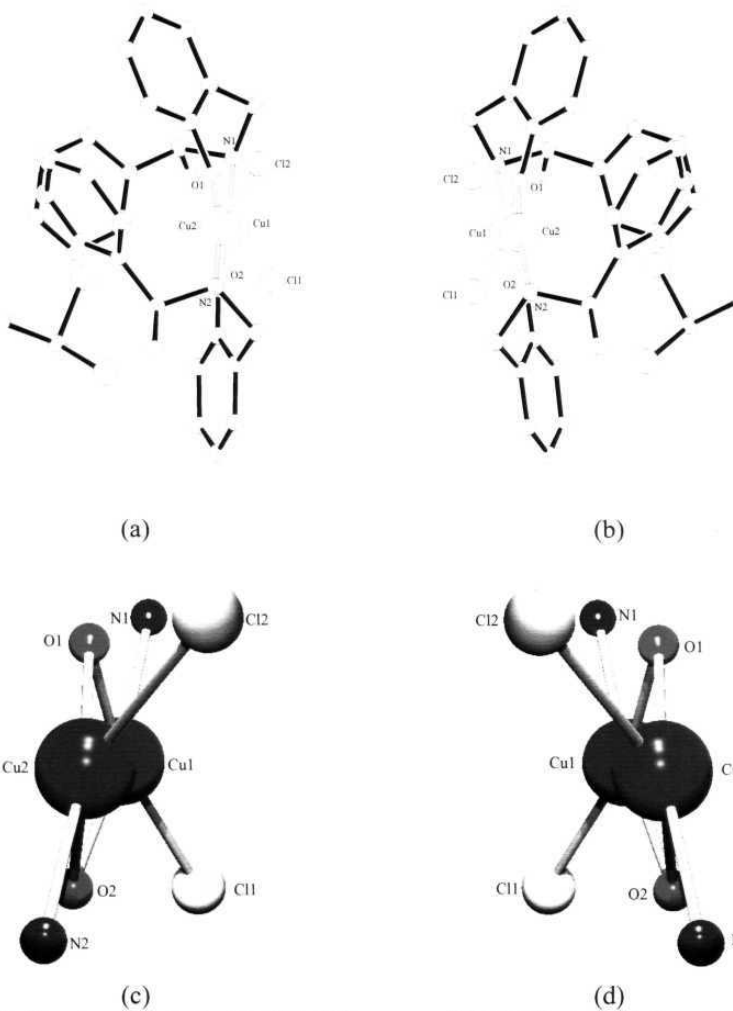


Figure 5. Structures and the $\text{Cu}_2\text{N}_2\text{O}_2\text{Cl}_2$ cores of $2 \cdot \text{CHCl}_3$ (a and c) and $1 \cdot \text{CHCl}_3$ (b and d).

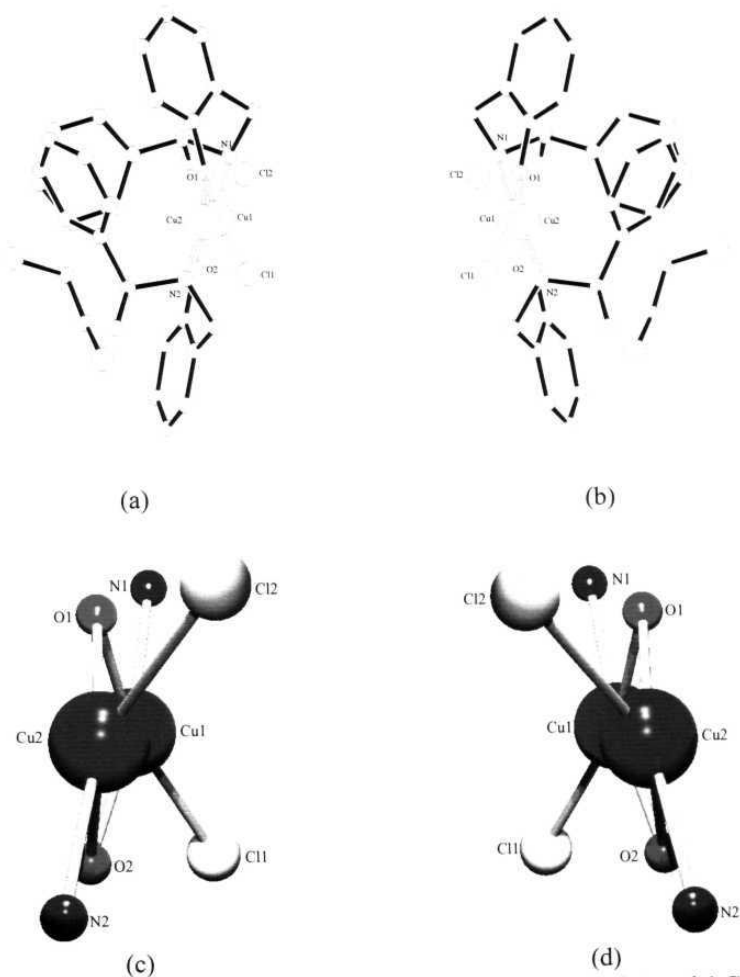


Figure 6. Structures and the $\text{Cu}_2\text{N}_2\text{O}_2\text{Cl}_2$ cores of $2 \cdot \text{C}_2\text{H}_4\text{Cl}_2$ (a and c) and $1 \cdot \text{C}_2\text{H}_4\text{Cl}_2$ (b and d).

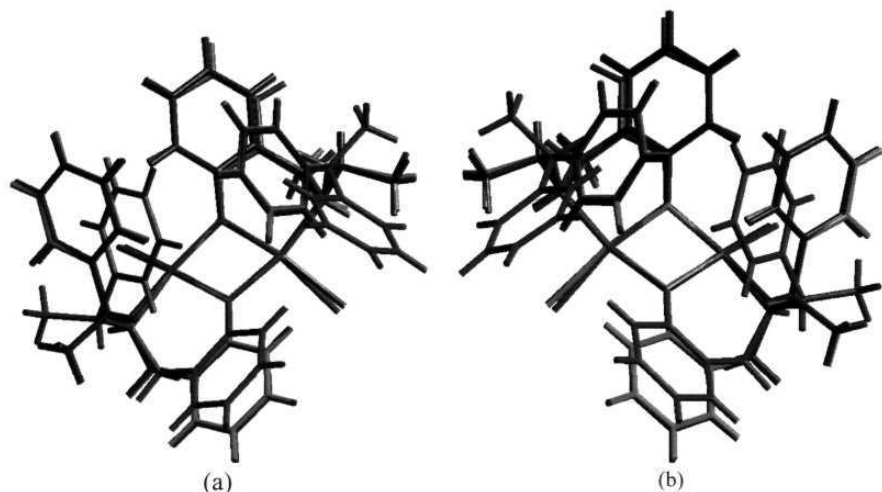


Figure 7. (a) Overlay diagrams of the molecule of **1** in **1**·CH₂Cl₂ (green), **1**·CHCl₃ (red) and **1**·C₂H₄Cl₂ (blue) (b) Overlay diagrams of the molecule of **2** in **2**·CH₂Cl₂ (green), **2**·CHCl₃ (red) and **2**·C₂H₄Cl₂ (blue)

2.4.5. Host-guest interactions

The complexes with opposite chirality, **1** and **2** are new chiral host materials with considerable structural adaptability to accommodate a range of chlorinated solvents. Recently much effort has been concentrated to hydrogen bond acceptor capabilities of the Cl-atom in C–Cl and M–Cl moieties.¹⁶ It has been shown both experimentally and theoretically that M–Cl (M = transition metal) moiety is much better hydrogen bond acceptor when compared with C–Cl moiety.¹⁷ In the case of inclusion compounds **1**·CH₂Cl₂ and **2**·CH₂Cl₂, the Cl-atom of the guest C–Cl moiety acts as hydrogen bond acceptor. On the other hand, for inclusion compounds **1**·CHCl₃, **2**·CHCl₃, **1**·C₂H₄Cl₂ and **2**·C₂H₄Cl₂, metal coordinated Cl-atom acts as hydrogen bond acceptor. The parameters associated with the C–H···Cl interactions involving the host and guest molecules in the present series of inclusion compounds are listed in Table 5. These C–H···Cl interactions play the decisive roles in the enclathration of small chloroalkane molecules in the host lattices formed by **1** and **2**. Calculations using

PLATON squeeze program show that the effective volume for inclusion is in between 12.1-20.6 % of the total crystal volume (Table 6).¹⁶ The individual packing patterns of enantiomeric pairs of the present series of inclusion compounds are described in the following sub-sections.

Table 6. Details of the solvent access area for all inclusion compounds

Inclusion compound	Effective volume for inclusion / Å³	Unit cell Volume / Å³	% of crystal volume
1·(CH ₂ Cl ₂)	193.5	1582.3	12.2
2·(CH ₂ Cl ₂)	191.6	1577.9	12.1
1·(CHCl ₃)	690.7	3408.4	20.3
2·(CHCl ₃)	700.2	3404.8	20.6
1·(C ₂ H ₄ Cl ₂)	679.8	3375.9	20.1
2·(C ₂ H ₄ Cl ₂)	663.6	3359.5	19.8

2.4.5.1. $1\cdot\text{CH}_2\text{Cl}_2$ and $2\cdot\text{CH}_2\text{Cl}_2$

Crystallization of binuclear complexes **1** and **2** from dichloromethane results in the formation of lattice inclusion compounds with 1:1 stoichiometric ratio. These inclusion compounds with opposite chirality crystallized in the monoclinic space group $P2_1$. There is one host and one guest molecule in the asymmetric unit. The crystal structure analysis reveals that the inclusion of solvent molecules is facilitated by weak inter-molecular $\text{C-H}\cdots\text{Cl}$ interactions. The C–H of the methylene group (C22) and the C–H of an aromatic ring (C11) participate in these $\text{C-H}\cdots\text{Cl}$ interactions as donors (Table 7). On the other hand, two chlorine atoms of dichloromethane participate as acceptors. These two inclusion compounds are enantiomeric pairs. They exhibit the mirror image relationship in the molecular level as well as in the crystal packing features (Figure 8).

2.4.5.2. $1\cdot\text{CHCl}_3$ and $2\cdot\text{CHCl}_3$

Crystallization of binuclear complexes **1** and **2** from chloroform results in the formation of lattice inclusion compounds with 1:1 stoichiometric ratio. The inclusion compounds with opposite chirality crystallized in the orthorhombic space group $P2_12_12_1$. There is one host and one guest molecule in the asymmetric unit. The crystal structure analysis reveals that the solvent molecules are stabilized in the lattice through weak inter-molecular $\text{C-H}\cdots\text{Cl}$ interaction. The C–H fragment of solvent chloroform (C31) participates as the donor and the metal coordinated chlorine (Cl2) acts as the acceptor (Table 7). As these two inclusion compounds are enantiomeric pairs, they exhibit mirror image relationship in the molecular level as well as in the supramolecular level (Figure 9).

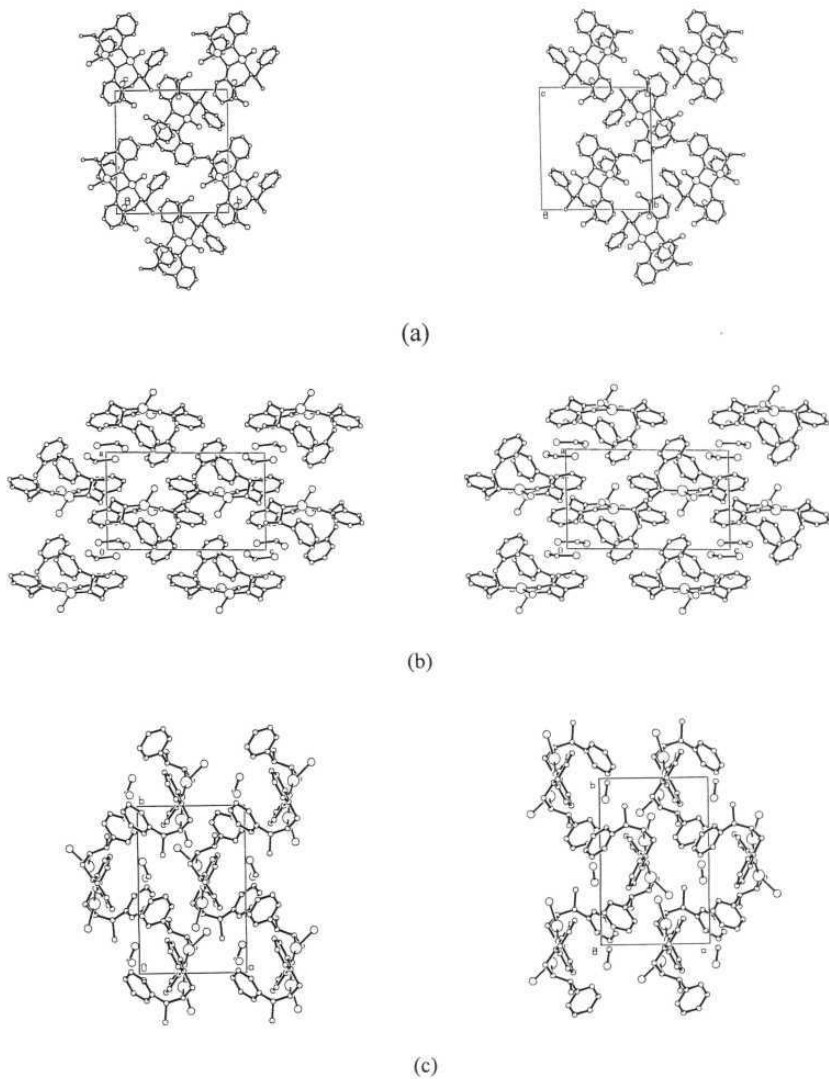


Figure 8. Projections of the crystal lattices of $1 \cdot \text{CH}_2\text{Cl}_2$ and $2 \cdot \text{CH}_2\text{Cl}_2$ onto the (a) bc -plane (b) ac -plane and (c) ab -plane

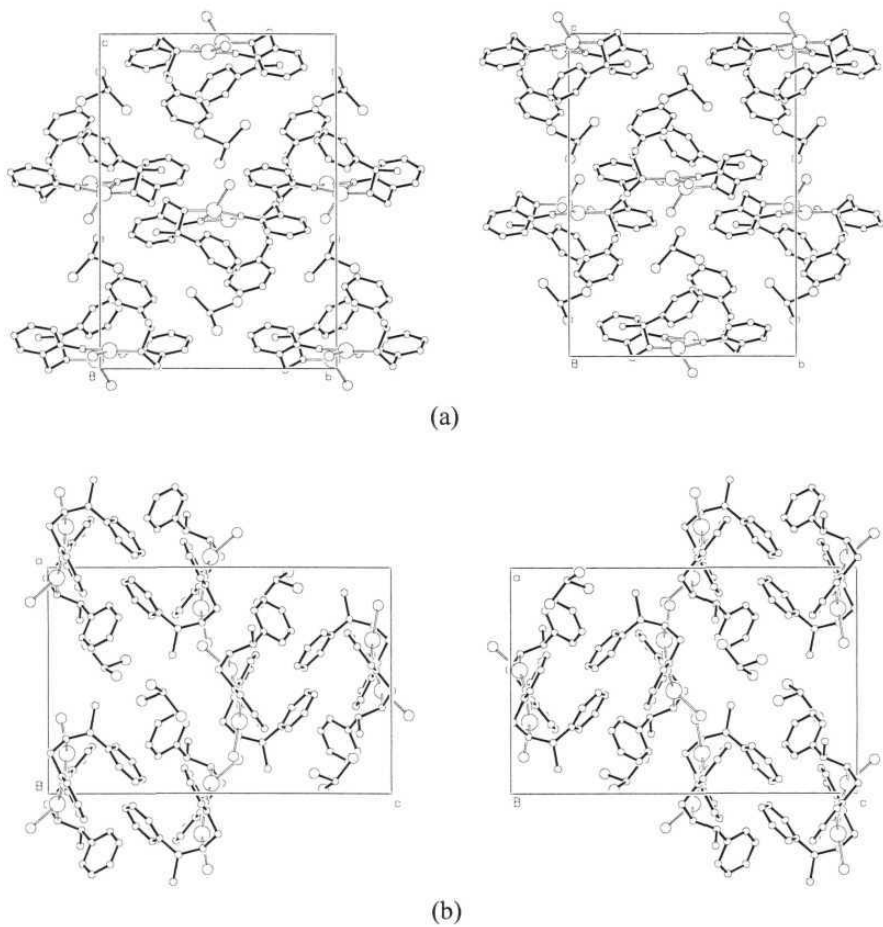


Figure 9. Projections of the crystal lattices of **1**·CHCl₃ and **2**·CHCl₃ onto the (a) *bc*-plane and (b) *ac*-plane

2.4.5.3. $1 \cdot C_2H_4Cl_2$ and $2 \cdot C_2H_4Cl_2$

Crystallization of binuclear complexes **1** and **2** from 1,2-dichloroethane results in the formation of lattice inclusion compounds with 1:1 stoichiometric ratio. The inclusion compounds with opposite chirality crystallized in the orthorhombic space group $P2_12_12_1$. There is one host and one guest molecule in the asymmetric unit. The crystal structure analysis reveals that the inclusion of solvent molecules are aided by weak intermolecular C–H \cdots Cl interactions. The C–H moiety of the methylene group of solvent 1,2-dichloroethane (C31) participates as hydrogen bond donor and the metal coordinated chlorine (Cl2) acts as a hydrogen bond acceptor (Table 7). As observed in the other two inclusion compounds, $1 \cdot C_2H_4Cl_2$ and $2 \cdot C_2H_4Cl_2$ exhibit mirror image relationship in molecular as well as supramolecular level. Projections of the crystal packing of these two enantiomeric compounds onto different planes (Figure 10) display the mirror image relationship of the molecules as well as packing patterns.

Table 7. Geometrical parameters of hydrogen bonds in compounds $1 \cdot CH_2Cl_2$, $2 \cdot CH_2Cl_2$, $1 \cdot CHCl_3$, $2 \cdot CHCl_3$, $1 \cdot C_2H_4Cl_2$ and $2 \cdot C_2H_4Cl_2$

Compound	D \cdots A	(D–H)/Å	$d(H \cdots A)/\text{\AA}$	$D(D \cdots A)/\text{\AA}$	D–H \cdots A/ $^\circ$
$1 \cdot (CH_2Cl_2)$	C(11) \cdots Cl(3)	0.93	2.75	3.444(7)	132
	C(22) \cdots Cl(4)	0.97	2.79	3.726(4)	161
$2 \cdot (CH_2Cl_2)$	C(11) \cdots Cl(3)	0.93	2.74	3.451(8)	134
	C(22) \cdots Cl(4)	0.97	2.79	3.724(4)	161
$1 \cdot (CHCl_3)$	C(31) \cdots Cl(2)	1.00	2.53	3.450(11)	153
$2 \cdot (CHCl_3)$	C(31) \cdots Cl(2)	0.98	2.55	3.446(10)	152
$1 \cdot (C_2H_4Cl_2)$	C(31) \cdots Cl(2)	0.968	2.886	3.697	142
$2 \cdot (C_2H_4Cl_2)$	C(31) \cdots Cl(2)	0.970	2.843	3.679	145

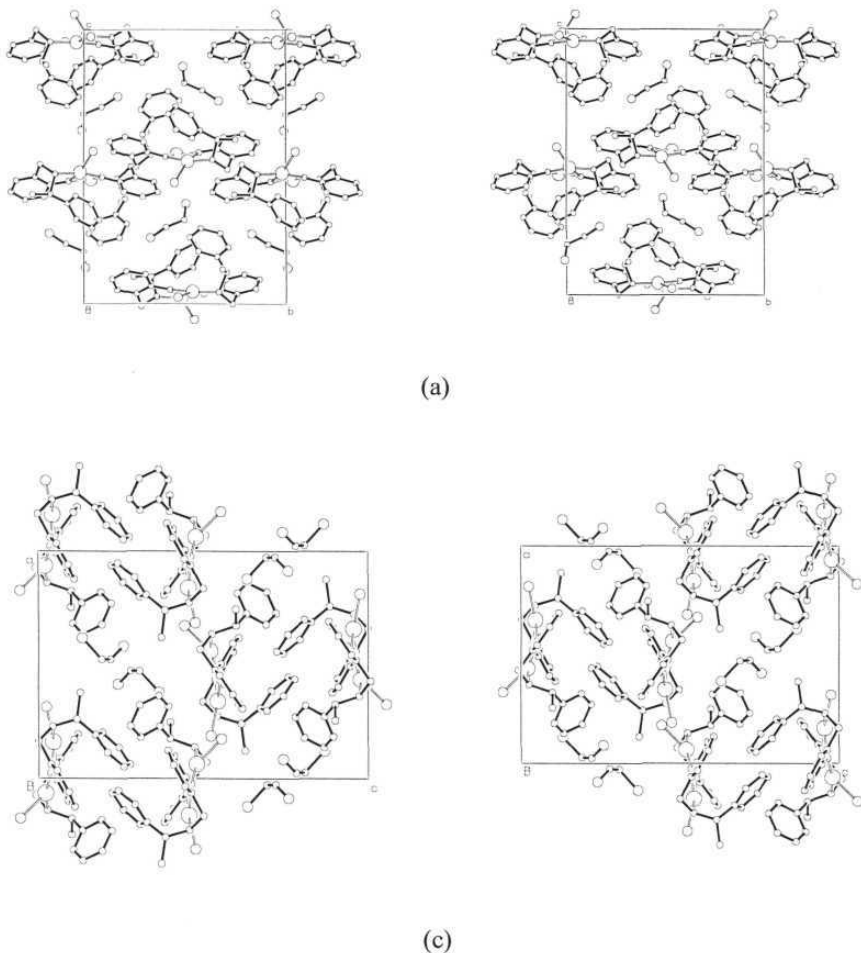


Figure 10. Projections of the crystal lattices of $1 \cdot \text{C}_2\text{H}_4\text{Cl}_2$ and $2 \cdot \text{C}_2\text{H}_4\text{Cl}_3$ onto the (a) *bc*-plane and (b) *ac*-plane

2.4.6. Enantio-specific inclusion of chiral 1,2-dichloroethane rotamers

The conformations of 1,2-dihaloethanes have been extensively studied by various physical methods especially by dipole moment measurements, raman, IR and microwave spectroscopy.¹⁷ A molecule without a plane of symmetry, a centre of inversion, or an improper axis of rotation is chiral. 1,2-dichloroethane is, of course, an

achiral molecular system. However, this is true when the Cl–C–C–Cl torsion angle is either 0° or 180° . Three rotamers (rotational isomers) are possible for 1,2-dichloroethane (Figure 11). These are *trans* or anti, *cis* or eclipsed and *gauche* forms. Eclipsed form ($\theta = 0$) is energetically most unfavourable due to the strong repulsions between not only the chlorine atoms but also hydrogen atoms. Between the *trans* and the *gauche* forms the former is more stable (by $\sim 1 \text{ kcal mol}^{-1}$). The existence of 1,2-dichloroethane in the *trans* form ($\theta = 180$) has been shown by X-ray analysis of 1,2-dichloroethane crystallized at 212 K using a miniature zone melting procedures.¹⁸ However, the isolation of the *gauche* form has never been reported.

The molecules which adopt the *gauche* form are chiral. One of the enantiomers has the right-handed (*P*) helical form and the other one has the left-handed (*M*) helical form. Recently, Toda *et al* reported a nearly eclipsed form of chiral 1,2-dichloromethane rotamer as inclusion crystal with the chiral host compound, (S)-(–)-2-bromo-3,3a,8-triphenyl-1,3a-dihydrocyclopenta[α]inden-1-one using the X-ray crystallographic technique.²¹ In the crystal lattices $1 \cdot \text{C}_2\text{H}_4\text{Cl}_2$ and $2 \cdot \text{C}_2\text{H}_4\text{Cl}_2$, the C–H \cdots Cl interactions between host and guest molecules play a crucial role in stabilizing the *gauche* form (chiral form) of 1,2-dichloroethane. The torsion angles involving Cl–C–C–Cl are 58.2° and 50.3° in $1 \cdot \text{C}_2\text{H}_4\text{Cl}_2$ and $2 \cdot \text{C}_2\text{H}_4\text{Cl}_2$, respectively. We have mentioned in the previous section that $1 \cdot \text{C}_2\text{H}_4\text{Cl}_2$ and $2 \cdot \text{C}_2\text{H}_4\text{Cl}_2$ have the mirror image relationship in the crystal lattice. The interesting implication of this relationship is enantio-selective trapping of the chiral rotamers of 1,2-dichloroethane in the host lattices formed by **1** and **2**. The 1,2-dichloroethane molecule is in the *P*-form in $1 \cdot \text{C}_2\text{H}_4\text{Cl}_2$. On the other hand, in the case of $2 \cdot \text{C}_2\text{H}_4\text{Cl}_2$ only the *M*-form of it exists (Figure 12). To the best of our knowledge, this is the first example of enantio-specific isolation of nearly *gauche* form of the right handed (*P*-form) and left handed (*M*-form) chiral 1,2-dichloroethane rotamers using the enantiomeric pair of an inorganic chiral host compound.

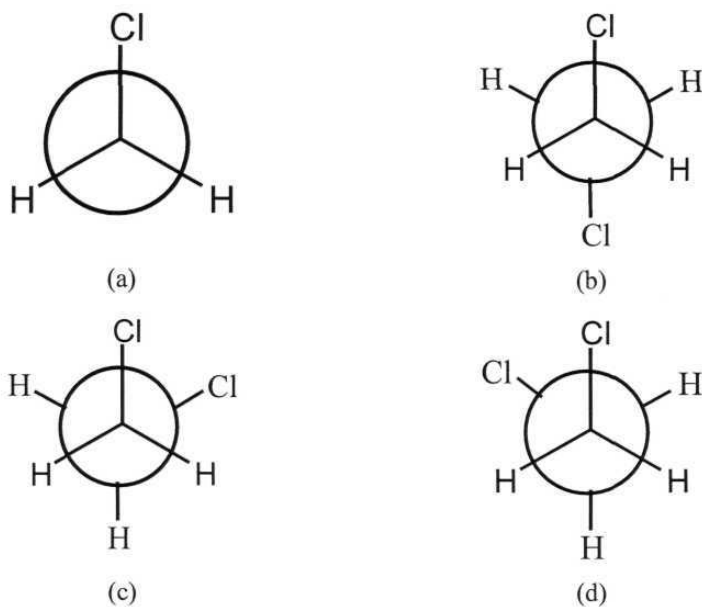


Figure 11. Possible conformations of 1,2-dichloroethane: (a) eclipsed form ($\theta = 0^\circ$) (b) staggered form ($\theta = 180^\circ$) (c) (*P*)-gauche form ($\theta = +60^\circ$) and (d) (*M*)-gauche form ($\theta = -60^\circ$)

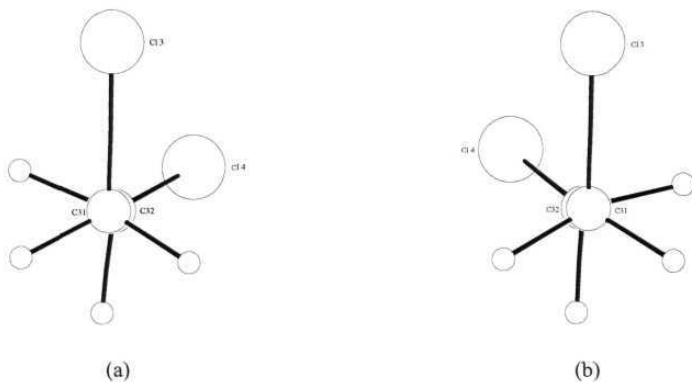


Figure 12. (a) The right-handed (*P*) and (b) the left-handed (*M*) helical forms of 1,2-dichloroethane in $1\cdot\text{C}_2\text{H}_4\text{Cl}_2$ and $2\cdot\text{C}_2\text{H}_4\text{Cl}_2$, respectively.

2.5. Conclusion

We have synthesized and characterized the enantiomers (**1** and **2**) of a chiral dinuclear copper(II) complex with the R- and S- form of a chiral reduced Schiff base (HL). The deprotonated chelating ligand coordinates a metal ion *via* the secondary amine N-atom and the phenolate-O atom. In the two complexes of general formula $[\text{Cu}_2\text{L}_2\text{Cl}_2]$, the phenoxy bridged copper(II) centres have distorted square-planar geometry. These complexes are found to be good chiral hosts, which can accommodate selectively chlorinated solvents such as dichloromethane, chloroform and 1,2-dichloroethane *via* intermolecular C–H \cdots Cl interactions. All the inclusion compounds are structurally characterized and the compounds with opposite chirality show mirror image relationship in both molecular and supramolecular level. The crystal structures of **1**·(*P*)-C₂H₄Cl₂ and **2**·(*M*)-C₂H₄Cl₂ reveal the unprecedented enantio-specific trapping of right handed (*P*) and the left-handed (*M*) *gauche* form of 1,2-dichloroethane rotamers.

1.5.9 References

1. F. Toda, *Pure Appl. Chem.*, **2001**, 73, 1137.
2. *Separations and Reactions in Organic Supramolecular Chemistry*, Edited by F. Toda and R. Bishop, John Wiley & sons, Ltd., **2004**.
3. *Comprehensive Supramolecular Chemistry*, Vol. 6, Eds. D. D. MacNicol, F. Toda and R. Bishop, Pergamon Press, Oxford, **1996**.
4. (a) H. Miyamoto, M. Sakamoto, K. Yoshioka, R. Takaoka and F. Toda, *Tetrahedron: Asymmetry*, **2000**, 11, 3045; (b) F. Toda, K. Mori, Z. Stein and I. Goldberg, *J. Org. Chem.*, **1988**, 53, 308; (c) X. Yuan, J. Li, Y. Tian, G.-H. Lee, X.-M. Peng, R. Zhu and X. You, *Tetrahedron: Asymmetry*, **2001**, 12, 3015; (d) K. Kato, K. Aburaya, Y. Miyake, K. Sada, N. Tohnai and M. Miyata, *Chem. Commun.*, **2003**, 23, 2872; (e) F. Toda, K. Tanaka, H. Ueda and T. Oshima, *J. Chem. Soc., Chem. Commun.*, **1983**, 743; (f) K. Sada, T. Kondo and M. Miyata, *Tetrahedron: Asymmetry*, **1996**, B52, 728; (g) K.

- Tanaka, S. Honke and Z. Urbanczyk-Lipkowska, *Eur. J. Org. Chem.*, **2000**, 3171; (h) G. Fantin, M. Fogagnolo, O. Bortolini and N. Masciocchi, S. Galli and A. Sironi, *New. J. Chem.*, **2004**, 11, 1295; (i) M. Akazome, M. Noguchi, O. Tanaka, A. Sumikawa, T. Uchida and K. Ogura, *Tetrahedron*, **1997**, 53, 8315; (j) F. Toda, K. Tanaka and S. Nagamatsu, *Tetrahedron Lett.*, **1984**, 25, 4929.
5. (a) F. Toda, H. Miyamoto, K. Kanemoto, K. Tanaka, Y. Takahashi and Y. Takenaka, *J. Org. Chem.*, **1999**, 64, 2096; (b) D. Seebach, A. K. Beck, R. Imwinkelried, S. Roggo and A. Wannacott, *Hel. Chim. Acta*, **1987**, 70, 954; (c) F. Toda and K. Tanaka, *Tetrahedron Lett.*, **1988**, 29, 551; (d) H. Hosomi, S. Ohba, K. Tanaka and F. Toda, *J. Am. Chem. Soc.*, **2000**, 122, 1818; (e) K. Tanaka, F. Toda, E. Mochizuki, N. Yasui, Y. Kai, I. Miyahara and K. Hirotsu, *Angew. Chem. Int. Ed.*, **1999**, 38, 3523; (f) M. Botoshansky, D. Braga, M. Kaftory, L. Maini, B. O. Patrick, J. R. Scheffer and K. Wang, *Tetrahedron Lett.*, **2005**, 46, 1141; (g) T. Bach, B. Grosch, T. Strassner and E. Herdtweck, *J. Org. Chem.*, **2003**, 68, 1107; (h) J. Shailaja, S. Karthikeyan and V. Ramamurthy, *Tetrahedron Lett.*, **2002**, 43, 9335; (i) K. Tanaka, T. Fujiwara and Z. Urbanczyk-Lipkowska, *Org. Lett.*, **2002**, 4, 3255; (j) K. Tanaka, R. Nagahiro and Z. Urbanczyk-Lipkowska, *Chirality*, **2002**, 14, 568; (k) K. Tanaka, R. Nagahiro and Z. Urbanczyk-Lipkowska, *Org. Lett.*, **2001**, 3, 1567; (l) M. Leibovitch, G. Olovsson, J. R. Scheffer and J. Trotter, *J. Am. Chem. Soc.*, **1997**, 119, 1462; (m) F. Toda, K. Tanaka, O. Kakinoki and T. Kawakami, *J. Org. Chem.*, **1993**, 58, 3783; (n) F. Toda, H. Miyamoto, K. Takeda, R. Matsugawa and N. Maruyama, *J. Org. Chem.*, **1993**, 58, 6208.
6. (a) J. S. Seo, D. Whang, H. Lee, S. I. Jun, J. Oh, Y. J. Jeon and K. Kimoon, *Nature*, **2000**, 404, 982; (b) O. R. Evans, H. L. Ngo and W. Lin, *J. Am. Chem. Soc.*, **2001**, 123, 10395.
7. SMART & SAINT Software Reference Manuals, Version 6.22, Bruker AXS Analytic X-Ray Systems, Inc., Madison, WI, **2000**.

8. G. M. Sheldrick, SADABS, Software for Empirical Absorption Correction, University of Göttingen, Germany, **2000**.
9. SHELXTL Reference Manual, Version 5.1, Bruker AXS, Analytic X-Ray Systems, Inc., WI, **1997**.
10. L. J. Farrugia, *J. Appl. Cryst.*, **1997**, 30, 567.
11. A. L. Spek, *Platon, Molecular Graphics Software*, University of Glasgow, UK, **2001**.
12. (a) R. J. Butcher and E. Sinn, *Inorg. Chem.*, **1976**, 15, 1604; (b) B. Chiari, O. Piovesana, T. Tarantelli and P. F. Zanazzi, *Inorg. Chem.*, **1987**, 26, 952; (c) E. Sinn and W. T. Robinson, *J. Chem. Soc., Chem. Commun.*, **1972**, 359; (d) P. Gluvchinsky, G. M. Mockler, P. C. Healy and E. Sinn, *J. Chem. Soc., Dalton Trans.*, **1974**, 1156; (e) R. Paschke, S. Liebsch, C. Tschierske, M. A. Oakley and E. Sinn, *Inorg. Chem.*, **2003**, 42, 8230.
13. K. M. Sureshan, R. G. Gonnade, M. S. Shashidhar, V. G. Puranik and M. M. Bhadbhade, *Chem. Commun.*, **2001**, 10, 881.
14. (a) E. C. Constable, *Tetrahedron*, **1992**, 48, 10013; (b) C. Piguet, G. Bernadinelli and G. Hopfgartner, *Chem. Rev.*, **1997**, 97, 2005; (c) M. Albrecht, *Chem. Soc. Rev.*, **1998**, 27, 281; (d) D. L. Caulder, K. N. Raymond, *Acc. Chem. Res.*, **1999**, 32, 975; (e) B. Quinodoz, G. Labat, H. Stoeckli-Evans and A. von Zelewsky, *Inorg. Chem.*, **2004**, 43, 7994.
15. H. D. Flack, *Acta Crystallogr.*, **1983**, A39, 876.
16. (a) L. Brammer, *Chem. Soc. Rev.*, **2004**, 33, 476; (b) M. Prabhakar, P. S. Zacharias and S. K. Das, *Inorg. Chem.*, **2005**, 44, 2585; (c) V. Balamurugan, M. S. Hundal and R. Mukherjee, *Eur. J. Chem.*, **2004**, 10, 1683.
17. (a) L. Brammer, E. A. Bruton and P. Sherwood, *Cryst. Growth Des.*, **2001**, 1, 277; (b) G. Allon, D. Bellamy, L. Bramer, E. A. Bruton and A. G. Orpen, *Chem. Commun.*, **1998**, 653.
18. P. V. Sluis and A. L. Spek, *Acta Crystallogr., Sect. A*, **1990**, 46, 194.

19. E. L. Eliel and S. H. Wilen, *Stereochemistry of Organic Compounds*, Wiley, New York, **1994**, p. 606.
20. R. Boese, D. Blaser and T. Haumann, *Z. Kristallogr.*, **1992**, 198, 311.
21. F. Toda, K. Tanaka and R. Kuroda, *Chem. Commun.*, **1997**, 1227.

**Inclusion compounds of polar solvents with chiral Cu(II) complexes:
Perfectly polar alignment of guest and host molecules and enantio-
specific inclusion of chiral 1,2-dihaloethane rotamers**

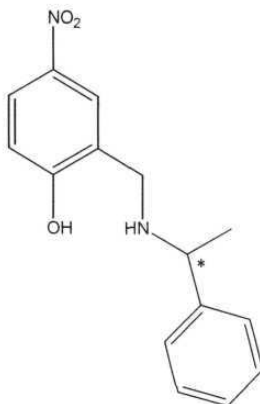
3.1. Abstract

Two chiral square-pyramidal Cu(II) complexes having the general formula $[\text{CuL}^n_2(\text{H}_2\text{O})]$ (**3** ($n = 3$) and **4** ($n = 4$); $\text{HL}^3 = \text{N}-(2\text{-hydroxy-5-nitrobenzyl})-(R)\text{-}\alpha\text{-methylbenzylamine}$ and $\text{HL}^4 = \text{N}-(2\text{-hydroxy-5-nitrobenzyl})-(S)\text{-}\alpha\text{-methylbenzylamine}$) are shown to form 1:1 inclusion compounds with acetonitrile, 1,2-dichloroethane and 1,2-dibromoethane. All the inclusion compounds (**3**·CH₃CN, **4**·CH₃CN, **3**·C₂H₄Cl₂, **4**·C₂H₄Cl₂, **3**·C₂H₄Br₂ and **4**·C₂H₄Br₂) crystallize in the monoclinic space group *C*2. The homo chiral host frameworks, constructed by intermolecular hydrogen bonding interactions, sustain one dimensional channels that are occupied by guest molecules during the crystallization. In each case, the chiral host framework is polar and it guides the alignment of guest molecules into a perfectly polar order. In addition, the structures of **3**·C₂H₄Cl₂, **4**·C₂H₄Cl₂, **3**·C₂H₄Br₂ and **4**·C₂H₄Br₂ reveal the enantio-selective confinement of chiral rotamers of 1,2-dihaloethane (halo = chloro, bromo) due to intermolecular hydrogen bonding.

3.2. Introduction

Polar and non-centrosymmetric organization of molecules in the crystalline state is a prerequisite for molecular materials having technologically important physical properties such as ferro-, pyro- or piezo-electricity and nonlinear optical effects.¹ Inclusion of chirality in the molecule is a common approach to ensure non-centrosymmetric organization in the crystals.² On the other hand, perfectly polar assembly in the crystal lattice is rare and requires special design strategies.³ Synthesis of inclusion compounds having polar host frameworks that can confine and align guest molecules in a polar order is one of the successful strategies.⁴ In this regard, it may well be noted that the synthesis of host frameworks with chiral cavities is a noteworthy challenge as these solids also have potential applications in the separation of enantiomers and in asymmetric catalysis.⁵ Recently some studies on coordination complexes of metal ions with chiral Schiff bases and their non-linear optical properties have been reported.⁶ Compared to the Schiff bases, reduced Schiff bases are expected to be more flexible as they are not constrained to be planar.⁷

In the preceding chapter, we have discussed the synthesis and inclusion properties of dinuclear Cu(II) complexes with unsubstituted chiral reduced Schiff bases. In this chapter, we have discussed the synthesis and inclusion properties of two chiral square-pyramidal Cu(II) complexes of general formula $[\text{CuL}^n_2(\text{H}_2\text{O})]$ (**3** ($n = 3$) and **4** ($n = 4$); $\text{HL}^3 = \text{N}-(2\text{-hydroxy-5-nitrobenzyl})-(R)\text{-}\alpha\text{-methylbenzylamine}$ and $\text{HL}^4 = \text{N}-(2\text{-hydroxy-5-nitrobenzyl})-(S)\text{-}\alpha\text{-methylbenzylamine}$). The inclusion compounds **3**·CH₃CN, **4**·CH₃CN, **3**·C₂H₄Cl₂, **4**·C₂H₄Cl₂, **3**·C₂H₄Br₂ and **4**·C₂H₄Br₂ crystallize in the non-centrosymmetric space group *C2*. Intermolecular hydrogen bonding leads to a perfectly polar alignment of both host and guest molecules in all these inclusion compounds. As observed in the previous chapter inclusion of the chiral rotamers of 1,2-dichloroethane as well as 1,2-dibromoethane molecules in the host lattices formed by **3** and **4** occurs in enantioselective manner.



HL³ = N-(2-hydroxy-5-nitrobenzyl)-(R)-α-methylbenzylamine

HL⁴ = N-(2-hydroxy-5-nitrobenzyl)-(S)-α-methylbenzylamine

3.3. Experimental

3.3.1. Materials

All commercially available chemicals and the solvents utilized in this work were of analytical grade and were used as obtained. The chemicals and the sources are as follows: 5-nitrosalicylaldehyde, (R)-α-methylbenzylamine and (S)-α-methylbenzylamine, sodium borohydride, Lancaster (England); CDCl₃, methanol, dichloromethane, chloroform, 1,2-dichloroethane, Across (India); CuCl₂·2H₂O, LiOH·1H₂O, anhydrous sodium sulphate, S. D. Fine Chem. Ltd. (India).

3.3.2. Physical measurements

Elemental analysis was carried out on a Perkin-Elmer 240C CHN analyzer. Infrared spectra were collected by using KBr pellets on a Jasco-5300 FT-IR spectrophotometer. NMR spectra were recorded on a Bruker ACF-200 spectrometer. A Shimadzu 3101-PC UV/vis/NIR spectrophotometer was used to record the electronic spectra. X-ray crystallographic experiments were performed using a Bruker-Nonius SMART APEX CCD single crystal diffractometer. A Sherwood scientific magnetic susceptibility balance was used to measure the magnetic moments.

3.3.3. Synthesis of ligand and complexes

(a) N-(2-hydroxy-5-nitrobenzyl)-(R)- α -methylbenzylamine, HL³

A methanol solution (30 ml) of 5-nitrosalicylaldehyde (1.67 g, 10 mmol) was added to a methanol solution (30 ml) of (R)- α -methylbenzylamine (1.21 g, 10 mmol) and stirred at room temperature for ½ h. To the resulting yellow solution 0.74 g (20 mmol) of NaBH₄ was added and the mixture was stirred for another ½ h until a colourless solution was obtained. The reaction mixture was evaporated to dryness on a rotary evaporator followed by addition of 100 ml of water. The solid suspended in water was extracted with (2 x 30 ml) CH₂Cl₂. The CH₂Cl₂ extracts were dried over anhydrous Na₂SO₄ and then evaporated to dryness. The compound (HL³) was obtained in the form of light yellow solid.

Yield	: 1.9 g, (70%).
M. F.	: C ₁₅ H ₁₆ N ₂ O ₃
IR (ν cm ⁻¹ , KBr pellet)	: 3298, 1593, 1335
¹ H NMR (CDCl ₃ , δ , ppm)	: 1.52 (d, 3H, CH ₃), 3.84 and 3.98 (2H, CH _A H _B), ~ 3.83 (q, 1H, CH(CH ₃)), 5.68 (br, 2H, NH and OH), 6.87 (d, 1H, <i>ortho</i> to phenolic-OH), 7.28-7.44 (m, 5H, phenyl protons), 7.85 (s, 1H, <i>ortho</i> to both NO ₂ and CH ₂). 8.08 (d, 1H, <i>ortho</i> to NO ₂)
Anal. calcd. for C ₁₅ H ₁₆ N ₂ O ₃	: C, 66.16; H, 5.92; N, 10.21
Found	: C, 65.88; H, 5.97; N, 10.15.

(b) N-(2-hydroxy-5-nitrobenzyl)-(S)- α -methylbenzylamine, HL⁴

HL⁴ was prepared in similar yield by following the same procedure as described for HL³ using (S)- α -methylbenzylamine instead of (R)- α -methylbenzylamine.

Yield	: 1.9 g, (70%).
M. F.	: C ₁₅ H ₁₆ N ₂ O ₃
IR (ν cm ⁻¹ , KBr pellet)	: 3298, 1593, 1335

^1H NMR (CDCl_3 , δ , ppm) : 1.52 (d, 3H, CH_3), 3.84 and 3.98 (2H, $\text{CH}_\text{A}\text{H}_\text{B}$), \sim 3.83 (q, 1H, $\text{CH}(\text{CH}_3)$), 5.68 (br, 2H, NH and OH), 6.87 (d, 1H, *ortho* to phenolic-OH), 7.28-7.44 (m, 5H, phenyl protons), 7.85 (s, 1H, *ortho* to both NO_2 and CH_2). 8.08 (d, 1H, *ortho* to NO_2)

Anal. calcd. for $\text{C}_{15}\text{H}_{16}\text{N}_2\text{O}_3$: C, 66.16; H, 5.92; N, 10.21

Found : C, 65.76; H, 5.88; N, 10.18.

(c) **$[\text{CuL}^3_2(\text{H}_2\text{O})]$ (3):** A methanol solution (10 ml) of $\text{CuCl}_2 \cdot 2\text{H}_2\text{O}$ (0.089 g, 0.5 mmol) was added to a methanol solution (20 ml) of HL^3 (0.272 g, 1 mmol) and $\text{LiOH} \cdot \text{H}_2\text{O}$ (0.042 g, 1 mmol). The mixture was stirred at room temperature for 1 h. The green solid separated was collected by filtration, washed with methanol and dried in vacuum. Yield, 0.40 g, 76%. Anal. calcd. for $\text{CuC}_{30}\text{H}_{32}\text{N}_4\text{O}_7$: C, 57.73; H, 5.17; N, 8.98. Found: 58.04, 5.10, 8.91. Selected infrared bands (cm^{-1}) : 3462(br), 3271(w), 2972(w), 2926(w), 1597(s), 1566(s), 1477(s), 1439(w), 1294(s), 1180(m), 1128(w), 1089(m), 1047(w), 1016(w), 968(w), 923(m), 837(m), 756(m), 736(w), 702(m), 657(m), 555(m), 532(w), 491(w), 447(w), 420(w). Electronic spectral data in CHCl_3 (λ , nm (ϵ , $\text{M}^{-1}\text{cm}^{-1}$)): 645 sh (190), 377 (22,400), 337 sh (16,500), 306 sh (11,500), 237 (13,700). Effective magnetic moment at 298 K: $1.88 \mu_\text{B}$.

(d) **$[\text{CuL}^4_2(\text{H}_2\text{O})]$ (4):** A methanol solution (10 ml) of $\text{CuCl}_2 \cdot 2\text{H}_2\text{O}$ (0.089 g, 0.5 mmol) was added to a methanol solution (20 ml) of HL^4 (0.272 g, 1 mmol) and $\text{LiOH} \cdot \text{H}_2\text{O}$ (0.042 g, 1 mmol). The mixture was stirred at room temperature for 1 h. The green solid separated was collected by filtration, washed with methanol and dried in vacuum. Yield, 0.40 g, 76%. Anal. calcd. for $\text{CuC}_{30}\text{H}_{32}\text{N}_4\text{O}_7$: C, 57.73; H, 5.17; N, 8.98. Found: 58.10, 5.11, 8.87. Selected infrared bands (cm^{-1}): 3462(br), 3271(w), 2972(w), 2926(w), 1597(s), 1566(s), 1477(s), 1439(w), 1294(s), 1180(m), 1128(w), 1089(m), 1047(w), 1016(w), 968(w), 923(m), 837(m), 756(m), 736(w), 702(m), 657(m), 555(m), 532(w), 491(w), 447(w), 420(w). Electronic spectral data in CHCl_3

(λ , nm (ϵ , $\text{M}^{-1}\text{cm}^{-1}$)): 645 sh (255), 377 (22,450), 335 sh (16,300), 303 sh (11,300), 237 (14,000). Effective magnetic moment at 298 K: $1.87 \mu_{\text{B}}$.

3.3.4. X-ray crystallography

X-ray data were collected for green crystals of $3 \cdot \text{CH}_3\text{CN}$, $3 \cdot \text{C}_2\text{H}_4\text{Cl}_2$, $3 \cdot \text{C}_2\text{H}_4\text{Br}_2$, $4 \cdot \text{CH}_3\text{CN}$, $4 \cdot \text{C}_2\text{H}_4\text{Cl}_2$ and $4 \cdot \text{C}_2\text{H}_4\text{Br}_2$ on a Bruker-Nonius SMART APEX CCD single crystal diffractometer using graphite monochromated Mo-K α radiation (0.71073 \AA). The SMART software was used for intensity data acquisition and the SAINT-Plus software⁸ was used for data extraction. In each case, absorption correction was performed with help of SADABS program.⁹ The SHELXTL package¹⁰ was used for structure solution and least-square refinement on F^2 . All the non hydrogen atoms were refined anisotropically. The secondary amine hydrogen atoms were located in a difference map and refined with geometric restraints. All other hydrogen atoms were included in the structure factor calculation by using a riding model. The ORTEP3¹¹ and the PLATON¹² software were used for molecular graphics. The significant X-ray crystallographic data are given in Tables 1-3.

Table 1. Crystallographic data for **3**·CH₃CN and **4**·CH₃CN

Compound	3 ·CH ₃ CN	4 ·CH ₃ CN
Molecular formula	C ₃₂ H ₃₂ N ₅ O ₇ Cu	C ₃₂ H ₃₂ N ₅ O ₇ Cu
Crystal dimensions / mm	0.31 x 0.14 x 0.22	0.28 x 0.36 x 0.30
Host-guest ratio	1:1	1:1
<i>T</i> /K	293(2)	293(2)
<i>M</i>	662.18	662.18
Crystal system	Monoclinic	Monoclinic
Space group	<i>C</i> 2	<i>C</i> 2
<i>a</i> /Å	20.0776 (19)	20.080 (2)
<i>b</i> /Å	8.1722 (8)	8.1754 (8)
<i>c</i> /Å	12.7012 (12)	12.7018 (13)
α /°	90	90
β /°	127.9370(10)	127.9380 (10)
γ /°	90	90
<i>V</i> /Å ³	1643.6 (3)	1644.5 (3)
<i>Z</i>	2	2
Observed reflections	3850	3844
Parameters	214	214
Final <i>R</i> indices (<i>I</i> > 2σ(<i>I</i>))	0.0486, 0.1057	0.0345, 0.0840
Goodness-of-fit on <i>F</i> ²	1.069	1.062
Largest hole and peak e/ Å ³	-0.232, 0.841	-0.308, 0.383

Table 2. Crystallographic data for $3 \cdot C_2H_4Cl_2$ and $4 \cdot C_2H_4Cl_2$

Compound	$3 \cdot C_2H_4Cl_2$	$4 \cdot C_2H_4Cl_2$
Molecular formula	$C_{32}H_{36}N_4O_7CuCl_2$	$CuC_{32}H_{36}N_4O_7CuCl_2$
Crystal dimensions / mm	0.36 x 0.34 x 0.18	0.41 x 0.22 x 0.18
Host-guest ratio	1:1	1:1
T/K	293(2)	293(2)
M	723.09	723.09
Crystal system	Monoclinic	Monoclinic
Space group	$C2$	$C2$
$a/\text{\AA}$	20.2834(12)	20.1329(17)
$b/\text{\AA}$	8.1769(5)	8.0328(6)
$c/\text{\AA}$	12.8799(7)	12.7987(13)
$\alpha/^\circ$	90	90
$\beta/^\circ$	128.6480(10)	128.290(2)
$\gamma/^\circ$	90	90
$V/\text{\AA}^3$	1667.94(17)	1624.6(2)
Z	2	2
Observed reflections	3572	3661
Parameters	215	215
Final R indices ($I > 2\sigma(I)$)	0.0411, 0.1035	0.0433, 0.1063
Goodness-of-fit on F^2	1.068	1.053
Largest hole and peak $e/\text{\AA}^3$	-0.451, 0.647	-1.080, 1.187

Table 3. Crystallographic data for **3**·C₂H₄Br₂ and **4**·C₂H₄Br₂

Compound	3 ·C ₂ H ₄ Br ₂	4 ·C ₂ H ₄ Br ₂
Molecular formula	C ₃₂ H ₃₆ N ₄ O ₇ CuBr ₂	C ₃₂ H ₃₆ N ₄ O ₇ CuBr ₂
Crystal dimensions / mm	0.35 x 0.19 x 0.09	0.38 x 0.28 x 0.22
Host-guest ratio	1:1	1:1
<i>T</i> /K	293(2)	293(2)
<i>M</i>	812.01	812.01
Crystal system	Monoclinic	Monoclinic
Space group	<i>C</i> 2	<i>C</i> 2
<i>a</i> /Å	20.4437(15)	20.4407 (16)
<i>b</i> /Å	8.1977(6)	8.1984 (7)
<i>c</i> /Å	13.0089(9)	13.0093 (10)
α /°	90	90
β /°	129.0990(10)	129.1040(10)
γ /°	90	90
<i>V</i> /Å ³	1691.9(2)	1691.8 (2)
<i>Z</i>	2	2
Observed reflections	3972	3966
Parameters	218	218
Final <i>R</i> indices (<i>I</i> > 2σ(<i>I</i>))	0.0675, 0.1793	0.0676, 0.1824
Goodness-of-fit on <i>F</i> ²	1.039	1.056
Largest hole and peak e/ Å ³	-1.711, 0.969	-1.723, 0.967

3.4 Results and discussions

3.4.1 Synthesis and some properties

HL³ and HL⁴ were prepared by condensation reactions of one mole equivalent of 5-nitrosalicylaldehyde with one mole equivalent of the corresponding enantiomerically pure α -methylbenzylamine in methanol followed by reduction with NaBH₄. The elemental analysis and spectral data (infrared and proton NMR) for HL³ and HL⁴ are very similar and consistent with the expected molecular formula and structure.¹³ Infrared spectrum collected with a CH₂Cl₂ solution of HL displays a broad and weak band at $\sim 3400\text{ cm}^{-1}$ possibly due to the phenolic OH group. The N-H stretch appears as a sharp band at $\sim 3300\text{ cm}^{-1}$. Two strong bands observed at 1593 and 1335 cm^{-1} are most likely due to the ν_{asym} and the ν_{sym} stretches of the nitro group. The proton NMR spectrum was recorded with a CDCl₃ solution of HL. The methyl protons appear as a doublet at 1.52 δ . The protons of methylene group are observed as an AB type quartet centred at 3.91 δ . A broad signal spreaded in the range 5.0-6.2 δ corresponds to two protons. This signal is most likely associated with the N-H and O-H groups. The signal for the hydrogen atom attached to the chiral C-atom of HL is expected to be quartet. A signal observed at $\sim 3.83\text{ } \delta$ most likely belongs to this quartet. The remaining part buried under the δ_B signal of the AB type quartet observed due to the methylene group protons. A multiplet centred at $\sim 7.36\text{ } \delta$ corresponding to five protons is assigned to the phenyl group protons. Two doublets, each corresponding to a single proton, are observed at 6.87 and 8.08 δ . The former is assigned to proton *ortho* to the phenolic-OH and the latter is assigned to the proton *ortho* to the nitro group. The protons *ortho* to both nitro and methylene groups appear as a singlet at 7.85 δ .

Reactions of CuCl₂·2H₂O, HLⁿ (n = 3, 4) and LiOH·1H₂O (1:2:2 mole ratio) in methanol produce the complexes, [CuL³₂(H₂O)] (**3**) and [CuL⁴₂(H₂O)] (**4**) in good yields. Both complexes are electrically non-conducting in solutions. The elemental analysis data for these complexes **3** and **4** are consistent with the expected molecular formula. Representative chemical diagram of these complex molecules are shown in

Figure 1. The room temperature magnetic moments suggest an $S = \frac{1}{2}$ spin state indicating the +2 oxidation state of the metal ions in both complexes. The infrared spectra of **3** and **4** are very similar. The same is true for the electronic spectral features of **3** and **4**. Infrared spectra of the complexes display the N-H stretch as a sharp band at $\sim 3271 \text{ cm}^{-1}$. Two strong bands observed at ~ 1597 and 1294 cm^{-1} are most likely due to the ν_{asym} and ν_{sym} stretches of the nitro group, respectively. A broad peak observed at $\sim 3460 \text{ cm}^{-1}$ is assigned to the metal coordinated water molecule. Two medium to strong bands observed at 1566 and 1477 cm^{-1} are most probably due to the C=C stretches from the aromatic part of the ligands. The electronic spectral features of **3** and **4** are very similar. A weak absorption observed near 645 nm is assigned to d-d transition. Intense absorption in the range $377\text{--}237 \text{ nm}$ is likely to be due to intraligand transition.

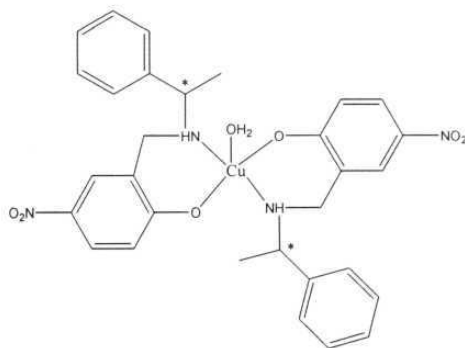


Figure 1. General molecular structure of **3** and **4**.

3.4.2 Crystallization

The complexes **3** and **4** with opposite chirality are proved to be excellent chiral hosts for inclusion of acetonitrile, 1,2-dichloroethane and 1,2-dibromoethane. X-ray quality crystals from acetonitrile, 1,2-dichloro- and 1,2-dibromoethane are grown very easily. In each inclusion compound the stoichiometric ratio for the host

and the solvent guest molecules is 1:1. The crystals of **3**·CH₃CN, **4**·CH₃CN, **3**·C₂H₄Cl₂, **4**·C₂H₄Cl₂, **3**·C₂H₄Br₂ and **4**·C₂H₄Br₂ have plate like morphology.

3.4.3 Description of the molecular structures of **3** and **4**

In the inclusion compounds **3**·CH₃CN, **3**·C₂H₄Cl₂ and **3**·C₂H₄Br₂, the chiral C-centre of the ligand has absolute configuration R or rectus. After metal coordination the N-atom of the ligand becomes chiral. The absolute configuration of this N-centre is also found to be R or rectus. Similarly the ligand in the inclusion compounds **4**·CH₃CN, **4**·C₂H₄Cl₂ and **4**·C₂H₄Br₂ contains the S or sinister C-centre. Here also the nitrogen center becomes chiral due to metal coordination and the absolute configuration of the N-centre is found to be S or sinister (Table 4).¹⁴ In both the cases, the generation of new chiral centre is homogeneous. The molecular structures of **3** and **4** having the opposite chirality are mirror images of each other. The thermal ellipsoid plots with the atom labeling schemes are shown in Figure 2. In each molecule, the metal centre is in a distorted square-pyramidal N₂O₃ coordination sphere. Two bidentate chelating ligands form the N₂O₂ basal plane and the water oxygen occupies the apical site. The bidentate ligands are related by a crystallographically imposed two-fold axis passing through the Cu and the apical water O. Both atoms are at special positions on the *b*-axis. The Cu–N distances are significantly longer than the Cu–O distances. The former range is in the 2.020(2)–2.036(4) Å whereas the latter is within 1.913(3)–1.9207(17) Å. The apical Cu(II)–O distance is significantly longer than the equatorial bond distances. The bond parameters associated with the Cu(II) centres are given in Table 5. The dihedral angles between the planes defined by Cu, N1 and O1 and that defined by Cu, N1' and O1' are in the range of 8.76(5)–18.97(5)° for all the inclusion compounds of **3** and **4** (Table 6). These values indicate a tetrahedral distortion of the N₂O₂ basal plane. In the inclusion compounds of **3**, the (R)-isomeric ligands exhibit right handed ($\Delta = P$) helical twist, whereas in the inclusion compounds of **4**, the (S)-isomeric ligands exhibit left handed ($\Lambda = M$) helical twist of N₂O₂ basal plane around the copper centres (Figure 3).

Table 4. Absolute configurations and the values of Flack parameters for $\mathbf{3} \cdot \text{CH}_3\text{CN}$, $\mathbf{3} \cdot \text{C}_2\text{H}_4\text{Cl}_2$, $\mathbf{3} \cdot \text{C}_2\text{H}_4\text{Br}_2$, $\mathbf{4} \cdot \text{CH}_3\text{CN}$, $\mathbf{4} \cdot \text{C}_2\text{H}_4\text{Cl}_2$ and $\mathbf{4} \cdot \text{C}_2\text{H}_4\text{Br}_2$

Compound	C(8), C(8') configuration	N(1), N(1') Configuration	Flack Parameter value
$\mathbf{3} \cdot \text{CH}_3\text{CN}$	R, R	R, R	0.018(14)
$\mathbf{3} \cdot \text{C}_2\text{H}_4\text{Cl}_2$	R, R	R, R	-0.012(13)
$\mathbf{3} \cdot \text{C}_2\text{H}_4\text{Br}_2$	R, R	R, R	0.05(2)
$\mathbf{4} \cdot \text{CH}_3\text{CN}$	S, S	S, S	0.016(9)
$\mathbf{4} \cdot \text{C}_2\text{H}_4\text{Cl}_2$	S, S	S, S	-0.005(14)
$\mathbf{4} \cdot \text{C}_2\text{H}_4\text{Br}_2$	S, S	S, S	0.05(2)

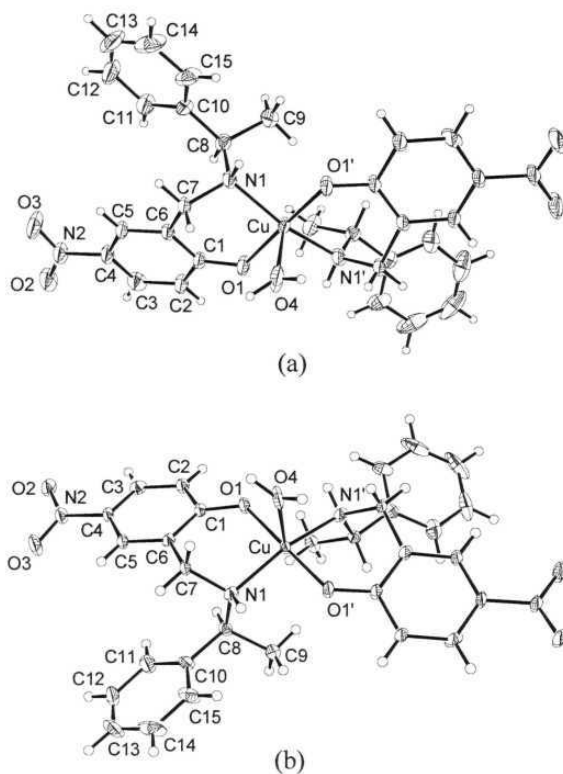


Figure 2. Molecular structures of (a) $[\text{CuL}^3_2(\text{H}_2\text{O})]$ (**3**) and (b) $[\text{CuL}^4_2(\text{H}_2\text{O})]$ (**4**) with the atom-labeling schemes. All non-hydrogen atoms are represented by their 35 and 50% probability thermal ellipsoids for **3** and **4**, respectively.

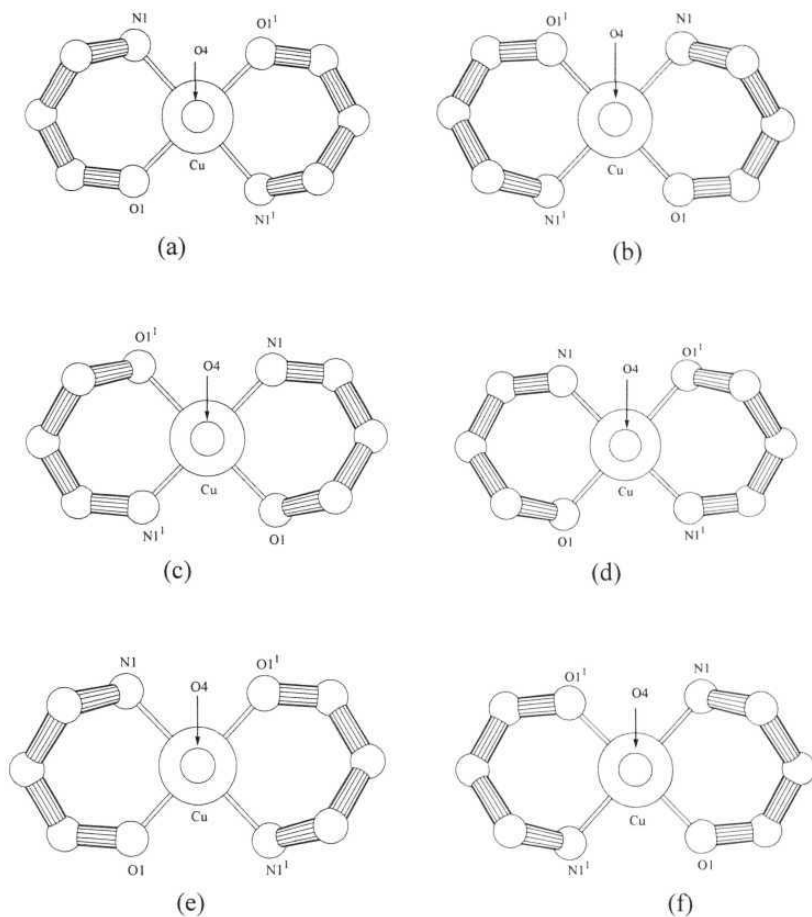


Figure 3. Absolute configuration of the tetrahedrally distorted N₂O₂ basal plane viewed down the C₂ axis: (a) Δ configuration in 3·CH₃CN, (b) Λ configuration in 4·CH₃CN (c) Δ configuration in 3·C₂H₄Cl₂ (d) Λ configuration in 4·C₂H₄Cl₂ (e) Δ configuration in 3·C₂H₄Br₂ (f) Λ configuration in 4·C₂H₄Br₂

Table 5. Selected bond lengths and bond angles for $3\cdot\text{CH}_3\text{CN}$, $3\cdot\text{C}_2\text{H}_4\text{Cl}_2$, $3\cdot\text{C}_2\text{H}_4\text{Br}_2$, $4\cdot\text{CH}_3\text{CN}$, $4\cdot\text{C}_2\text{H}_4\text{Cl}_2$ and $4\cdot\text{C}_2\text{H}_4\text{Br}_2$ **Bond lengths (Å)**

Compound	$3\cdot\text{CH}_3\text{CN}$	$3\cdot\text{C}_2\text{H}_4\text{Cl}_2$	$3\cdot\text{C}_2\text{H}_4\text{Br}_2$	$4\cdot\text{CH}_3\text{CN}$	$4\cdot\text{C}_2\text{H}_4\text{Cl}_2$	$4\cdot\text{C}_2\text{H}_4\text{Br}_2$
Cu – O(1)	1.9117(17)	1.9152(15)	1.915(3)	1.9127(12)	1.9207(17)	1.913(3)
Cu – O(1 ¹)	1.9117(17)	1.9152(15)	1.915(3)	1.9127(12)	1.9207(17)	1.913(3)
Cu – N(1)	2.032(2)	2.030(2)	2.034(4)	2.0310(16)	2.020(2)	2.036(4)
Cu – N(1 ¹)	2.032(2)	2.030(2)	2.034(4)	2.0310(16)	2.020(2)	2.036(4)
Cu – O(4)	2.307(5)	2.326(4)	2.331(8)	2.309(3)	2.271(4)	2.336(8)

Bond angles (°)

Compound	$3\cdot\text{CH}_3\text{CN}$	$3\cdot\text{C}_2\text{H}_4\text{Cl}_2$	$3\cdot\text{C}_2\text{H}_4\text{Br}_2$	$4\cdot\text{CH}_3\text{CN}$	$4\cdot\text{C}_2\text{H}_4\text{Cl}_2$	$4\cdot\text{C}_2\text{H}_4\text{Br}_2$
O (1) – Cu – O (1 ¹)	177.8(3)	177.5(2)	176.0(4)	177.54(18)	178.54(19)	175.8(4)
O (1) – Cu – N (1)	92.93(8)	93.14(8)	93.21(16)	93.08(6)	92.94(9)	93.35(16)
O (1 ¹) – Cu – N (1)	87.44(8)	87.25(8)	87.41(17)	87.32(6)	87.30(9)	87.32(17)
O (1) – Cu – N (1 ¹)	87.44(8)	87.25(8)	87.41(17)	87.32(6)	87.30(9)	87.32(17)
O (1 ¹) – Cu – N (1 ¹)	92.93(8)	93.14(8)	93.21(16)	93.08(6)	92.94(9)	93.35(16)
N (1) – Cu – N (1 ¹)	161.14(14)	161.65(12)	161.8(3)	161.54(9)	161.04(13)	161.9(3)
O (1) – Cu – O (4)	88.88(13)	88.76(10)	88.0(2)	88.77(9)	89.27(10)	87.9(2)
O (1 ¹) – Cu – O (4)	88.88(13)	88.76(10)	88.0(2)	88.77(9)	89.27(10)	87.9(2)
N (1) – Cu – O (4)	99.43(7)	99.17(6)	99.08(14)	99.23(5)	99.48(7)	99.03(13)
N (1 ¹) – Cu – O (4)	99.43(7)	99.17(6)	99.08(14)	99.23(5)	99.48(7)	99.03(13)

Table 6. Dihedral angles between the planes defined by Cu, N1, O1 and Cu, N1', O1'

Inclusion compound	Dihedral angle between the planes
3 ·CH ₃ CN	8.97 (3)
3 ·C ₂ H ₄ Cl ₂	18.41(4)
3 ·C ₂ H ₄ Br ₂	8.76 (5)
4 ·CH ₃ CN	8.83 (2)
4 ·C ₂ H ₄ Cl ₂	18.97(5)
4 ·C ₂ H ₄ Br ₂	9.05 (5)

3.4.5. Perfectly polar alignment of host and guest molecules

The complexes with opposite chirality, **3** and **4** are found to be good chiral hosts and crystallize in acetonitrile, 1,2-dichloroethane and 1,2-dibromoethane to give inclusion compounds. All these inclusion compounds crystallize in the non-centrosymmetric monoclinic space group *C*2. The consistency in the crystal packing is reflected in the small variations of the unit cell parameters *a* (20.0776(19)-20.4437(15) Å), *b* (8.0328(6)-8.1984(7) Å), *c* (12.7012(12)-13.0093(10) Å) and β (127.9370(10)-129.1040(10)°). These cell parameter values indicate that the host framework is highly rigid and the guest molecules are only altered. Calculations using PLATON squeeze program¹⁵ show that the effective volume for inclusion is in between the 14.6-16.0 % of the total crystal volume in these inclusion compounds (Table 7).

Table 7. Details of the solvent access area in all the inclusion compounds using the PLATON squeeze program

Inclusion compound	Effective volume for inclusion / Å³	Unit cell Volume / Å³	% of crystal volume
3·CH ₃ CN	239.7	1643.6	14.6
4·CH ₃ CN	237.8	1644.5	14.6
3·C ₂ H ₄ Cl ₂	258.6	1667.9	15.5
4·C ₂ H ₄ Cl ₂	236.7	1624.6	14.6
3·C ₂ H ₄ Br ₂	270.1	1691.9	16.0
4·C ₂ H ₄ Br ₂	270.5	1691.8	16.0

In the crystal lattice of each structure, the apical water molecule of the complex molecule is involved in hydrogen bonding interactions with the nitro groups of the neighboring molecules and leads to perfectly polar self-assembly. Most likely these O—H \cdots O interactions are primarily responsible for the alignment of the host molecules in a head-to-tail manner along the *b*-axis. In all the compounds, the O4—H, H \cdots O2 and O4 \cdots O2 distances and O4—H \cdots O2 angles are in the range of 0.64(4)–0.89(6) Å, 1.98(6)–2.30(7) Å and 2.816(3)–2.871(6) Å and 130(7)–167(7)°, respectively. The same O-atom of the nitro group participates in an additional weak intermolecular C—H \cdots O interaction involving one of the methylene hydrogens. The C7 \cdots O2 distances and the C7—H \cdots O2 angles are in the ranges of 3.336–3.407 Å and 146–147°, respectively. These O—H \cdots O and C—H \cdots O interactions connect the complex molecules and a polar two-dimensional layered structure is formed (Figures 4). In the channels formed by the parallel layers of the complex molecules, the guest molecules are trapped and oriented in a polar order. The methylene groups of the 1,2-dihaloethane are involved in intermolecular C—H \cdots O interactions with the other O-atom of the nitro group (Figures 5 and 6). The C16 \cdots O3 distance and the C16—H \cdots O3 angle are within of 3.195(11)–3.35(4) Å and 149–157° for 3·C₂H₄Cl₂, 4·C₂H₄Cl₂,

3·C₂H₄Br₂ and **4**·C₂H₄Br₂. These C–H···O interactions act as bridges between the parallel layers of the complex molecules and a three-dimensional network with the polar alignment of both host and guest molecules is formed. In the asymmetric units of **3**·CH₃CN and **4**·CH₃CN, the CH₃CN molecules are on the crystallographic two-fold axis. The N- and the two C-atoms are at special positions. Thus the hydrogen atoms of the methyl group are disordered. However, the distance between this methyl C-atom and one of nitro group O-atom indicates a C–H···O type of interaction in both cases. As a result the CH₃CN molecules are oriented in a perfectly polar manner and the C–H···O interactions bridge the parallel layers of the complex molecules (Figure 7).

Table 8. Geometrical parameters for the hydrogen bonds

Compound	D ... A	(D–H)/Å	d(H···A)/Å	D(D···A)/Å	D–H···A/°
3 ·CH ₃ CN	O(4) – O(2)	0.64(4)	2.20(4)	2.824(3)	167(7)
	C(7) – O(2)	0.97	2.55	3.392(5)	146
	C(16) – O(3)			3.339	
4 ·CH ₃ CN	O(4) – O(2)	0.66(3)	2.19(3)	2.827(2)	163(5)
	C(7) – O(2)	0.97	2.54	3.390(4)	146
	C(16) – O(3)			3.347	
3 ·C ₂ H ₄ Cl ₂	O(4) – O(2)	0.86(6)	2.03(7)	2.846(3)	160(9)
	C(7) – O(2)	0.97	2.54	3.388(4)	146
	C(16) – O(3)	0.97	2.41	3.285(14)	150
4 ·C ₂ H ₄ Cl ₂	O(4) – O(2)	0.89(5)	1.98(6)	2.816(3)	156(7)
	C(7) – O(2)	0.97	2.48	3.336(4)	147
	C(16) – O(3)	0.97	2.33	3.195(11)	149
3 ·C ₂ H ₄ Br ₂	O(4) – O(2)	0.78(6)	2.30(7)	2.871(6)	130(7)
	C(7) – O(2)	0.97	2.56	3.403(8)	146
	C(16) – O(3)	0.97	2.43	3.34(4)	156
4 ·C ₂ H ₄ Br ₂	O(4) – O(2)	0.76(8)	2.26(8)	2.868(6)	138(7)
	C(7) – O(2)	0.97	2.56	3.407(8)	146
	C(16) – O(3)	0.97	2.44	3.35(4)	157

In each case, the polar alignments of host and guest molecules are along the *b*-axis. It may be noted that for all the inclusion complexes with **3** and **4** the molecular dipole axis is along the *b*-axis or parallel to the *b*-axis. The polar alignments are in opposite directions due to the enantiomeric relationship between the two host molecules and that between the two guest molecules for all the inclusion complexes with opposite chirality (Figures 8,9,10). Details of the hydrogen bonding parameters are given in Table 8.

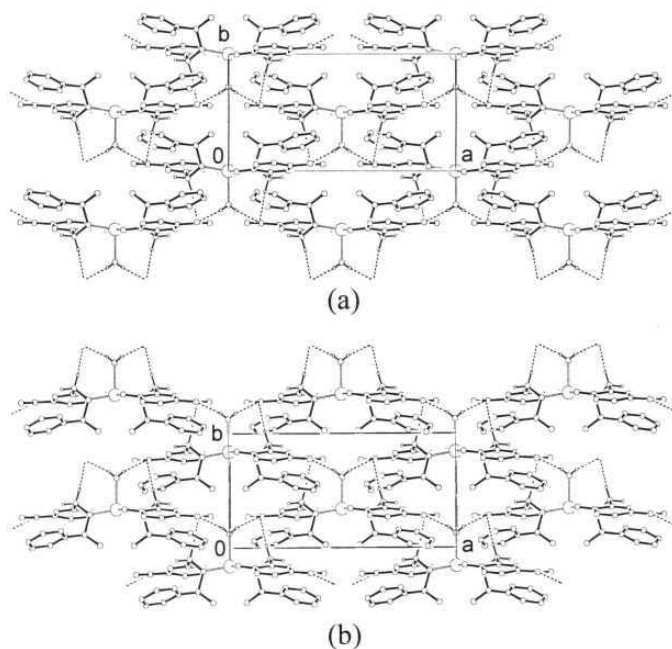


Figure 4. View of the two-dimensional layered structures of (a) **3** and (b) **4** along the *c*-axis in all the inclusion compounds; Only the H_2O and the CH_2 group H-atoms involved in the non-covalent interactions (dashed lines) are shown.

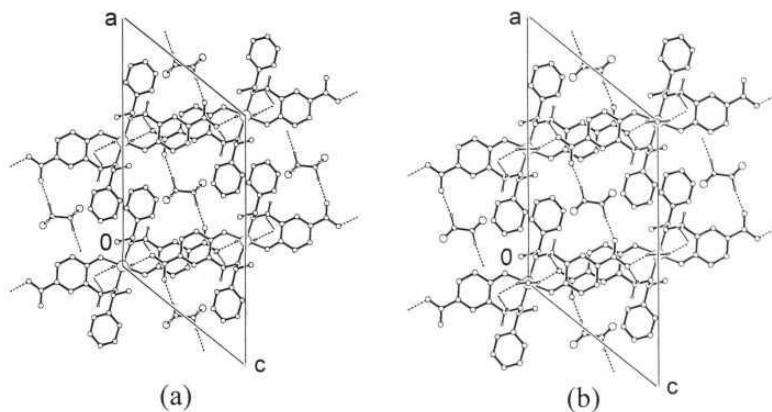


Figure 5. Projections of the crystal lattices of (a) $3 \cdot \text{C}_2\text{H}_4\text{Cl}_2$ and (b) $4 \cdot \text{C}_2\text{H}_4\text{Cl}_2$ onto the *ac*-plane.

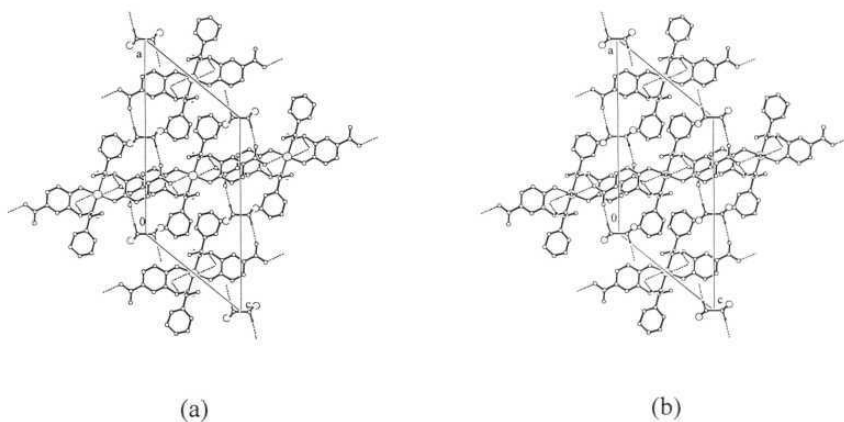
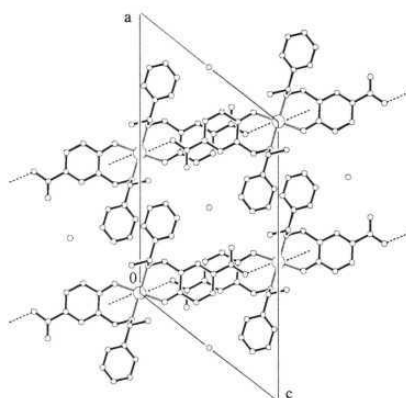
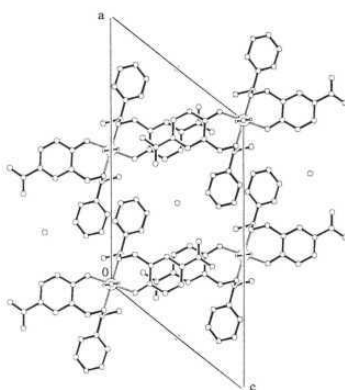


Figure 6. Projections of the crystal lattices of (a) $3 \cdot \text{C}_2\text{H}_4\text{Br}_2$ and (b) $4 \cdot \text{C}_2\text{H}_4\text{Br}_2$ onto the *ac*-plane.



(a)



(b)

Figure 7. Projections of the crystal lattices of (a) $1 \cdot \text{CH}_3\text{CN}$ and (b) $2 \cdot \text{CH}_3\text{CN}$ onto the *ac*-plane.

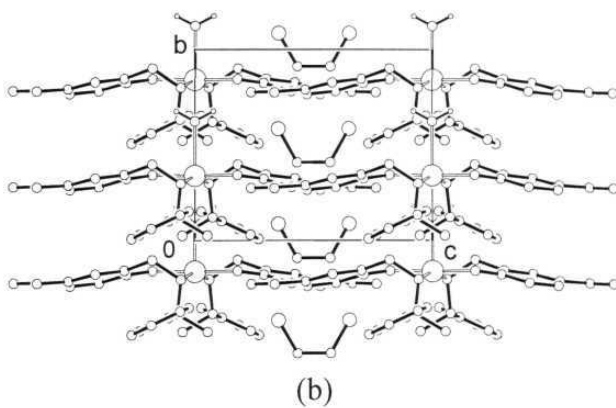
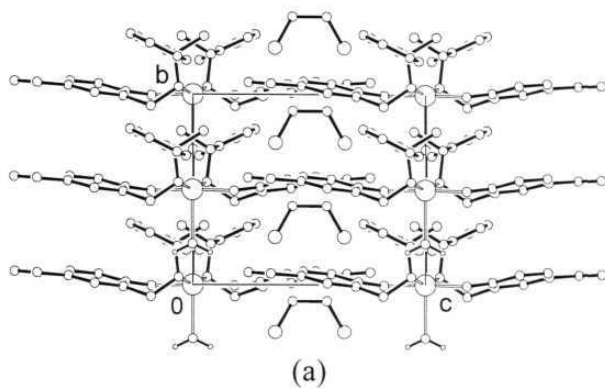
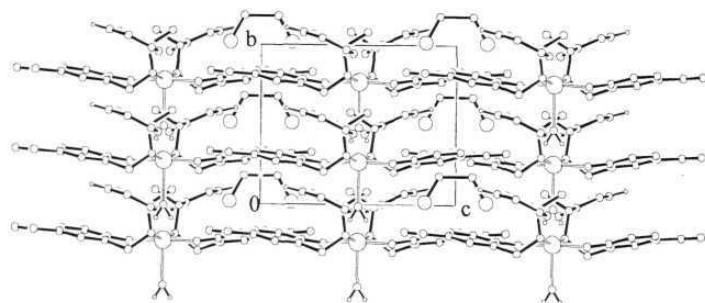
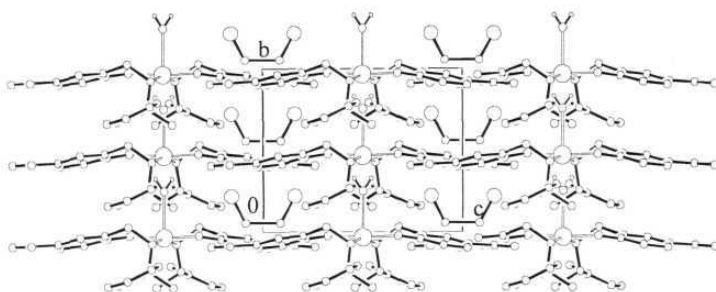


Figure 8. Polar alignments of (a) $3 \cdot \text{C}_2\text{H}_4\text{Cl}_2$ and (b) $4 \cdot \text{C}_2\text{H}_4\text{Cl}_2$ viewed along the a -axis; H-atoms of the ligands and 1,2-dichloroethane are omitted for clarity.

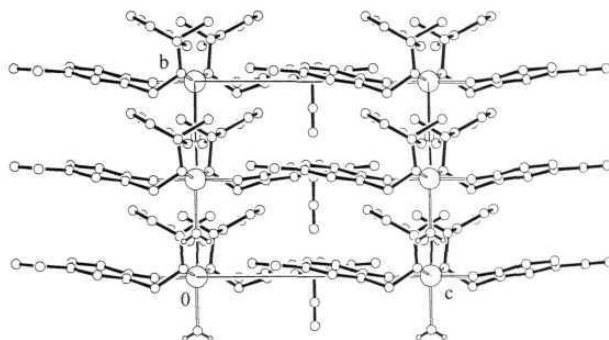


(a)

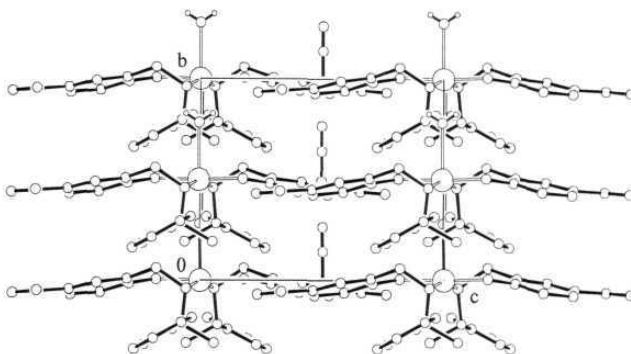


(b)

Figure 9. Polar alignments of (a) $3 \cdot \text{C}_2\text{H}_4\text{Br}_2$ and (b) $4 \cdot \text{C}_2\text{H}_4\text{Br}_2$ viewed along the a -axis; H-atoms of the ligands and 1,2-dibromoethane are omitted for clarity.



(a)



(b)

Figure 10. Polar alignments of (a) **3**·(CH₃CN) and (b) **4**·(CH₃CN) viewed along the *a* axis.

3.4.6. Enantio-specific inclusion of chiral 1,2-dichloroethane rotamers

As discussed in the previous chapter, three rotamers are possible for 1,2-dichloroethane. These are *trans* or anti, *cis* or eclipsed and *gauche* forms. Eclipsed form is energetically most unfavorable. Between the *trans* and the *gauche* forms the former is more stable (by $\sim 1 \text{ kcal mol}^{-1}$).¹⁶ The *gauche* form is chiral and also polar. One of the enantiomers has the right-handed (*P*) helical form and the other one has the left-handed (*M*) helical form. Report on inclusion crystal of a chiral host compound with an optically active rotamer of 1,2-dichloroethane is very rare.¹⁵ Enantiomeric pair of inclusion compounds with opposite chirality, $3 \cdot \text{C}_2\text{H}_4\text{Cl}_2$ and $4 \cdot \text{C}_2\text{H}_4\text{Cl}_2$ exhibit mirror image relationship in both molecular level as well as in supramolecular level. In both the structures, the asymmetric unit contains one-half of the 1,2-dichloroethane molecule. The other half can be generated by rotation about a two-fold axis passing through the mid-point of the C–C bond. The molecule is in *gauche* form in each structure (Figure 11). The torsion angles involving Cl–C–C–Cl are $63(1)^\circ$ and $64.6(9)^\circ$ in $3 \cdot \text{C}_2\text{H}_4\text{Cl}_2$ and $4 \cdot \text{C}_2\text{H}_4\text{Cl}_2$, respectively. The 1,2-dichloroethane molecule is trapped in the *P*-form in $3 \cdot \text{C}_2\text{H}_4\text{Cl}_2$ (Figure 11a). On the other hand, in the case of $4 \cdot \text{C}_2\text{H}_4\text{Cl}_2$ only the *M*-form of it exists (Figure 11b). Thus the chiral host complexes **3** and **4** produce the appropriate frameworks in the crystal lattice for exclusive accommodation of the *P*- and *M*-form of 1,2-dichloroethane, respectively (figure 12). There is no report on inclusion crystals of a chiral rotamers of 1,2-dichloroethane with the polar order of the guest molecules in the host framework. The crystals of $3 \cdot \text{C}_2\text{H}_4\text{Cl}_2$ and $4 \cdot \text{C}_2\text{H}_4\text{Cl}_2$ provide examples for not only enantio-selective isolation of the *P*- and *M*-form of the chiral rotamers but also for the unprecedented perfectly polar alignment of both host and guest molecules in the crystal lattice.

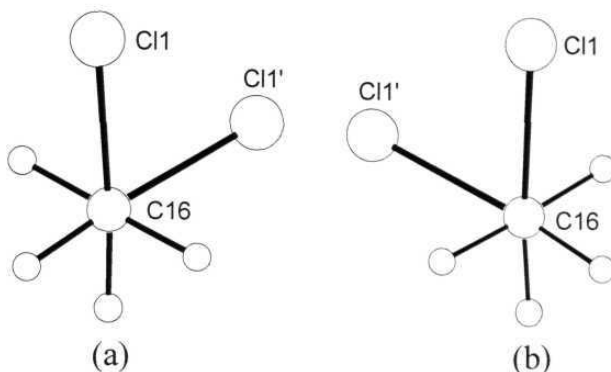


Figure 11: (a) The right-handed (*P*) and (b) the left-handed (*M*) helical forms of 1,2-dichloroethane in **3**·(*P*)-C₂H₄Cl₂ and **4**·(*M*)-C₂H₄Cl₂, respectively.

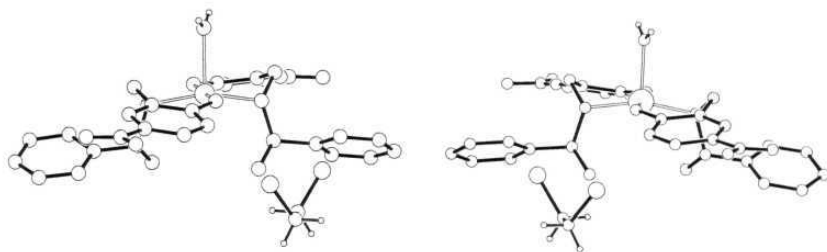


Figure 12: Molecular structures of **3**·(*P*)-C₂H₄Cl₂ and **4**·(*M*)-C₂H₄Cl₂

3.4.7. Enantio-specific inclusion of chiral 1,2-dibromoethane rotamers

Three rotamers are also possible for 1,2-dibromoethane (Figure 13). These are *trans* or *anti*, *cis* or eclipsed and *gauche* forms.¹⁶ The *trans* form ($\theta = 180^\circ$) is less energetic and favorable conformation. On the other hand, the eclipsed form ($\theta = 0^\circ$) of the 1,2-dibromoethane is most unfavorable, because of instability due to the strong repulsions between not only the heavier bromo atoms but also between the hydrogen atoms. In the solid state, the isolation of the *gauche* form ($\theta = 60^\circ$) of 1,2-dibromoethane never been reported.

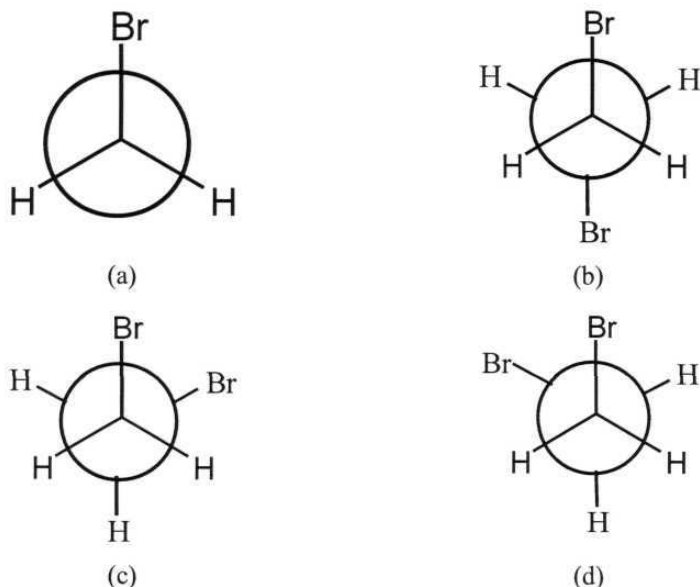


Figure 13. Possible conformations for 1,2-dibromoethane (a) eclipsed form ($\theta = 0^\circ$), (b) staggered form ($\theta = 180^\circ$), (c) *P*-gauche form ($\theta = +60^\circ$) and (d) *M*-gauche form ($\theta = -60^\circ$)

The molecules which adopt *gauche*, nearly *gauche* or nearly *eclipsed* forms are chiral and also polar. One of the enantiomers has the right-handed (*P*) helical form and the other one has the left-handed (*M*) helical form. The inclusion compounds $3 \cdot \text{C}_2\text{H}_4\text{Br}_2$ and $3 \cdot \text{C}_2\text{H}_4\text{Cl}_2$ are isostructural. Similarly the inclusion compounds $4 \cdot \text{C}_2\text{H}_4\text{Br}_2$ and $4 \cdot \text{C}_2\text{H}_4\text{Cl}_2$ are isostructural. In the structures of $3 \cdot \text{C}_2\text{H}_4\text{Br}_2$ and $4 \cdot \text{C}_2\text{H}_4\text{Br}_2$ (Figure 15) the asymmetric unit contains one-half of the 1,2-dibromoethane molecule. The other half can be generated by rotation about a two-fold axis passing through the mid-point of the C–C bond. The molecule is in nearly *gauche* form in each structure (Figure 14). The torsion angles involving Br–C–C–Br are 54.06° and 52.74° in $3 \cdot \text{C}_2\text{H}_4\text{Br}_2$ and $4 \cdot \text{C}_2\text{H}_4\text{Br}_2$, respectively. The 1,2-dibromoethane molecule is trapped in the *P*-form in $3 \cdot \text{C}_2\text{H}_4\text{Br}_2$ (Figure 14a). On the other hand, in the case of $4 \cdot \text{C}_2\text{H}_4\text{Br}_2$ only the *M*-form of it exists (Figure 14b). To the best of our knowledge,

this is the first example of enantio-specific isolation of right handed (*P*) and left handed (*M*) nearly gauche forms of 1,2-dibromoethane using the inclusion phenomenon. The structural features of the inclusion compounds **3**·(*P*)-C₂H₄Br₂ and **4**·(*M*)-C₂H₄Br₂ show not only the first isolation of chiral forms of 1,2-dibromoethane, but also perfectly polar alignment of 1,2-dibromoethane in the crystal lattice (see section 3.4.5).

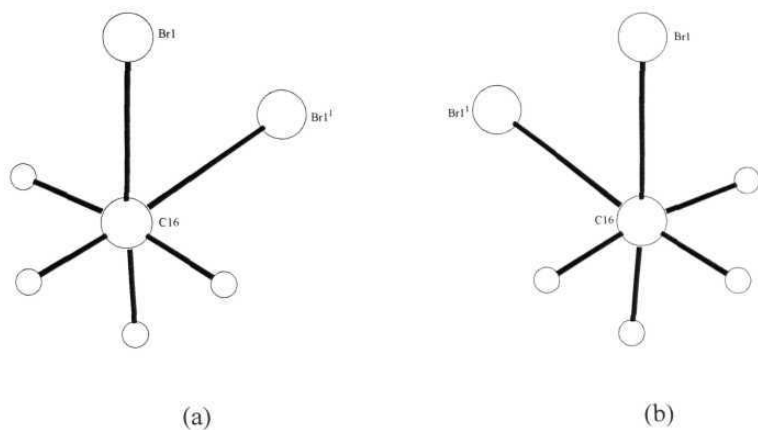


Figure 14. (a) The right-handed (*P*) and (b) the left-handed (*M*) helical forms of 1,2-dibromoethane in **3**·(*P*)-C₂H₄Br₂ and **4**·(*M*)-C₂H₄Br₂, respectively.

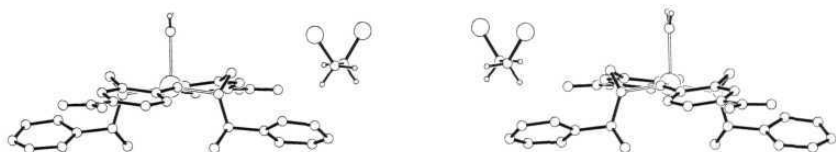


Figure 15. Molecular structures of **3**·(*P*)-C₂H₄Br₂ and **4**·(*M*)-C₂H₄Br₂

3.5. Conclusion

Self-assembly *via* intermolecular non-covalent interactions is one of the powerful tools for designing and synthesising polar crystals as well as enantio-selective chiral host frameworks. The spatial disposition of the functional groups participating in the intermolecular non-covalent interactions is expected to control the alignment of the host and guest molecules as well as spontaneous resolution of chiral guest compounds. The structures of **3**·(*P*)-C₂H₄Cl₂, **4**·(*M*)-C₂H₄Cl₂, **3**·(*P*)-C₂H₄Br₂ and **4**·(*M*)-C₂H₄Br₂ reveal this functional group directed alignment of molecules and enantio-selective trapping of guest molecules. The self-assembly of the host molecules (**3** and **4**) occurs through the O–H···O interactions and the guest molecules are held *via* the C–H···O interactions. In both intermolecular interactions, ligand nitro group O-atoms act as the acceptors. The positions and orientations of the nitro groups on the enantiomeric ligands in **3** and **4** are befitting for a perfectly polar alignment of the host molecules and for enantio-selective confinement of the chiral rotamers of 1,2-dihaloethane in a polar order.

3.6. References

1. *Molecular Nonlinear Optics: Materials, Physics and Devices*, ed. J. Zyss, Academic Press, London **1994**; *Handbook of Laser Science and Technology*, ed. M. J. Webber, CRC Press, Boca Raton, FL, **1995**.
2. (a) J. Zyss, J.-F. Nicoud and M. Coquillay, *J. Chem. Phys.*, **1984**, 81, 4160; (b) D. E. Eaton, *Science*, **1991**, 253, 281.
3. (a) S. R. Marder, J. W. Perry and W. P. Scafer, *Science*, **1989**, 245, 626; (b) S. R. Marder, J. W. Perry and C. P. Yakymyshyn, *Chem. Mater.*, **1994**, 6, 1137; (c) S. P. Anthony and T. P. Radhakrishnan, *Chem. Commun.*, **2001**, 931; (d) P. K. Thallapally, G. R. Desiraju, M. Bagieu-Beucher, R. Masse, C. Bourgogne and J.-F. Nicoud, *Chem. Commun.*, **2002**, 1052; (e) A. Jouaiti, M. W. Hosseini and N. Kyritsakas, *Chem. Commun.*, **2002**, 1898.

4. (a) W. Tam, D. F. Eaton, J. C. Calabrese, I. D. Williams, Y. Wang and A. G. Anderson, *Chem. Mater.*, **1989**, 1, 128; (b) O. König, H.-B. Bürgi, T. Armbruster, J. Hullinger and T. Weber, *J. Am. Chem. Soc.*, **1997**, 119, 10632; (c) A. Quintel, J. Hullinger, and M. Wübbenhorst, *J. Phys. Chem. B*, **1998**, 102, 4277; (d) K. T. Holman, A. M. Pivovar and M. D. Ward, *Science*, **2001**, 294, 1907.
5. (a) X. X. Zhang, J. S. Bradshaw and R. M. Izatt, *Chem. Rev.*, **1997**, 97, 3313; (b) E. Brunet, *Chirality*, **2002**, 14, 135; (c) L. Pérez-García and D. B. Amabilino, *Chem. Soc. Rev.*, **2002**, 31, 342; (d) B. Kesanli and W. Lin, *Coord. Chem. Rev.*, **2003**, 246, 305; (e) L.-X. Dai, *Angew. Chem. Int. Ed.*, **2004**, 43, 5726; (f) M. A. Mateos-Timoneda, M. Crego-Calama and D. N. Reinhoudt, *Chem. Soc. Rev.*, **2004**, 33, 363.
6. (a) F. Averseng, P.G. Lacroix, I. Malfant, F. Dahan, K. Nakatani, *J. Mater. Chem.*, **2000**, 10, 1013; (b) S.R. Korupoju, N. Mangayarkarasi, S. Ameerunisha, E.J. Valente, P.S. Zacharias, *J. Chem. Soc., Dalton Trans.*, **2000**, 2845; (c) C. Evans, D. Luneau, *J. Chem. Soc., Dalton Trans.*, **2002**, 83.
7. (a) L. L. Koh, J.O. Ranford, W. T. Robinson, J. O. Svensson, A. L. C. Tan, D. Wu, *Inorg. Chem.*, **1996**, 35, 6466; (b) J.J. Vittal, X. Yang, *Cryst. Growth Des.*, **2003**, 3, 635; (c) C. T. Yang, H. Moubaraki, K.S. Murray, J. J. Vittal, *J. Chem. Soc., Dalton Trans.*, **2003**, 880.
8. SMART & SAINT Software Reference Manuals, Version 6.22, Bruker AXS Analytic X-Ray Systems, Inc., Madison, WI, **2000**.
9. G. M. Sheldrick, SADABS, Software for Empirical Absorption Correction, University of Göttingen, Germany, **2000**.
10. SHELXTL Reference Manual, Version 5.1, Bruker AXS, Analytic X-Ray Systems, Inc., WI, **1997**.
11. L. J. Farrugia, *J. Appl. Cryst.*, 1997, 30, 567.
12. A. L. Spek, PLATON, *Molecular Graphics Software*, University of Glasgow, UK, 2001.
13. V. K. Muppidi, P. S. Zacharias and S. Pal, *Inorg. Chem. Commun.*, **2005**, 8, 543.

14. H. D. Flack, *Acta Crystallogr.*, **1983**, A39, 876
15. P. V. Sluis and A. L. Spek, *Acta Crystallogr., Sect. A*, **1990**, 46, 194.
16. (a) E. L. Eliel and S. H. Wilen, *Stereochemistry of Organic Compounds*, Wiley, New York, **1994**; (b) D. Nasipuri, *Stereochemistry of Organic Compounds*, New Age International (P) Limited, Publishers, New Delhi, **1994**.
17. F. Toda, K. Tanaka and R. Kuroda, *Chem. Commun.*, **1997**, 1227.

Mononuclear Copper(II) complexes with chloro-substituted chiral reduced Schiff bases: Activated C—H...O interaction induced Self-assembly to homo chiral helices.

4.1. Abstract

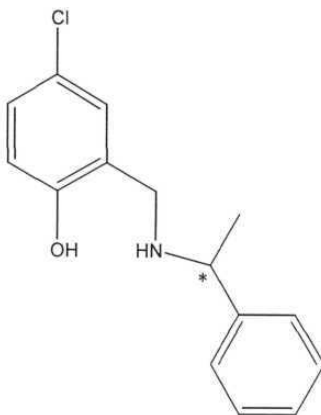
The enantiomerically pure chiral reduced Schiff bases N-(2-hydroxy-5-chlorobenzyl)-(R)- α -methylbenzylamine (HL⁵), N-(2-hydroxy-5-chlorobenzyl)-(S)- α -methylbenzylamine (HL⁶) were prepared by condensation of 5-chlorosalicylaldehyde with (R)- or (S)- α -methylbenzylamine followed by reduction with sodium borohydride in methanol. Reactions of these ligands with CuCl₂·2H₂O and NaOH in 2:1:2 stoichiometric ratio produced mononuclear complexes of general formula [CuLⁿ₂] (n = 5, 6). We were able to crystallize these complexes in both solvated and unsolvated forms. X-ray crystallographic studies revealed that the solvated complexes (**5A**, **6A**) crystallize in the space group *P*2₁2₁2 and the unsolvated complexes (**5**, **6**) crystallize in the space group *P*2₁2₁2₁. The Cu(II) center is in distorted N₂O₂ square planar assembled by the two N,O-donor ligands. The complexes (**5**, **5A**) with HL⁵ have the Δ absolute configuration and the complexes (**6**, **6A**) with HL⁶ have the Λ absolute configuration around the metal center. In the crystal lattice, the molecules self assemble via C—H...O interactions into infinite supramolecular helices. The C—H...O interactions are highly specific and involve the activated C-H group (*ortho* to the chloro group) and metal coordinated phenolate (MCP) oxygen. The complexes with the (R)- enantiomeric ligand form right handed helices. On the other hand, the complexes with the (S)-enantiomeric ligand form left-handed helices. Thus the complexes with opposite chirality exhibit mirror image relationship in molecular as well as in supramolecular level.

4.2. Introduction

Helical architecture is vital for biologically important molecules such as proteins, peptides and nucleic acids.¹ In self assembly process, chiral molecules assemble *via* non-covalent interactions such as metal-ligand binding, hydrogen bonds and π - π interaction which often lead to the generation of helical architectures.² Applications are therefore anticipated as functional solid materials for nonlinear optics,³ molecular recognition⁴ and asymmetric catalysis.⁵ The combined coordination chemistry and hydrogen bonding approach have given particularly interesting supramolecular systems.⁶ Recently, weak hydrogen bonds (such as C-H \cdots O) have received much attention in the construction of novel self assemblies like helices, host-guest, square grids and so on.⁷ Evidence for C-H \cdots O hydrogen bond assisted recognition of a pyrimidine base in the parallel DNA triple helical motif is reported.⁸ The C-H group is activated if it is α to the carbon atom bound to an electron withdrawing group.⁹ Such hydrogen bonds between main-chain C $_{\alpha}$ -H groups and back bone or side chain oxygen atoms are often observed in protein molecules.¹⁰ In our earlier work we reported that chiral C₂ symmetric ferrocene molecule and pseudo C₂ symmetric zinc(II) complex exhibit helical self assembly *via* weak hydrogen bonded interactions.¹¹ The flexibility and the influence of intrinsic ligand chirality generate novel supramolecular networks like helical coordination polymers, chiral capsules etc. These studies were focused on how the metal-ligand coordination leads to generation of this interesting supramolecular networks.¹²

In the previous chapters, we have described Cu(II) complexes with chiral reduced Schiff bases and enantio-specific inclusion of chiral rotamers in their crystal lattices. In this chapter, synthesis and structural investigations of new mononuclear Cu(II) bis complexes with R- and S- enantiopure reduced Schiff bases HL⁵ and HL⁶ are discussed. In the crystal lattice, the complex molecules exhibit helical and/or host-guest self assemblies *via* hydrogen bonded interactions. Interestingly, these complexes crystallize in both solvated and unsolvated forms. The solvated forms crystallize in the orthorhombic space group $P2_12_12$, whereas the unsolvated forms

(apohost) crystallize in the orthorhombic space group $P2_12_12_1$. All these complexes show infinite one dimensional helical self assembly *via* activated C-H...O interactions.



HL⁵ = N-(2-hydroxy-5-chlorobenzyl)-(R)- α -methylbenzylamine

HL⁶ = N-(2-hydroxy-5-chlorobenzyl)-(S)- α -methylbenzylamine

4.3. Experimental

4.3.1. Materials

All commercially available chemicals and the solvents utilized in this work were of analytical grade and were used as obtained. The chemicals and the sources are as follows: 5-chlorosalicylaldehyde, (R)- α -methylbenzylamine and (S)- α -methylbenzylamine, sodium borohydride Lancaster (England); CDCl_3 , methanol, dichloromethane, hexane, acetonitrile, Acros (India); $\text{CuCl}_2 \cdot 2\text{H}_2\text{O}$, anhydrous sodium sulphate, sodium hydroxide, S. D. Fine Chem. Ltd. (India).

4.3.2. Physical measurements

Elemental analysis was carried out on a Perkin-Elmer 240C CHN analyzer. Infrared spectra were collected by using KBr pellets on a Jasco-5300 FT-IR spectrophotometer. NMR spectra were recorded on a Bruker ACF-200 spectrometer.

A Shimadzu 3101-PC UV/vis/NIR spectrophotometer was used to record the electronic spectra. X-ray crystallographic experiments were performed using a Bruker-Nonius SMART APEX CCD single crystal diffractometer. A Sherwood scientific magnetic susceptibility balance was used to measure the magnetic moments.

4.3.3. Synthesis of the reduced Schiff bases and the complexes

(a) N-(2-hydroxy-5-chlorobenzyl)-(R)- α -methyl benzyl amine, HL⁵

A methanol solution (30 ml) of 5-chlorosalicylaldehyde (1.56 g, 10 mmol) was added to a methanol solution (30 ml) of (R)- α -methylbenzylamine (1.21 g, 10 mmol) and stirred at room temperature for ½ h. To the resulting yellow solution 0.74 g (20 mmol) of NaBH₄ was added and the mixture was stirred for another ½ h until a colourless solution was obtained. The reaction mixture was evaporated to dryness on a rotary evaporator followed by addition of 100 ml of water. The suspended solid in water was extracted with (2 x 30 ml) CH₂Cl₂. The CH₂Cl₂ extracts were dried over anhydrous Na₂SO₄ and then evaporated to dryness. The compound (HL⁵) was obtained in the form of white solid.

Yield : 2.01 g, (80 %)

M. F. : C₁₅H₁₆NOCl

IR ($\nu_{\text{N-H}}$ cm⁻¹, KBr pellet) : ~ 3302

¹H NMR (CDCl₃, δ , ppm) : 1.48 (d, 3H, CH₃), 3.71 and 3.88 (2H, CH_AH_B), ~ 3.78 (q, 1H, CH(CH₃)), 6.86 (s, 1H, *ortho* to both Cl and CH₂), 6.79 (d, 1H, *ortho* to phenolic-OH), 7.09 (d, 1H, *ortho* to Cl), 7.24-7.39 (m, 5H, phenyl protons).

Anal. calcd. for C₁₅H₁₆NOCl : C, 68.83; H, 6.16; N, 5.35

Found : C, 69.07; H, 6.06; N, 5.48.

(b) N-(2-Hydroxy-5-chlorobenzyl)-(S)- α -methyl benzyl amine, HL⁶

HL⁶ was prepared in similar yield by following the same procedure as described for HL⁵ using (S)- α -methylbenzylamine instead of (R)- α -methylbenzylamine.

Yield : 2.0 g, (79 %)

M. F. : C₁₅H₁₆ClNO

IR ($\nu_{\text{N-H}}$ cm⁻¹, KBr pellet) : ~ 3302

¹H NMR (CD₃CN, δ , ppm) : 1.48 (d, 3H, CH₃), 3.71 and 3.88 (2H, CH_AH_B), ~ 3.78 (q, 1H, CH(CH₃)), 6.86 (s, 1H, *ortho* to both Cl and CH₂), 6.79 (d, 1H, *ortho* to phenolic-OH), 7.09 (d, 1H, *ortho* to Cl), 7.24-7.39 (m, 5H, phenyl protons).

Anal. calcd. for C₁₅H₁₆NOCl : C, 68.83; H, 6.16; N, 5.35

Found : C, 68.96; H, 6.08; N, 5.43.

(c) [CuL⁵₂] (5): A methanol solution (10 ml) of CuCl₂·2H₂O (0.089 g, 0.5 mmol) was added to a methanol solution (20 ml) of HL⁵ (0.261 g, 1 mmol) and NaOH (0.040 g, 1 mmol). The mixture was stirred at room temperature for 1 h. The solvent was removed under vacuum and the residue was dissolved in dichloromethane and dried over sodium sulphate. Evaporation of the dichloromethane under vacuum condition gave dark brown solid. The complex thus obtained was recrystallized from acetonitrile and obtained in the unsolvated form. Yield 0.41 g (70%), Anal. calcd. for CuC₃₀H₃₀N₂O₂Cl₂: C, 61.59; H, 5.17; N, 4.79. Found: 61.42, 5.31, 4.64. Selected infrared bands (cm⁻¹): 3260(w), 3032(w), 2964(w), 1591(s), 1550(w), 1469(vs), 1354(w), 1292(vs), 1180(w), 1087(m), 1045(m), 1005(m), 970(m), 895(w), 873(w), 823(w), 777(m), 754(w), 704(s), 679(s), 611(w), 557(w), 536(w), 493(w). Electronic spectral data in CHCl₃ (λ , nm (ϵ , M⁻¹cm⁻¹)): 676 sh (198), 438 (2,130), 346 sh (1,407), 272 (8,254). Effective magnetic moment at 298 K: 1.77 μ_B

(d) [CuL⁶₂] (6): A methanol solution (10 ml) of CuCl₂·2H₂O (0.089 g, 0.5 mmol) was added to a methanol solution (20 ml) of HL⁶ (0.261 g, 1 mmol) and NaOH (0.040 g, 1mmol). The mixture was stirred at room temperature for 1 h. The solvent was removed under vacuum and the residue was dissolved in dichloromethane and dried over sodium sulphate. Evaporation of the dichloromethane under vacuum gave dark brown solid. The complex thus obtained was recrystallized from acetonitrile and obtained in the unsolvated form. Yield 0.41 g, (70%). Anal. calcd. for CuC₃₀H₃₀N₂O₂Cl₂: C, 61.59; H, 5.17; N, 4.79. Found: 61.38, 5.26, 4.71. Selected infrared bands (cm⁻¹): 3260 (w), 3032(w), 2964(w), 1591(s), 1552(w), 1469(vs), 1354(w), 1292(vs), 1180(w), 1086(m), 1045(m), 1005(m), 970(m), 895(w), 873(w), 823(w), 775(m), 754(w), 704(s), 679(s), 611(w), 557(w), 536(w), 493(w). Electronic spectral data in CHCl₃ (λ, nm (ε, M⁻¹cm⁻¹)): 676 sh (208), 438 (2,341), 346 sh (1,555), 272 (8,882). Effective magnetic moment at 298 K: 1.76 μ_B

4.3.4. X-ray crystallography

Single crystals of **5** and **6** were grown from acetonitrile while **5A** and **6A** were grown from CH₂Cl₂–hexane (1:1) mixture by slow evaporation at ambient temperature. X- ray data were collected for dark brown crystals of **5**, **6**, **5A** and **6A** on a Bruker-Nonius SMART APEX CCD single crystal diffractometer using graphite monochromated Mo-Kα radiation (0.71073Å). The SMART software was used for intensity data acquisition and the SAINT-Plus software¹³ was used for data extraction. In each case, absorption correction was performed with help of SADABS program.¹⁴ The SHELXTL package¹⁵ was used for structure solution and least square refinement on F². All the non hydrogen atoms were refined anisotropically. The secondary amine hydrogen atoms and lattice water hydrogen atoms were located in a difference map and refined with geometric restraints. All other hydrogen atoms were included in the structure factor calculation by using a riding model. The hexane molecules found in the lattice of **5A** and **6A** showed disorder. The ORTEP3¹⁶ and the PLATON¹⁷

softwares were used for molecular graphics. The significant X-ray crystallographic data are given in Tables 1 and 2.

Table 1. Crystallographic data for **5** and **6**

Compound	5	6
Molecular formula	C ₃₀ H ₃₀ Cl ₂ CuN ₂ O ₂	C ₃₀ H ₃₀ Cl ₂ CuN ₂ O ₂
Crystal dimensions / mm	0.24 x 0.31 x 0.18	0.40 x 0.34 x 0.32
Host-guest ratio	-	-
<i>T</i> /K	298	298
<i>M</i>	585.00	585.00
Crystal system	Orthorhombic	Orthorhombic
Space group	<i>P</i> 2 ₁ 2 ₁ 2 ₁	<i>P</i> 2 ₁ 2 ₁ 2 ₁
<i>a</i> /Å	12.5356(9)	12.5430(10)
<i>b</i> /Å	13.3293(10)	13.3376(10)
<i>c</i> /Å	16.4773(12)	16.4855(12)
α /°	90	90
β /°	90	90
γ /°	90	90
<i>V</i> /Å ³	2753.2(3)	2757.9(4)
<i>Z</i>	4	4
Observed reflections	6383	6438
Parameters	344	332
Final <i>R</i> indices	0.0519, 0.0956	0.0350, 0.0827
(<i>I</i> > 2σ(<i>I</i>))		
Goodness-of-fit on <i>F</i> ²	1.011	1.011
Largest hole and peak e/ Å ³	-0.250, 0.758	-0.224, 0.489

Table 2. Crystallographic data for **5A** and **6A**

Compound	5A	6A
Molecular formula	$C_{33.5}H_{31}Cl_2CuN_2O_{2.5}$	$C_{33.5}H_{31}Cl_2CuN_2O_{2.5}$
Crystal dimensions / mm	0.30 x 0.03 x 0.2	0.32 x 0.05 x 0.24
Host-guest ratio	1: 0.5: 0.5	1: 0.5: 0.5
<i>T</i> /K	100	298
<i>M</i>	630.04	630.04
Crystal system	Orthorhombic	Orthorhombic
Space group	$P2_12_12$	$P2_12_12$
<i>a</i> /Å	16.9258(14)	16.9060(13)
<i>b</i> /Å	13.6056(11)	13.5845(11)
<i>c</i> /Å	14.1338(11)	14.1040(11)
α /°	90	90
β /°	90	90
γ /°	90	90
<i>V</i> /Å ³	3254.8(5)	3239.1(4)
<i>Z</i>	4	4
Observed reflections	7635	7540
Parameters	378	378
Final <i>R</i> indices (<i>I</i> > 2σ(<i>I</i>))	0.0736, 0.1242	0.0816, 0.1347
Goodness-of-fit on <i>F</i> ²	1.001	1.013
Largest hole and peak e/ Å ³	-0.221, 0.438	-0.240, 0.330

4.4. Results and discussion

4.4.1. Synthesis and some properties

Chloro substituted chiral reduced Schiff bases HL^5 and HL^6 were prepared by condensation of 5-chlorosalicylaldehyde with (R)- or (S)- α -methylbenzylamine followed by reduction with sodium borohydride in methanol. The elemental analysis and spectral (infrared and proton NMR) data for HL^5 and HL^6 are very similar and consistent with the expected molecular formula and structure. Reactions of HL^5 and HL^6 with $CuCl_2$ and NaOH in 2:1:2 stoichiometry gave mononuclear complexes of general formula $[CuL^n_2]$ ($n = 5, 6$). Representative chemical diagram of these complex molecules are shown in Figure 1.

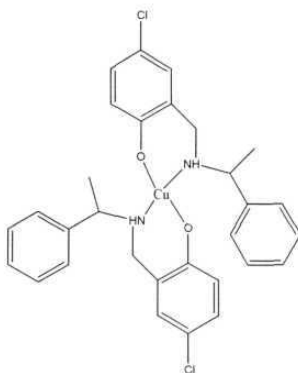


Figure 1: General molecular structure of the **5** and **6**.

The infrared spectra of both reduced Schiff bases and their complexes exhibit the N-H stretching band ($3250\text{--}3300\text{ cm}^{-1}$) for the secondary amine. The broad band around 3200 cm^{-1} is likely to be due to the lattice water molecule for solvates **5A** and **6A**. The weak bands in the range $2900\text{--}3100\text{ cm}^{-1}$ are most likely due to the aliphatic and aromatic CH stretches.

Electronic spectra of **5** and **6** in $CHCl_3$ solutions are essentially identical (Figure 2). The low intensity absorption at $\sim 676\text{ nm}$ is assigned to the d-d transition. The other intense absorptions observed in the range $438\text{--}272\text{ nm}$ are most likely due to the ligand-to-metal charge transfer and intraligand transitions.

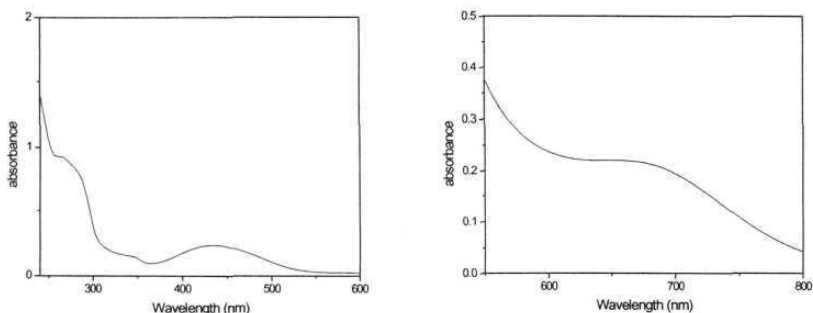


Figure 2: Electronic spectrum of **5** in CHCl_3 .

4.4.2. CSD search

A Search for activated $\text{C-H}\cdots\text{O}$ interactions was performed on the Cambridge Structural Database (November 2004 release). Primary search was performed for complexes where 4-chloro substituted metal coordinated phenolate oxygen, and the *ortho* to chloro substituent aromatic C-H participate in intermolecular $\text{C-H}\cdots\text{O}$ interaction with $\text{H}\cdots\text{O}$ distance in the range 1.8 to 2.8 Å and $\text{C-H}\cdots\text{O}$ angle in the range 120° - 180° (three carbon atoms of the aromatic ring contain hydrogen or alkyl group). Search analysis shows 66 hits within this range. Second search defined for 4-chloro substituted metal coordinated phenolate (four carbon atoms of aromatic ring contain hydrogen or alkyl group) yielded 184 hits. The analysis of these results show that in 35.86 % of metal-organic crystals, C-H groups *ortho* to chloro substituent are activated and participate in $\text{C-H}\cdots\text{O}$ interactions. These search results encouraged us to study the activated $\text{C-H}\cdots\text{O}$ interactions in the present complexes. η

4.4.3. Crystallization

Unsolvated forms (**5** and **6**) were obtained by recrystallization of the complexes from acetonitrile as dark brown block shaped crystals. X-ray crystallographic analysis reveals that both the complexes crystallize in the

orthorhombic space group $P2_12_12_1$. In each case, the asymmetric unit contains one full molecule. Alternatively, solvated forms (**5A** and **6A**) were obtained by recrystallization of these complexes from dichloromethane/hexane as dark brown plate like crystals. X-ray crystallographic analysis reveals that both complexes crystallize in slightly different orthorhombic space group $P2_12_12$. In each case, the asymmetric unit contains one full complex molecule, half water and half *n*-hexane molecules. The *n*-hexane molecule is disordered and the water oxygen sits at the special position. Notably, both solvated complexes (**5A** and **6A**) of opposite chirality crystallize in plate-like morphology in similar crystallization conditions. On the other hand, guest-free complexes (**5** and **6**) of opposite chirality crystallize in cubic morphology in similar crystallization conditions. The R factors of the solvated complexes are slightly higher when compared with those of the unsolvated complexes. This is most probably due to severe guest disorder. However, the host molecules are well ordered for solvated complexes. The absolute configurations of the complex molecules (Figure 3) are successfully confirmed by flack parameter values¹⁸ and details are given in Table 3.

Table 3: Absolute configurations of **5**, **5A**, **6** and **6A**

Compound	C(8), C(23) configuration	N(1), N(2) Configuration	Flack Parameter value
5	R, R	R, R	0.001(13)
5A	R, R	R, R	0.01(2)
6	S, S	S, S	0.002(9)
6A	S, S	S, S	0.02(2)

4.4.4. Description of Structures

The coordination environment around the metal ion in all the mononuclear complexes of the solvated and unsolvated forms is grossly similar with respect to bond parameters (Table 4). In these complexes, the ligands coordinate through the phenolato-O and the secondary amine N-atoms forming two five-membered chelate rings and a distorted N_2O_2 square plane around the Cu(II) center. The Cu-N distances (2.021(3)-2.037(3) Å) are significantly longer than Cu-O distances (1.880(2)-1.897(4)

Å). The chelate bite angles are in the range of $84.79(7)^\circ$ - $94.30(8)^\circ$. The trans O-Cu-O angles are in the range of $163.85(19)^\circ$ - $167.06(9)^\circ$. Although there are no significant changes in the metal to coordinating atom bond distances for the solvated and the unsolvated complexes, noticeable changes are observed in the case of bond angles. The molecular structures of **5** and **6** are mirror images of each other (Figure 3). The dihedral angles between the plane defined by Cu, N1 and O1 and that defined by Cu, N2 and O2 are $13.1(2)^\circ$, $21.37(31)^\circ$, $12.98(13)^\circ$ and $21.29(33)^\circ$ for **5**, **5A**, **6** and **6A**, respectively. These values indicate a tetrahedral distortion of the N_2O_2 plane. Solvated complexes show more tetrahedral distortion when compared with unsolvated complexes. The chiral information of the helical structure very often is embedded in the preferred coordination geometry at the metal ions. Unsymmetrical bidentate ligands in pseudo-tetrahedral and pseudo-octahedral mononuclear metal complexes already possess helical twist and are loosely called helical.^{2a,2b} Alternatively, in a tetrahedrally distorted square planar complex the metal ion will also force the ligands to adopt a helically twisted configuration. Herein complexes with HL^5 exhibit right handed helical twist (Δ or P), whereas complexes with HL^6 exhibit left handed helical twist (Λ or M) of the ligands around the central copper ion (Figure 4). This feature is retained for both solvated and unsolvated forms of the complexes with opposite chirality.

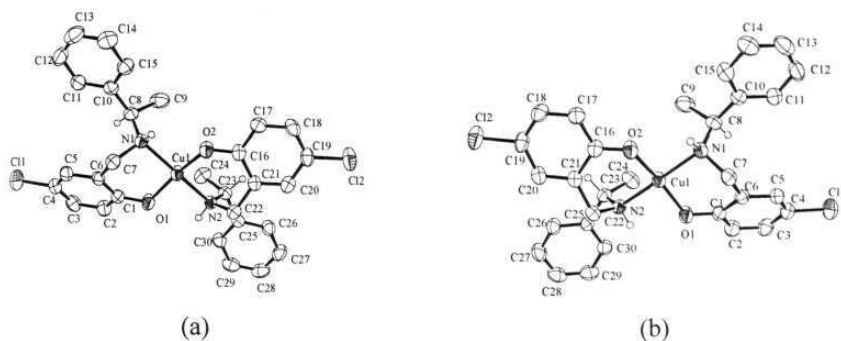


Figure 3. Molecular structures of (a) $[\text{CuL}^5_2]$ (**5**) and (b) $[\text{CuL}^6_2]$ (**6**) with the atom-labeling schemes. Hydrogen atoms other than the chiral center hydrogen atoms are omitted for clarity. All non-hydrogen atoms are represented by their 40% probability thermal ellipsoids.

Table 4. Selected bond parameters for **5**, **5A**, **6** and **6A**

Compound	5	5A	6	6A
Cu(1) - O(1)	1.885(3)	1.897(4)	1.8897(16)	1.897(4)
Cu(1) - O(2)	1.880(2)	1.870(4)	1.8821(16)	1.878(4)
Cu(1) - N(1)	2.037(3)	2.030(5)	2.0368(18)	2.031(5)
Cu(1) - N(2)	2.021(3)	2.028(5)	2.0232(18)	2.023(5)
O(2) - Cu(1) - O(1)	166.96(13)	163.85(19)	167.06(9)	164.1(2)
O(2) - Cu(1) - N(2)	94.24(12)	94.0(2)	94.30(8)	94.3(2)
O(1) - Cu(1) - N(2)	84.85(11)	90.0(2)	84.79(7)	89.6(2)
O(2) - Cu(1) - N(1)	87.42(12)f	87.9(2)	87.50(7)	88.2(2)
O(1) - Cu(1) - N(1)	94.09(12)	92.2(2)	94.01(7)	91.9(2)
N(2) - Cu(1) - N(1)	177.00(13)	165.1(2)	176.93(8)	165.0(2)

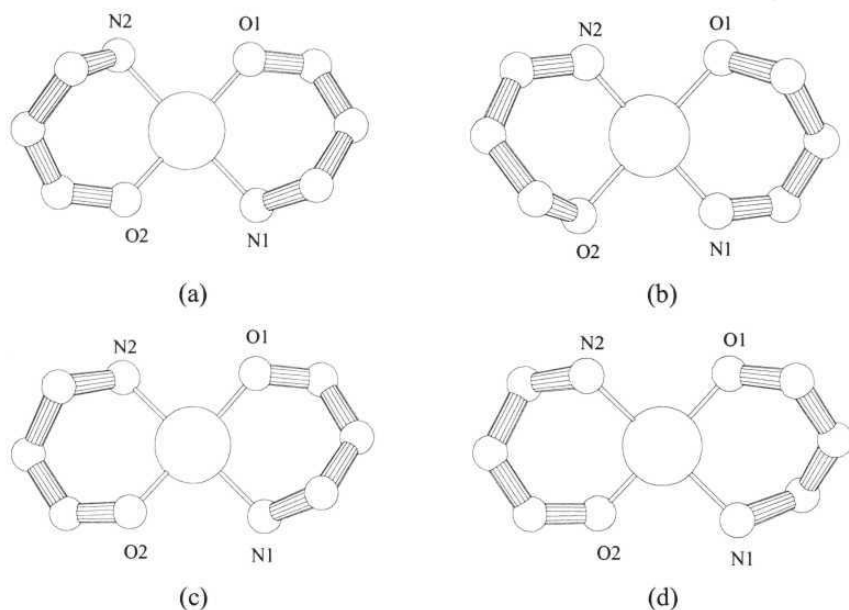


Figure 4. Absolute configuration viewed down C_2 axis: (a) right handed configuration (Δ or P) in **5** (b) left handed configuration (Λ or M) in **6** (c) right handed configuration (Δ or P) in **5A** and (d) left handed configuration (Λ or M) in **6A**.

4.4.5. One-dimensional helical self assembly *via* intermolecular C–H \cdots O interactions

In the crystal lattices, all these molecules (solvated and unsolvated) exhibit infinite one-dimensional helical self assembly *via* intermolecular C–H \cdots O interactions. This C–H \cdots O interaction is highly specific and involves the C–H group at *ortho* position with respect to the chloro substituent on the benzene ring of one molecule and the metal coordinated phenolate O-atom of another molecule. The C \cdots O distances and the C–H \cdots O angles are in the ranges 3.2–3.5 Å and 145–152°, respectively. The C \cdots O distances observed for the unsolvated complexes are longer when compared with those observed for the solvated ones (Table 5). The *ortho* C–H group with respect to the electron withdrawing chloro substituent on the benzene ring is expected to be more activated hydrogen bond donor compared to the other C–H

groups. It is interesting to note that although each molecule contains four such *ortho* C-H groups, only C5-H participates in C-H...O interaction and other three remain as spectators. Although we cannot give any specific reason for this observation, but it may be assumed that this is because of the position of this C-H group is most suited due to the chirality of ligand for the observed C-H...O interaction which leads to efficient crystal packing. The studies on hydrogen bonding have led to the establishment of several experimental scales of H-bonding acidity / basicity and donor / acceptor ability.¹⁹ Herein probably the C-H group *ortho* to chloro substituent is acidic and therefore participates in C-H...O interaction. On the other hand, the metal coordinated phenolate oxygen, is the best available with respect to acceptor ability and its position in the molecular architecture for this C-H...O interactions. This C-H...O interaction pattern is shown in the Figure 5.

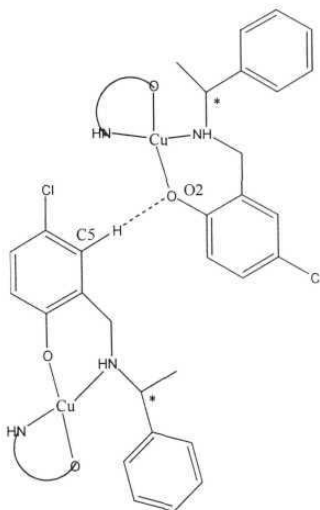


Figure 5. C-H...O pattern in the complexes **5**, **5A**, **6** and **6A**.

The path of the helix can be traced by following the hydrogen bonds clock wise / counter clock wise around the two-fold screw axis of the helix. It is worth mentioning that if compounds contain at least one two-fold screw axis, symmetry elements may favor the helical organization. The copper(II) complexes (**5** and **5A**)

containing (R)-isomeric chloro substituted ligand form right handed helices (*P*-form), whereas copper(II) complexes (**6** and **6A**) of (S)-isomeric chloro substituted ligand form left handed helices (*M*-form) in the supramolecular level (Figures 6-9). The chirality at the C8 and C23 and the flexibility of the CH₂-NH bond (Figure 3) lead to a twisted conformation around the metal ion and this feature is translated to right or left handed helical self assembly *via* C-H...O interactions. It has been shown in the previous section and in earlier work that molecular helicity around the central metal atom is right handed for (R) enantiomeric ligands and left handed for (S) enantiomeric ligands. Although the extent of tetrahedral distortion in each of these complex molecules is rather low, it may be sufficient to dictate the handedness of the helical supramolecular structure. Pitch distances of these helices vary from 12-13 Å. In each case, a full turn comprises of three molecules. To the best of our knowledge this is the first example where homochiral metal-organic molecules self assemble through weak hydrogen bonding interactions leading to helical organization and this feature is retained for both solvated and unsolvated forms. As expected the helices formed by [CuL⁵₂] and [CuL⁶₂] show mirror image relationship (Figures 7 and 9). Thus these molecules exhibit helical chirality not only in the molecular level, also in the supramolecular level.

Table 5. Geometrical parameters for hydrogen bonds in **5**, **5A**, **6** and **6A**

Compound	D...A	(D-H)/Å	d(H...A)/Å	D(D...A)/Å	D-H...A/ ^o
5	C5...O2 ^a	0.93	2.56	3.408(3)	152
5A	C5...O2 ^a	0.93	2.53	3.356(8)	148
	O3...O1	0.82(6)	1.89(5)	2.667(5)	156(5)
	N2...O3	0.80(5)	2.29(5)	3.074(7)	171(4)
	C30...O3	0.93	2.58	3.475(8)	162
6	C5...O2 ^a	0.93	2.55	3.403(4)	152
6A	C5...O2 ^a	0.93	2.54	3.366(7)	148

O3...O1	0.73(6)	1.97(5)	2.670(5)	160(6)
N2...O3	0.73(5)	2.35(5)	3.078(7)	175(6)
C30...O3	0.93	2.59	3.483(10)	162

^a activated C-H...O interaction

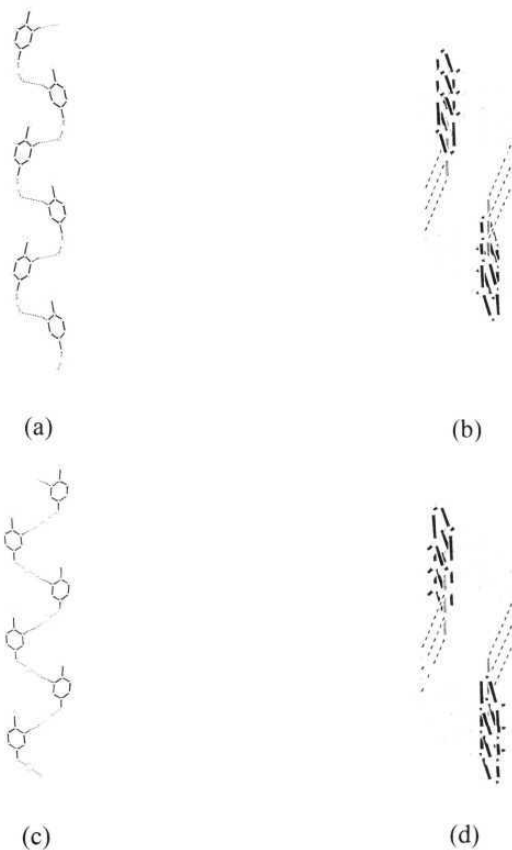


Figure 6. Helical packing of $[\text{CuL}^5_2]$ (**5**) and $[\text{CuL}^6_2]$ (**6**) through C-H...O interactions: (a) the right handed helical packing of **5** (view perpendicular to *a*-axis), (b) channel through the helix (view down *a*-axis), (c) the left handed helical packing of **6** (view perpendicular to *a*-axis), (d) channel through the helix (view down *a*-axis).

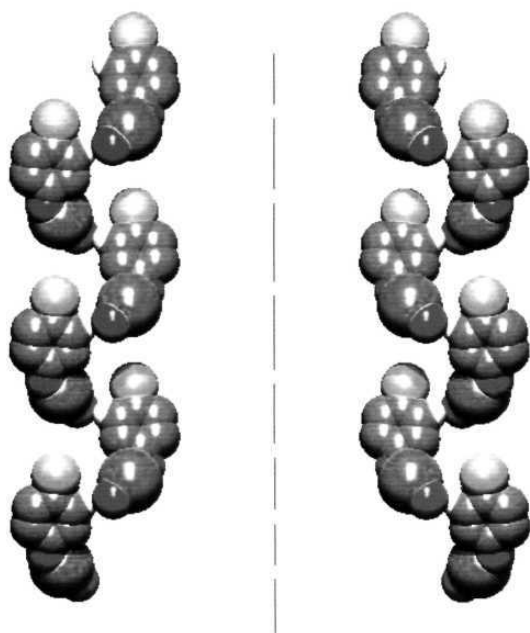


Figure 7. Mirror image relationship of the helices formed by **5** and **6**.

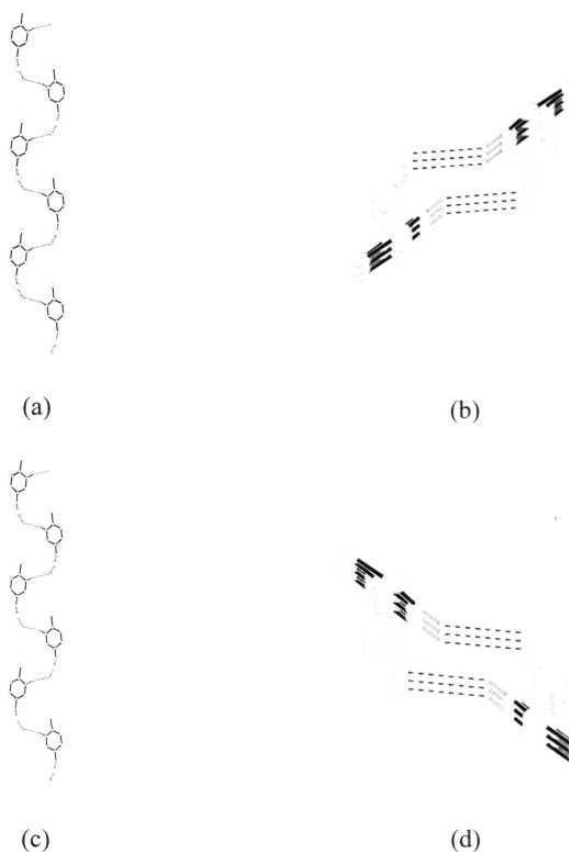


Figure 8. C–H \cdots O interactions and the helical packing of $[\text{CuL}^5_2]$ and $[\text{CuL}^6_2]$ in **5A** and **6A**, respectively: (a) the right handed helical packing of $[\text{CuL}^5_2]$ (view perpendicular to b -axis), (b) channel through the helix (view down b -axis), (c) the left handed helical packing of $[\text{CuL}^6_2]$ (view perpendicular to b -axis), (d) channel through the helix (view down b -axis).]

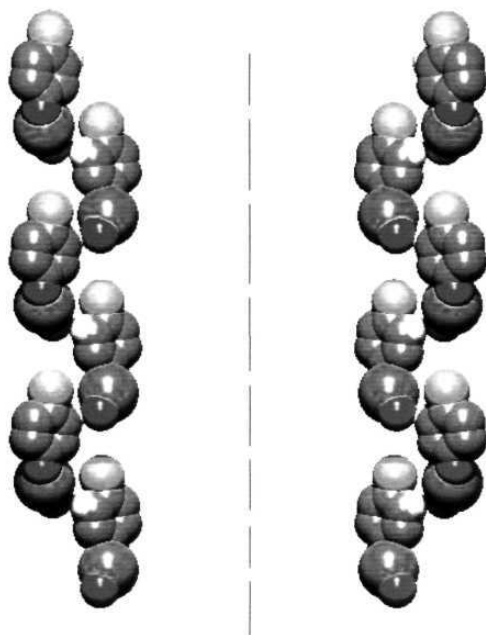


Figure 9. Mirror image relationship of the helices formed by $[\text{CuL}^5_2]$ and $[\text{CuL}^6_2]$ present in **5A** and **6A**, respectively.

4.5.6. Non-covalent interactions involving the solvent molecules in **5A** and **6A**

One serious difficulty for construction of isostructural hydrogen bonded networks for solvates is the influence of polar solvents. Such solvents (e.g. H_2O , DMF, DMSO, etc) are themselves very efficient in hydrogen bond formation with the building blocks. Thus they can disturb the intended network.²⁰ The *n*-hexane molecule present in both **5A** and **6A** are severely disordered. We also could not find any weak interaction involving the disordered molecule in either case. However in both solvated complexes (**5A** and **6A**) water molecules are not disordered and play an important role in interconnecting the two parallel helices without disturbing the path of the helix caused by this activated $\text{C-H}\cdots\text{O}$ interactions. Herein water molecule is involved in six hydrogen bonding interactions. It acts as tetra furcated hydrogen bond acceptor for

two N-H...O and two C-H...O interactions, whereas it is hydrogen bond donor to two metal coordinated phenolate oxygen of the two molecules (Figure 10 and 11). Each helix is connected to adjacent helices through the N-H...O...H-N, C-H...O...H-C and O...H-O-H...O interactions and an infinite two-dimensional network is formed. Only one of the N-H groups of each complex is involved in connecting parallel helices while other N-H remains a noninteractive spectator. Calculations using PLATON squeeze program show that effective volume for inclusion is $\sim 517 \text{ \AA}^3$, which is $\sim 16 \%$ of the crystal volume.²¹

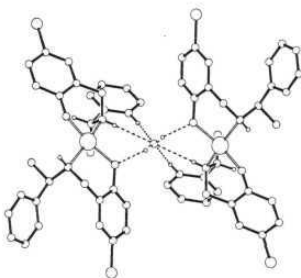


Figure 10. Water molecule involved in six hydrogen bonding interactions in **5A**.

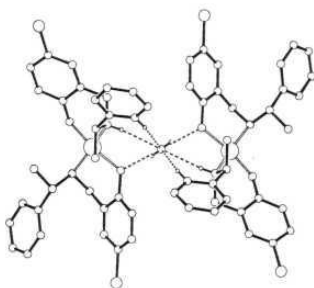


Figure 11. Water molecule involved in six hydrogen bonding interactions in **6A**.

4.6. Conclusions

In summary, we have synthesized and structurally characterized mononuclear Cu(II) complexes with chloro substituted chiral reduced schiff bases. X-ray crystallographic studies reveal that both solvated and unsolvated forms of these complexes exhibit helical self assembly *via* activated C–H...O interactions. In all the cases, the C–H...O interactions are highly specific and involve the *ortho* C–H with respect to the chloro substituent on the benzene ring of one molecule and the metal coordinated phenolate oxygen atom of another molecule. The complexes with (R)-enantiomeric ligand show right handed absolute configuration (Δ or P) around metal ion in molecular level and this feature is translated to right handed single helix self-assembled through activated C–H...O interactions in supramolecular level. The complexes with (S)-enantiomeric ligand show opposite handedness in both molecular level as well as supramolecular level.

4.7. References

1. J.-M. Lehn, *Supramolecular chemistry: concepts and perspectives*, VCH: Weinheim, **1995**.
2. (a) M. Albrecht, *Chem. Rev.*, **2001**, 101, 3457; (b) C. Piguet, G. Bernardinelli and G. Hopfgartner *Chem. Rev.*, **1997**, 97, 2005; (c) J.-M Lehn, *Chem. Eur. J.* **2000**, 6, 2097; (d) I. E. Rowan and R. J. M. Nolte, *Angew. Chem., Int. Ed. Engl.*, **1998**, 37, 62; (e) M. C. Feiters and R. J. M. Nolte, *Adv. Supramol. Chem.*, **2000**, 6, 41.
3. (a) P. Gangopadhyay and T. P. Radhakrishnan, *Angew. Chem. Int. Ed.*, **2001**, 40, 2451; (b) S. P. Anthony and T. P. Radhakrishnan, *Chem. Commun.*, **2004**, 1058; (c) S. Jayanthi and T. P. Radhakrishnan, *Chem. Eur. J.*, **2004**, 10, 2661; (d) J. Nishida, T. Suzuki, M. Ohkita and T. Tsuji, *Angew. Chem. Int. Ed.*, **2001**, 40, 3251; (e) B. Busson, M. Kauranen, C. Nuckolls and T. J. Katz, *Phys. Rev. Lett.*, **2000**, 84, 79; (f) T. Verbiest, S. V. Elshocht, M. Kauranen,

- L. Helleman, J. Snauwaert, C. Noukolls, T. J. Katz and A. Persoons, *Science*, **1998**, 282, 913.
4. (a) S. Hanessian, A. Gomtsyan, M. Simard, and S. Rolens; *J. Am. Chem. Soc.*, **1994**, 116, 4495; (b) S. Hanessian, M. Simard and S. Rolens, *J. Am. Chem. Soc.*, **1995**, 117, 7630; (c) L. R. M. Gillivray, J. L. Atwood, *J. Am. Chem. Soc.*, **1997**, 119, 2592; (d) H. C. Chou, C. H. Hsu, Y. M. Cheng, C. C. Cheng, H. W. Liu, S. C. Pu and P. T. Chou, *J. Am. Chem. Soc.*, **2004**, 126, 1650.
 5. T. D Owens, F. J. Hollander, A. G. Oliver and J. A. Ellman, *J. Am. Chem. Soc.* **2001**, 123, 1539.
 6. (a) M. Eddaoudi, D. B. Moler, H. Li, B. Chen, T. M. Reineke, M. O'Keefe and O. M. Yaghi, *Acc. Chem. Res.*, **2001**, 34, 319; (b) A. M. Beatty, *Coord. Chem. Rev.*, **2003**, 246, 131.
 7. G. R. Desiraju and T. Steiner. *The weak hydrogen bond in structural chemistry and biology*, New York: Oxford University Press, **1999**.
 8. J. Marfurt and C. Leumann, *Angew. Chem. Int. Ed.*, **1998**, 37, 175.
 9. T. Steiner, *Chem. Comm.*, **1997**, 727.
 10. (a) Z. S. Derewenda, L. Lee and U. Derewenda, *J. Mol. Biol.*, **1995**, 252, 248; (b) J. Bella and H. M. Berman, *J. Mol. Biol.*, **1996**, 264, 734; (c) A. Senes, I. U. Belandia and D. M. Engelman, *PNAS*, **2001**, 98, 9061.
 11. (a) V. K. Muppidi, T. Htwe, P. S. Zacharias and S. Pal, *Inorg. Chem. Commun.*, **2004**, 7, 1045; (b) V. K. Muppidi, P. S. Zacharias and S. Pal, *Inorg. Chem. Commun.*, **2005**, 8, 543-547.
 12. (a) J. D. Ranford, J. J. Vittal and D. Wu, *Angew. Chem., Int. Ed.*, **1998**, 37, 1114; (b) J. D. Ranford, J. J. Vittal, D. Wu and X. Yang, *Angew. Chem., Int. Ed.* **1999**, 38, 3498; (c) J. J. Vittal and X. Yang, *Cryst. Growth Des.*, **2002**, 2, 259; (d) M. A. Alam, M. Netaji and M. Ray, *Angew. Chem., Int. Ed.* **2003**, 42, 1940; (e) S. R. Korupolu and P. S. Zacharias, *Chem. Commun.*, **1998**, 1267.
 13. SMART & SAINT Software Reference Manuals, Version 6.22, Bruker AXS Analytic X-Ray Systems, Inc., Madison, WI, **2000**.

14. G. M. Sheldrick, SADABS, Software for Empirical Absorption Correction, University of Göttingen, Germany, **2000**.
15. SHELXTL Reference Manual, Version 5.1, Bruker AXS, Analytic X-Ray Systems, Inc., WI, **1997**.
16. L. J. Farrugia, *J. Appl. Cryst.*, **1997**, 30, 567.
17. A. L. Spek, *Platon, Molecular Graphics Software*, University of Glasgow, UK, 2001.
18. H. D. Flack, *Acta Crystallogr.*, **1983**, A39, 876.
19. F. T. T. Huque and J. A. Platts, *Org. Biomol. Chem.*, **2003**, 1, 1419.
20. (a) L. Bramer, *Chem. Soc. Rev.*, **2004**, 33, 476; (b) L. Bramer, J. C. M. Rivas, R. Atencio, S. Fang and F. C. Pigge, *J. Chem.Soc., Dalton Trans.*, **2000**, 3855.
21. P. V. Sluis and A. L. Spek, *Acta Crystallogr., Sect., A*, **1990**, 46, 194.

Inclusion properties of Cu(II) complexes of bromo substituted chiral reduced Schiff bases: Stabilization of guest molecules *via* O–H \cdots O interactions

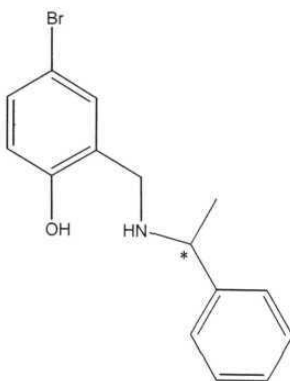
5.1. Abstract:

Mononuclear copper(II) complexes with enantiomerically pure N-(2-hydroxy-5-bromobenzyl)-(R)- α -methylbenzylamine (HL⁷) and N-(2-hydroxy-5-bromobenzyl)-(S)- α -methylbenzylamine (HL⁸) have been synthesized and structurally characterized. Crystal packing features reveal that the complex (7) with HL⁷ exhibit host-guest interactions with solvent molecules. Inclusion of solvent (methanol, ethanol and acetonitrile) molecules is facilitated by intermolecular hydrogen bonding interactions. The molecules of 7 form zig-zag chain like structure *via* C–H \cdots O interactions involving the metal coordinated phenolate-O and the C–H group *ortho* to the bromo substituent. Interestingly, the complex (8) with HL⁸ crystallizes in the unsolvated form and assembles to a helical superstructure *via* the same bromo activated C–H \cdots O interactions.

5.2. Introduction

In the previous chapters we have shown that copper(II) complexes with chiral reduced Schiff bases (HL¹-HL⁶) are good flexible chiral hosts and capable of inclusion of various solvent molecules *via* intermolecular non-covalent interactions. Binuclear copper(II) complexes (**1** and **2**) with unsubstituted ligands (HL¹ and HL²) display enantio-specific inclusion of chiral 1,2-dichloroethane rotamers and other achiral chloroalkanes. Mononuclear copper(II) complexes (**3** and **4**) with nitro-substituted ligands (HL³ and HL⁴) show the perfectly polar alignment of guest and host molecules and also the enantio-specific inclusion of chiral 1,2-dihaloethane rotamers in the crystal lattice. On the other hand, the mononuclear Cu(II) complexes (**5** and **6**) with chloro substituted ligands (HL⁵ and HL⁶) exhibit helical self assembly *via* activated C-H...O interactions. This feature is retained for both solvated and unsolvated forms of **5** and **6**.

In this chapter, we have described the synthesis and the structural features of the mononuclear Cu(II) complexes with bromo substituted enantiomerically pure chiral reduced Schiff bases N-(2-hydroxy-5-bromobenzyl)-(R)- α -methylbenzylamine (HL⁷) and N-(2-hydroxy-5-bromobenzyl)-(S)- α -methylbenzylamine (HL⁸). The crystal structure analysis of these complexes reveals that the Cu(II) complex (**7**) with HL⁷ are capable of host-guest interactions with solvent molecules. The inclusion of the solvent molecules in the crystal lattice occurs *via* intermolecular hydrogen bonding interactions. The host molecules (**7**) form a zig-zag chain due to bromo activated intermolecular C-H...O interactions, when the guest molecule is small size. However, for larger guest molecule the C-H...O interactions do not take place. On the other hand, the complex (**8**) with HL⁸ crystallizes in the unsolvated form and self-assembly *via* activated C-H...O interactions leads to a helical superstructure. Herein, we have described the similarities and the differences between the packing patterns of the complexes with the chloro substituted ligands (Chapter 4) and with the bromo substituted ligands.



HL⁷ = N-(2-hydroxy-5-bromobenzyl)-(R)- α -methylbenzylamine

HL⁸ = N-(2-hydroxy-5-bromobenzyl)-(S)- α -methylbenzylamine

5.3. Experimental

5.3.1. Materials

All commercially available chemicals and the solvents utilized in this work were of analytical grade and were used as obtained. The chemicals and the sources are as follows: 5-bromosalicylaldehyde, (R)- α -methylbenzylamine and (S)- α -methylbenzylamine, sodium borohydride, Lancaster (England); CDCl_3 , methanol, dichloromethane, chloroform, 1,2-dichloroethane, Acros (India); $\text{CuCl}_2 \cdot 2\text{H}_2\text{O}$, sodium hydroxide, anhydrous sodium sulphate, S. D. Fine Chem. Ltd. (India).

5.3.2. Physical measurements

Elemental analysis was carried out on a Perkin-Elmer 240C CHN analyzer. Infrared spectra were collected by using KBr pellets on a Jasco-5300 FT-IR spectrophotometer. NMR spectra were recorded on a Bruker ACF-200 spectrometer. A Shimadzu 3101-PC UV/vis/NIR spectrophotometer was used to record the electronic spectra. X-ray crystallographic experiments were performed using a Bruker-Nonius SMART APEX CCD single crystal diffractometer. A Sherwood scientific magnetic susceptibility balance was used to measure the magnetic moments.

5.3.3. Synthesis of ligand and complexes

(a) N-(2-hydroxy-5bromobenzyl)-(R)- α -methylbenzylamine, HL⁷

A methanol solution (30 ml) of 5-bromosalicylaldehyde (2.01 g, 10 mmol) was added to a methanol solution (30 ml) of (R)- α -methylbenzylamine (1.21 g, 10 mmol) and stirred at room temperature for ½ h. To the resulting yellow solution 0.74 g (20 mmol) of NaBH₄ was added and the mixture was stirred for another ½ h until a colourless solution was obtained. The reaction mixture was evaporated to dryness on a rotary evaporator followed by addition of 100 ml of water. The suspended solid in water was extracted with (2 x 30 ml) CH₂Cl₂. The CH₂Cl₂ extracts were dried over anhydrous Na₂SO₄ and then evaporated to dryness. The compound (HL⁷) was obtained in the form of white solid.

Yield	: 2.26 g, (74%)
M. F.	: C ₁₅ H ₁₆ NOBr
IR ($\nu_{\text{N-H}}$ cm ⁻¹ , KBr pellet)	: 3304
¹ H NMR (CDCl ₃ , δ , ppm)	: 1.48 (d, 3H, CH ₃), 3.71 and 3.88 (2H, CH _A H _B), ~ 3.78 (q, 1H, CH(CH ₃), 6.99 (s, 1H, <i>ortho</i> to both Br and CH ₂), 6.74 (d, 1H, <i>ortho</i> to phenolic-OH), 7.00 (d, 1H, <i>ortho</i> to Br), 7.23-7.40 (m, 5H, phenyl protons).
Anal. calcd. for C ₁₅ H ₁₆ NOBr	: C, 58.84; H, 5.27; N, 4.57
Found	: C, 58.42; H, 5.12; N, 4.40.

(b) N-(2-hydroxy-5bromobenzyl)-(S)- α -methylbenzylamine, HL⁸

HL⁸ was prepared in similar yield by following the same procedure as described for HL⁷ using (S)- α -methylbenzylamine instead of (R)- α -methylbenzylamine.

Yield	: 2.28 g, (74%)
M. F.	: C ₁₅ H ₁₆ NOBr
IR ($\nu_{\text{N-H}}$ cm ⁻¹ , KBr pellet)	: 3304

^1H NMR (CDCl_3 , δ , ppm) : 1.48 (d, 3H, CH_3), 3.71 and 3.88 (2H, CH_AH_B), ~ 3.78 (q, 1H, $\text{CH}(\text{CH}_3)$), 6.99 (s, 1H, *ortho* to both Br and CH_2), 6.74 (d, 1H, *ortho* to phenolic-OH), 7.00 (d, 1H, *ortho* to Br), 7.23-7.40 (m, 5H, phenyl protons).

Anal. calcd. for $\text{C}_{15}\text{H}_{16}\text{NOBr}$: C, 58.84; H, 5.27; N, 4.57

Found : C, 59.18; H, 5.08; N, 4.35.

(c) $[\text{CuL}^7_2]$ (7): A methanol solution (10 ml) of $\text{CuCl}_2 \cdot 2\text{H}_2\text{O}$ (0.089 g, 0.5 mmol) was added to a methanol solution (20 ml) of HL^7 (0.306 g, 1 mmol) and NaOH (0.040 g, 1 mmol). The mixture was stirred at room temperature for 1 h. The resulting dark brown precipitate was filtered and the slow evaporation of filtrate gave dark brown crystals (yield: 0.54 g, 80%). Anal. calcd. for $\text{CuC}_{30}\text{H}_{30}\text{N}_2\text{O}_2\text{Br}_2$: C, 53.47; H, 4.49; N, 4.16. Found: C, 53.31; H, 4.42; N, 4.07. Selected infrared bands (cm^{-1}): 3265(w), 2969(w), 2926(w), 2860(w), 1583(s), 1551(vs), 1469(m), 1408(s), 1292(w), 1182(w), 1116(w), 1080(m), 1045(m), 1011(m), 962(m), 875(m), 845(m), 815(m), 771(m), 758(m), 702(s), 652(m), 555(w), 532(w), 499(m). Electronic spectral data in CHCl_3 (λ , nm (ϵ , $\text{M}^{-1}\text{cm}^{-1}$)): 678sh (235), 444 (2,313), 355sh (1,774), 282 (7,270). Effective magnetic moment at 298 K: 1.68 μ_B

(d) $[\text{CuL}^8_2]$ 8: A methanol solution (10 ml) of $\text{CuCl}_2 \cdot 2\text{H}_2\text{O}$ (0.089 mg, 0.5 mmol) was added to a methanol solution (20 ml) of HL^8 (0.306 g, 1 mmol) and NaOH (0.040 g, 1mmol). The resulting solution was stirred for 1h. Slow evaporation of solvent gave a dark brown crystalline material (yield 0.55 g, 82%). Anal. calcd. for $\text{CuC}_{30}\text{H}_{30}\text{N}_2\text{O}_2\text{Br}_2$: C, 53.47; H, 4.49; N, 4.16. Found: C, 53.40; H, 4.38; N, 4.21. Selected infrared bands (cm^{-1}): 3264(w), 2969(w), 2924(w), 2860(w), 1583(s), 1551(vs), 1470(m), 1408(s), 1292(w), 1182(w), 1116(w), 1078(m), 1045(m), 1011(m), 962(m), 875(m), 845(m), 815(m), 771(m), 758(m), 702(s), 652(m), 555(w), 532(w), 499(m). Electronic spectral data in CHCl_3 (λ , nm (ϵ , $\text{M}^{-1}\text{cm}^{-1}$)): 678sh (226),

444 (2,578), 355sh (1,811), 282 (7,932). Effective magnetic moment at 298 K: 1.68 μ_B

5.3.4. X-ray crystallography

X-ray data were collected for dark brown crystals of **7**·CH₃OH and **7**·CH₃CN·H₂O (obtained from solution of **7** in CH₃OH and CH₃CN, respectively) on a Bruker-Nonius SMART APEX CCD single crystal diffractometer using graphite monochromated Mo-K α radiation (0.71073 Å). The SMART software was used for intensity data acquisition and the SAINT-Plus software¹ was used for data extraction. In each case, absorption correction was performed with the help of SADABS program.² The SHELXTL package³ was used for structure solution and least-square refinement on F². All the non hydrogen atoms were refined anisotropically. The secondary amine hydrogen atoms were located in a difference map and refined with geometric restraints. All other hydrogen atoms were included in the structure factor calculation by using a riding model.

X-ray data were collected for dark brown crystals of **7**·C₂H₅OH (obtained from C₂H₅OH solution of **7**) and **8** on a Enraf-Nonious Mach3 diffractometer using graphite monochromated Mo K α radiation (0.71073 Å). Unit cell parameters were determined by least-squares fit of 25 reflections having 2 θ values in the range 18-30°. Stability of the crystal was monitored by measuring the intensities of three check reflections after every 1.5 h during the data collection. The structure was solved by direct methods and refined on F² by full-matrix least-square procedures. The semi-empirical absorption correction based on ψ -scan was applied for the both complexes.⁴ All non-hydrogen atoms were refined using anisotropic thermal parameters. Geometric constraints were applied for the refinement of the secondary amine hydrogens after locating them from difference maps. Other hydrogen atoms of the complexes were added at calculated positions using a riding model. The ORTEP⁵ and the PLATON⁶ software were used for molecular graphics. The significant X-ray crystallographic data are given in Tables 1 and 2.

Table 1. Crystallographic data for 7·CH₃OH and 7·C₂H₅OH

Compound	7·CH ₃ OH	7·C ₂ H ₅ OH
Molecular formula	C ₃₁ H ₃₄ Br ₂ CuN ₂ O ₃	C ₃₂ H ₃₆ Br ₂ CuN ₂ O ₃
Crystal dimensions / mm	0.28 × 0.30 × 0.16	0.30 × 0.42 × 0.36
Host-guest ratio	1 : 1	1 : 1
<i>T</i> /K	100	293
<i>M</i>	705.96	719.99
Crystal system	Monoclinic	Monoclinic
Space group	<i>P</i> 2 ₁	<i>P</i> 2 ₁
<i>a</i> /Å	10.6569(14)	11.0104(14)
<i>b</i> /Å	10.2104(14)	10.326(2)
<i>c</i> /Å	13.6498(18)	14.3339(18)
<i>α</i> °	90	90
<i>β</i> °	92.706(2)	101.582(10)
<i>γ</i> °	90	90
<i>V</i> /Å ³	1483.6(3)	1596.5(5)
<i>Z</i>	2	2
Observed reflections	6798	3869
Parameters	362	366
Final <i>R</i> indices	0.0336, 0.0817	0.0862, 0.2011
(<i>I</i> > 2σ(<i>I</i>))		
Goodness-of-fit on <i>F</i> ²	1.028	0.997
Largest hole and peak e/ Å ³	-0.485, 1.146	-1.268, 0.835

Table 2. Crystallographic data for **7**·CH₃CN·H₂O and **8**

Compound	7 ·CH ₃ CN·H ₂ O	8
Molecular formula	C ₃₂ H ₃₅ Br ₂ CuN ₃ O ₃	C ₃₀ H ₃₀ Br ₂ CuN ₂ O ₂
Crystal dimensions / mm	0.32 × 0.26 × 0.38	0.40 × 0.38 × 0.24
Host-guest ratio	1 : 1 : 1	-
<i>T</i> /K	293	293
<i>M</i>	732.99	673.92
Crystal system	Monoclinic	Monoclinic
Space group	<i>P</i> 2 ₁	<i>P</i> 2 ₁
<i>a</i> /Å	10.8817(8)	10.9424(12)
<i>b</i> /Å	10.5154(7)	10.036(5)
<i>c</i> /Å	13.9207(10)	13.8223(15)
<i>α</i> /°	90	90
<i>β</i> /°	101.7090(10)	90.893(10)
<i>γ</i> /°	90	90
<i>V</i> /Å ³	1559.74(19)	1517.8(8)
<i>Z</i>	2	2
Observed reflections	7258	3662
Parameters	377	342
Final <i>R</i> indices (<i>I</i> > 2σ(<i>I</i>))	0.0220, 0.0521	0.044, 0.0805
Goodness-of-fit on <i>F</i> ²	1.030	1.045
Largest hole and peak e/ Å ³	-0.339, 0.697	-0.406, 0.349

5.4. Results and discussions

5.4.1. Synthesis and Some properties

Bromo substituted chiral reduced Schiff bases HL⁷ and HL⁸ were prepared as described in the experimental section 5.3.3. IR, NMR and elemental analysis data of these compounds are satisfactory with their empirical formulae. Reactions of these reduced Schiff bases with CuCl₂ and NaOH in 2:1:2 stoichiometry gave mononuclear complexes of general formula [CuLⁿ₂] (n = 7, 8). Representative chemical diagram of these complex molecules are shown in Figure 1. The infrared spectra of both ligands and complexes exhibited N-H stretching bands (3250-3300 cm⁻¹) of the secondary amine. Electronic spectra of **7** and **8** in CHCl₃ solutions are essentially identical (Figure 2). The low intensity absorption at ~678 nm is assigned to the d-d transition. The other intense bands observed in the range 444-282 nm are most likely due to ligand-to-metal charge transfer and intraligand transitions.

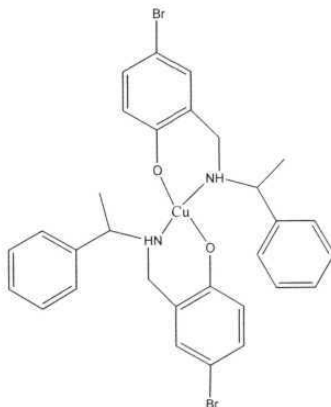


Figure 1. General molecular structure of **7** and **8**.

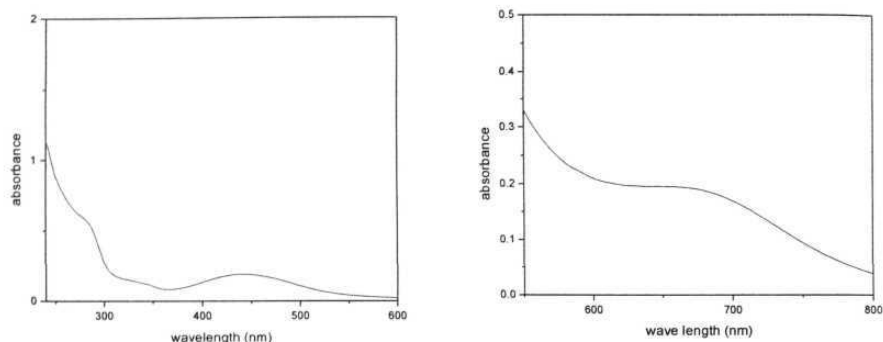


Figure 2. Electronic spectrum of **7** in CHCl_3 .

5.4.2. Crystallization

Suitable crystals of inclusion compounds for X-ray crystallographic studies $7 \cdot \text{CH}_3\text{OH}$, $7 \cdot \text{C}_2\text{H}_5\text{OH}$ were grown by slow evaporation of mother liquor over a period of 3 days. The X-ray quality single crystals of the inclusion compound $7 \cdot \text{CH}_3\text{CN} \cdot \text{H}_2\text{O}$ were grown by recrystallization of **7** in acetonitrile. Suitable crystals of compound **8** were grown by slow evaporation of mother liquor over a period of 3 days. All these compounds crystallize in monoclinic space group $P2_1$. The crystals are needle shaped and loose the guest solvent molecules over a period of 7 days. The absolute configurations of all these complexes are successfully confirmed by flack parameter values and details are given in Table 3.⁷

Table 3. Absolute configurations of $7 \cdot \text{CH}_3\text{OH}$, $7 \cdot \text{C}_2\text{H}_5\text{OH}$, $7 \cdot \text{CH}_3\text{CN} \cdot \text{H}_2\text{O}$ and **8**

Complex	C(8), C(23) configuration	N(1), N(2) Configuration	Flack Parameter value
$7 \cdot \text{CH}_3\text{OH}$	R, R	R, R	0.001(7)
$7 \cdot \text{C}_2\text{H}_5\text{OH}$	R, R	R, R	-0.04(3)
$7 \cdot \text{CH}_3\text{CN} \cdot \text{H}_2\text{O}$	R, R	R, R	0.005(5)
8	S, S	S, S	0.007(13)

5.4.3. Description of Structures

The molecular structures of **7** and **8** are very similar. In these complexes, the ligands coordinate through the phenolato-O and the secondary amine N- atoms forming a distorted N_2O_2 square plane around the Cu(II) centers. As shown by most of the Cu(II) complexes with Schiff bases and reduced Schiff bases derived from salicylaldehyde, the Cu-N bond distances are significantly longer than Cu-O bond distances. Slight changes are observed for bond angles and bond distances around the coordination spheres which are common for crystalline inclusion compounds. The bond parameters associated with the coordination spheres of all the compounds are given in Table 4. The molecular structures of **7** and **8** are shown in Figure 2. The dihedral angles between the planes defined by Cu, N1 and O1 and that defined by Cu, N2 and O2 are $19.98(16)^\circ$, $20.04(84)^\circ$, $17.71(11)^\circ$ and $18.84(31)^\circ$ for **7**-CH₃OH, **7**-C₂H₅OH, **7**-CH₃CN·H₂O and **8**, respectively. These dihedral angles indicate the distortion of N_2O_2 coordination sphere from square planar geometry. The complexes with HL⁷ exhibit right handed helical twist (Δ or P), where as complexes with HL⁸ exhibit left handed helical twist (Λ or M) around the central copper ion (Figure 3).

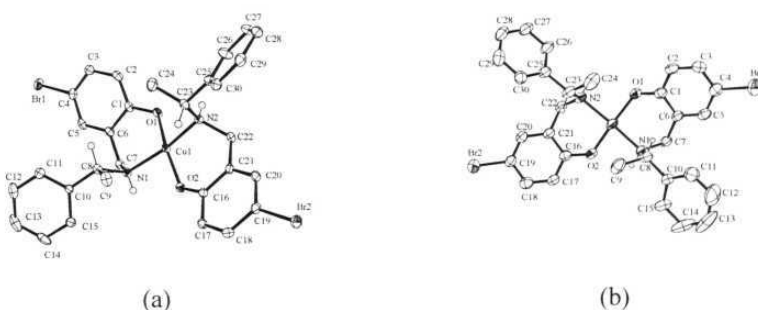


Figure 2. Molecular structures of (a) **7** and (b) **8** with the atom-labeling schemes. Hydrogen atoms other than the chiral center hydrogens are omitted for clarity. All non-hydrogen atoms are represented by their 40 and 30% probability thermal ellipsoids.

Table 4. Selected bond parameters for $7\cdot\text{CH}_3\text{OH}$, $7\cdot\text{C}_2\text{H}_5\text{OH}$, $7\cdot\text{CH}_3\text{CN}\cdot\text{H}_2\text{O}$ and **8**

Compound	$7\cdot\text{CH}_3\text{OH}$	$7\cdot\text{C}_2\text{H}_5\text{OH}$	$7\cdot\text{CH}_3\text{CN}\cdot\text{H}_2\text{O}$	8
Cu(1) - O(1)	1.915(2)	1.910(13)	1.9082(15)	1.881(4)
Cu(1) - O(2)	1.877(2)	1.894(12)	1.8829(14)	1.872(5)
Cu(1) - N(1)	2.027(3)	2.019(12)	2.0246(17)	2.022(5)
Cu(1) - N(2)	2.015(2)	2.047(14)	2.0197(17)	2.024(4)
O(2) - Cu(1) - O(1)	166.41(10)	163.9(5)	166.61(7)	165.6(2)
O(2) - Cu(1) - N(2)	93.72(10)	92.5(5)	93.55(7)	94.2(2)
O(1) - Cu(1) - N(2)	90.01(10)	86.8(5)	91.63(7)	89.5(2)
O(2) - Cu(1) - N(1)	86.61(10)	92.7(5)	84.42(7)	85.8(2)
O(1) - Cu(1) - N(1)	93.29(10)	91.5(5)	93.29(7)	93.8(2)
N(2) - Cu(1) - N(1)	164.42(11)	166.8(5)	166.63(7)	166.66(19)

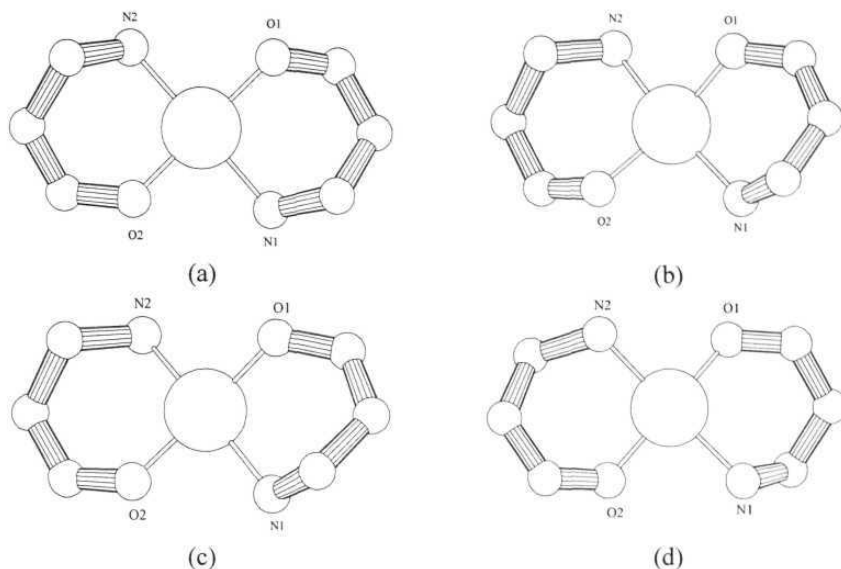


Figure 3. Absolute configurations viewed down C_2 axis: (a) right handed configuration (Δ or P) in $7\cdot\text{CH}_3\text{OH}$ (b) right handed configuration (Δ or P) in $7\cdot\text{C}_2\text{H}_5\text{OH}$ (c) right handed configuration (Δ or P) in $7\cdot\text{CH}_3\text{CN}\cdot\text{H}_2\text{O}$ and (d) left handed configuration (Λ or M) in **8**.

5.4.4. Host-guest interactions

Complex $[\text{CuL}^7_2]$ (**7**) is found to be good chiral host and crystallizes in methanol, ethanol and acetonitrile to give inclusion compounds. X-ray crystallographic studies reveal that all these solvates are isostructural and crystallizes in monoclinic space group $P2_1$. In all the cases, $\text{O}-\text{H}\cdots\text{O}$ hydrogen bonding interactions are found to exist between the alcoholic hydroxyl group or water molecule and the metal coordinated phenolate oxygen (Figure 4). The consistency in the crystal packing is reflected in the very small variation of the unit cell parameters a (10.6569–11.0104 Å), b (10.2104–10.5154 Å) and c (13.6498–14.3339 Å) in the three structures. However, the cell parameter β varies significantly. The β - values are 92.71° , 101.71° and 101.58° for $7\cdot\text{CH}_3\text{OH}$, $7\cdot\text{CH}_3\text{CN}\cdot\text{H}_2\text{O}$ and $7\cdot\text{C}_2\text{H}_5\text{OH}$,

respectively. This may be due to accommodation of the larger or more than one guest molecules in the crystal lattice. Hydrogen bonding distances and angles for all the compounds are given in Table 5.

Table 5. Geometrical parameters of hydrogen bonds in $7\cdot\text{CH}_3\text{OH}$, $7\cdot\text{C}_2\text{H}_5\text{OH}$, $7\cdot\text{CH}_3\text{CN}\cdot\text{H}_2\text{O}$ and **8**

Compound	D...A	$d(\text{D-H})/\text{\AA}$	$d(\text{H-A})/\text{\AA}$	$d(\text{D...A})/\text{\AA}$	$\text{D-H...A}/^\circ$
$7\cdot\text{CH}_3\text{OH}$	C3...O1^a	0.93	2.673	3.486	146
	O3...O1^b	0.82	2.09	2.828(4)	150
	Br2...O3	-	-	3.133	-
	C7...O3	0.97	2.53	3.360(4)	143
	C28...O2	0.93	2.50	3.273(4)	141
$7\cdot\text{C}_2\text{H}_5\text{OH}$	O3...O2^b	0.82	1.86	2.67(2)	173
	N1...O3	1.00(12)	2.35(11)	3.23(2)	146(8)
$7\cdot\text{CH}_3\text{CN}\cdot\text{H}_2\text{O}$	C3...O3^a	0.93	2.51	3.295(3)	142
	O3...O1^b	0.78	1.94	2.709(2)	168
	N2...O3	0.80(2)	2.34(2)	3.120(2)	164(2)
	O...N	0.87	2.13	2.9908(9)	170
	C...Br	0.97	2.88	3.514	124
8	C3...O1^a	0.93	2.58	3.391(8)	145

^a activated C-H...O interaction

^b O-H...O interaction between the host and guest molecules

(a) $7\cdot\text{CH}_3\text{OH}$: A closer scrutiny of the structure reveals that the inclusion of methanol solvent is not only through O-H...O interactions, but C-H...O and Br...O interactions also play some roles in hosting the guest molecules. All these interactions are found to be shorter than the sum of Van der Waals radii of the involved atoms. Host and guest molecules form an infinite one dimensional chain *via* alternating

O—H \cdots O (2.828 Å, 151°) and Br \cdots O (3.134 Å) interactions (Figure 5a). The *ortho* C—H with respect to the bromo substituent participates in activated C—H \cdots O interaction involving the metal coordinated phenolate O- atom and lead to an infinite one dimensional zigzag chain (Figure 5b) instead of a helical chain observed for **5** and **6** (chapter 4). Along with the activated C—H \cdots O interactions, the CH₂ (C7) which is adjacent to the NH group and the aromatic C28-H also participate in the C—H \cdots O interactions (Table 5). Calculations using PLATON squeeze program show that effective volume for inclusion is 147.3 Å³, comprising 9.9% of the crystal volume.⁸ The packing diagram of **7**·CH₃OH is shown in Figure 6.

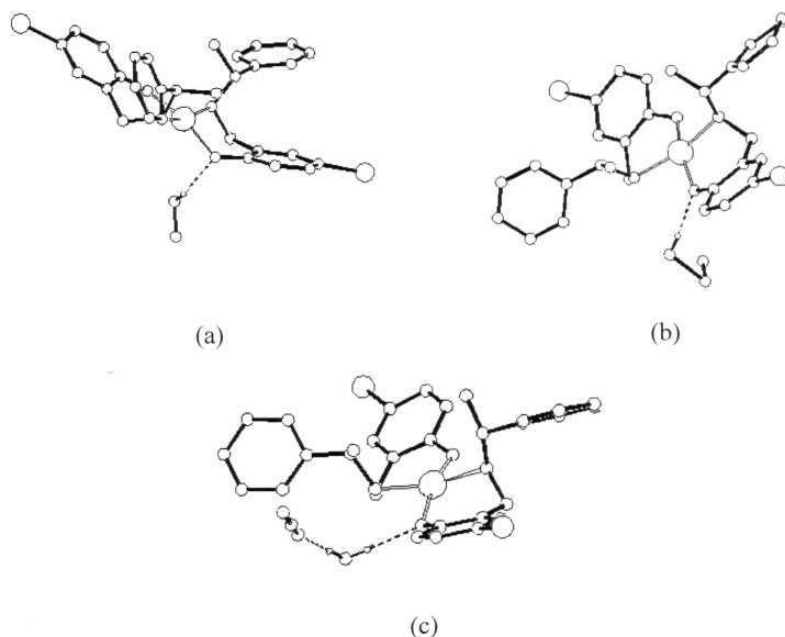


Figure 4. Inclusion of guest solvent via O—H \cdots O interaction in (a) **7**·CH₃OH, (b) **7**·C₂H₅OH and (c) **7**·CH₃CN·H₂O.

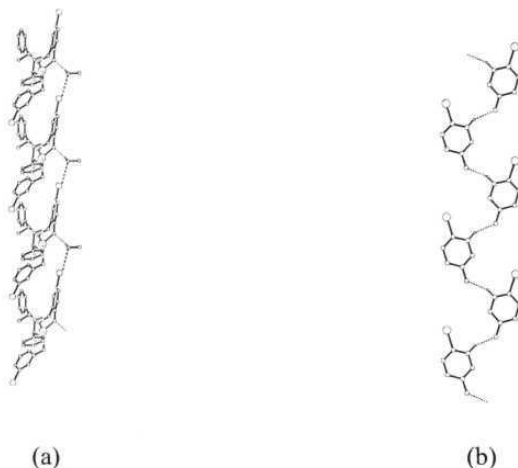


Figure 5. (a) Host molecules aggregate with guest methanol molecules to form infinite one-dimensional chain via alternating O-H...O and Br...O interactions. (b) One-dimensional zigzag chain via C-H...O interactions.

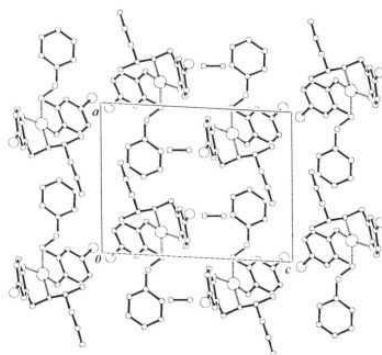


Figure 6. Packing of 7·CH₃OH in the crystal lattice.

(b) $7 \cdot \text{C}_2\text{H}_5\text{OH}$: Here the inclusion of ethanol solvent is stabilized by intermolecular $\text{O}-\text{H} \cdots \text{O}$ interaction involving the metal coordinated phenolate oxygen and the alcoholic OH group of the guest molecule. Calculations using PLATON squeeze program shows that effective volume for inclusion (251.5 \AA^3) comprises 15.8% of the crystal volume. The packing diagram of $7 \cdot \text{C}_2\text{H}_5\text{OH}$ is shown in Figure 7. Interesting the halo activated intermolecular $\text{C}-\text{H} \cdots \text{O}$ interactions leading to helical (as observed for **5** and **6**) and zig-zag chain structure (as observed for $7 \cdot \text{CH}_3\text{OH}$) are absent here. Possibly the larger guest molecules ($\text{C}_2\text{H}_5\text{OH}$) in the lattice do not allow the complex molecules to approach each other for activated $\text{C}-\text{H} \cdots \text{O}$ interactions.

(c) $7 \cdot \text{CH}_3\text{CN} \cdot \text{H}_2\text{O}$: Here, on crystallization from acetonitrile results into inclusion of water molecules along with acetonitrile molecules in the crystal lattice. The asymmetric unit contains the complex, acetonitrile and water molecules in 1:1:1 stoichiometric ratio. The water oxygen acts as acceptor in bifurcated hydrogen bonding ($\text{N}-\text{H} \cdots \text{O}$ and $\text{C}-\text{H} \cdots \text{O}$) interactions. The $\text{C}-\text{H}$ *ortho* to the bromo substituent participates in hydrogen bonding with water molecules and is not exhibiting any helical arrangement of host molecules. On the other hand, water molecules act as hydrogen bond donors to metal coordinated phenolate oxygen atoms ($\text{O}-\text{H} \cdots \text{O}$, 2.7 \AA , 168°) and to the cyano group of acetonitrile molecule ($\text{O}-\text{H} \cdots \text{N}$, 3.0 \AA , 168°). Calculations using PLATON squeeze program show that the effective volume (241.7 \AA^3) comprises 15.5% of the crystal volume. The packing diagram of $7 \cdot \text{CH}_3\text{CN} \cdot \text{H}_2\text{O}$ is shown in Figure 8.

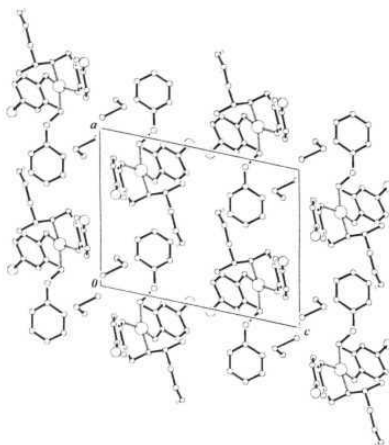


Figure 7. Packing of 7·C₂H₅OH in the crystal lattice

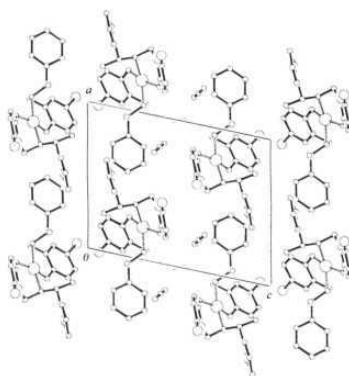


Figure 8. Packing of 7·CH₃CN·H₂O in the crystal lattice.

5.4.5. Helical self assembly

The copper(II) complex (**8**) with the (S)-enantiomeric reduced Schiff base HL⁸ was crystallized from methanol in the monoclinic space group $P2_1$ with $Z = 4$. The asymmetric unit contains one complex molecule with no inclusion of solvent molecule. Under similar crystallization conditions the copper(II) complex (**7**) with the (R)-enantiomeric reduced Schiff base HL⁷ crystallizes in the same monoclinic space group $P2_1$ but with solvent methanol. It may be noted that the packing features of solvated **7**·CH₃OH and guest free crystals of complex **8** are somewhat different although the crystallization conditions for both are similar.

Crystal packing of **8** reveals helical self assembly *via* activated C-H...O interaction as observed for the chloro substituted copper(II) complexes (chapter 4). Here also *ortho* C-H group with respect to bromine atom is activated and participates in C-H...O interaction. Metal coordinate phenolate oxygen acts as hydrogen bond acceptor. These intermolecular C-H...O hydrogen bonds drive the formation of the helix. The path of the helix can be traced by following the hydrogen bonds counter clockwise around the two-fold screw axis of the helix. Only one of the *ortho* to bromine C-H groups is involved in intermolecular hydrogen bonding while other three C-H groups act as spectators. The local chirality at the C8 and C23 and the flexibility of the CH₂-NH fragment (Figure 2b) lead to a twisted conformation and this feature is translated *via* C-H...O interactions into the formation of only right handed (*P*-form) helices at the supramolecular level (Figure 9). Interestingly absolute configuration around the metal centre is left handed (Λ or M) and the molecules assembled through C-H...O interactions form right handed helices. Two complex molecules make up a single turn of the helix generating a helical pitch of 10.04 Å. Copper(II) complex (**6**) with the (S)-enantiomeric chloro substituted reduced Schiff base shows larger helical twist and opposite handedness (chapter 4), when compared with the copper(II) complex (**8**) of the (S)-enantiomeric bromo substituted reduced Schiff base. In **6**, C5-H (*ortho* to both CH₂ and Cl) participates in the C-H...O interaction. On the other hand, C3-H (*ortho* to only Br) participates in the C-H...O

interaction in **8**. Perhaps this difference in the location of C–H group that participates in the helix forming C–H \cdots O interactions is responsible for the opposite handedness of two helical structures formed by **6** and **8**.



Figure 9. The right handed helical packing of $[\text{CuL}^8_2]$ (**8**) molecules through C–H \cdots O interactions; (a) view perpendicular to the *a*-axis and (b) channel of the helix (view down *a*-axis). Only the 4-bromophenolate moiety is shown for clarity.

5.5. Conclusion

The copper(II) complex (**7**) with R-enantiomeric ligand forms host-guest species when crystallized from CH_3OH , $\text{C}_2\text{H}_5\text{OH}$ and CH_3CN . However, under same crystallization condition the copper(II) complex (**8**) with S-enantiomeric ligand crystallizes in the unsolvated form. All the species crystallize in the same non-centrosymmetric monoclinic space group $P2_1$. The intermolecular C–H \cdots O interactions involving the *ortho* C–H with respect to the bromo substituent and the metal coordinated phenolate oxygen are present in all the cases except for $7 \cdot \text{C}_2\text{H}_5\text{OH}$. The other solvated species of **7** form zig-zag chain structures *via* these C–H \cdots O interactions. However, the unsolvated species (**8**) form a helical superstructure *via* this interaction.

5.6. References

1. SMART & SAINT Software Reference Manuals, Version 6.22, Bruker AXS Analytic X-Ray Systems, Inc., Madison, WI, **2000**.
2. G. M. Sheldrick, SADABS, Software for Empirical Absorption Correction, University of Göttingen, Germany, **2000**.
3. SHELXTL Reference Manual, Version 5.1, Bruker AXS, Analytic X-Ray Systems, Inc., WI, **1997**.
4. WinGX-Version 1.63.02 – An integrated system of windows program for the solution, refinement and analysis of single crystal X-ray diffraction data, L. J. Farrugia, *J. Appl. Cryst.*, **1999**, 32, 837.
5. L. J. Farrugia, *J. Appl. Cryst.*, **1997**, 30, 567.
6. A. L. Spek, *Platon, Molecular Graphics Software*, University of Glasgow, UK, **2001**.
7. H. D. Flack, *Acta Crystallogr.*, **1983**, A39, 876.
8. P. V. Sluis and A. L. Spek, *Acta Crystallogr., Sect., A*, **1990**, 46, 194.

List of Publications

1. Self-assembly of a hydrated chiral C_2 - symmetric bisferrocenylimine *via* C—H $\cdots\pi$ and N \cdots H—O—H \cdots N interactions.

Vamsee Krishna Muppidi, Tin Htwe, Panthapally S. Zacharias and Samudranil Pal

Inorg. Chem. Commun., **2004**, 7, 1045-1048.

2. Enantio-specific inclusion of chiral 1,2-dichloroethane rotamers in the crystal lattice of chiral square-pyramidal Cu(II) complexes with perfectly polar alignment of guest and host molecules.

Vamsee Krishna Muppidi, Panthapally S. Zacharias and Samudranil Pal

Chem. Commun., **2005**, 2515-2517.

3. Self-assembly of a pseudo-tetrahedral Zn(II) complex with a chiral reduced Schiff base into a helical superstructure.

Vamsee Krishna Muppidi, Panthapally S. Zacharias and Samudranil Pal

Inorg. Chem. Commun., **2005**, 8, 543-547.

4. Crystal and molecular structures of two mononuclear nickel(II) complexes with tridentate anthracene based Schiff bases.

Tin Htwe, **Vamsee Krishna Muppidi**, Chullikkattil P. Pradeep, Panthapally S. Zacharias and Samudranil Pal

Communicated.

5. Inclusion compounds of CH_3CN and $\text{XCH}_2\text{CH}_2\text{X}$ ($\text{X} = \text{Cl}, \text{Br}$) in the crystal lattice of chiral square-pyramidal Cu(II) complexes: Perfectly polar alignment and enantioselectivity.

Vamsee Krishna Muppidi and Samudranil Pal

To be communicated.

6. Dicopper(II) complexes with an enantiomeric pair of reduced Schiff bases: Inclusion of chlorinated solvents and enantioselective trapping of 1,2-dichloroethane rotamers in the crystal lattice.

Vamsee Krishna Muppidi and Samudranil Pal

To be communicated.

7. Crystal structures of chiral mononuclear Cu(II) complexes: Investigations of intermolecular interactions and supramolecular motifs.

Vamsee Krishna Muppidi, Pallepogu Raghavaiah and Samudranil Pal

To be communicated.